Republic of Iraq

Ministry of Higher Education and Scientific Research

University of Babylon

College of Materials Engineering

Department of Polymer and Petrochemical Industries

Study the Fillers Effect on the Viscoelastic Behavior of LDPE

A Thesis

Submitted to the Council of the College of Materials Engineering / University of Babylon in Partial Fulfillment of the Requirements for the Master Degree in Materials Engineering / Polymer

By

Ahmed Saeed Hashim Abbas

Supervised By

(Prof. D) Najim Abd Al-meer Saad

2021 AD 1442 AH

بسم الله الرحمن الرحيم

((اللَّهُ نُورُ السَّمَاوَاتِ وَالأَرْضِ مَثَلُ نُورِهِ كَمِشْكَاةٍ فِيهَا مِصْبَاحٌ الْمِصْبَاحُ فِي زُجَاجَةٍ الزُّجَاجَةُ كَأَنَّهَا كَوْكَبٌ دُرِّيٌّ يُوقَدُ مِن شَجَرَةٍ مُّبَارَكَةٍ زَيْتُونَةٍ لَّا شَرْقِيَّةٍ وَلَا غَرْبِيَّةٍ يَكَادُ زَيْتُهَا يُضِيءُ وَلَوْ لَمْ تَمْسَسْهُ نَارٌ نُّورٌ عَلَى نُورٍ يَهْدِي اللَّهُ لِنُورِهِ مَن يَشَاء وَيَضْرِبُ اللَّهُ الأَمْثَالَ لِلنَّاسِ وَاللَّهُ بِكُلِّ شَيْءٍ عَلِيمٌ))

صدق الله العلي العظيم

سورة النور/ الاية 35

Acknowledgements

First of all, I thank Allah who gave me the ability and desire to

complete this work.

I would like to express my deep appreciation and sincere thanks to my supervisors

Prof. Dr. Najim Abd Al-meer Saad for his continued encouragement, knowledgeable advice guidance and support throughout this study.

Sincere thanks are also expressed to all staff of Department of Polymer and Petrochemical Engineering / College of Materials Engineering / University of Babylon for their appreciable support. Thanks are also expressed to the staff of the Material Engineering College especially in Polymers laboratories

Finally, I would like to express my appreciation and love to the members of my family and my friends for their support, inspiration, and care during this work.

Ahmed 2021

Dedication

To

The One Who Worth's Praise and Thanks…..
The one who Revives the skies by His Throne and Decorates the Universe by his Mention…..

Allah

To

Our great Prophet Mohammad and his Relatives (Peace and Blessings of Allah be Upon Him and Them) …..

To

The one who embraced me like my mother…..
The one who is my light in life…..

My dear father

To

The one who is my angel on earth…..
The secret of my existence, strength and joy…..

My beloved mother

To

The whispers of flowers and fragrance of morning…..
The shoulder of tenderness and miracle of all time…..

My brother and sister

To

To write my life lines...

To my companion in the road and my life partner.....

My dear wife

Ahmed Saeed 2021

Supervisor Certification

I certify that this thesis entitled " **Study the Fillers Effect on the Viscoelastic Behavior of LDPE**" is Prepared by (**Ahmed Saeed Hashim**) under our supervision at the University of Babylon/ College of Material's Engineering/ Department of Polymer and petrochemical industries in partial fulfillment of the requirements for the degree of Master in Material's Engineering/Polymer and petrochemical industries.

Signature:

(Prof. D) Najm Abd Al-meer Saad

Supervisor

Date: / / 2021

Abstract

Some polymers show a solid elastic behavior and another, viscous liquid, especially low molecular weight polymers, and some polymers possess this behavior at room temperature, especially those that have a low transformation temperature, which negatively affects the properties and performance of parts during service, especially the creep behavior, so improving the performance of these Polymers require the addition of reinforcing materials to form new composite materials capable of overcoming this type of behavior. Fillers were used as reinforcing materials in this work.

Two types of composite materials were prepared, low-density polyethylene (LDPE) reinforced by (10,20,30,40) % weight fraction of alumina (AL_2O_3) powder and LDPE reinforced by (10,20,30,40) % weight fraction of calcium carbonate ($CaCO_3$) powder, the two mixing process were used the first is dry mixing mechanical the (ball mill) and second is fusion process to mixes the materials by the twin extruder, to obtain the new modified composites materials (LDPE/ AL_2O_3),(LDPE/$CaCO_3$) respectively.

To purpose study the effect of fillers on the visco- elastic properties and morphology, several tests are performed including, Fourier transforms infrared, melt flow index MFI examination, density, tensile strength, impact, creep, and scanning electron microscope (SEM).

The results are, a clear improvement in the creep performance of all LDPE composite when adding fillers, but reasonable proportions of fillers gave the best performance, Where the adding of 10wt% alumina to the LDPE matrix is provided the best performance of creep resistance, superior to the best performance provided

by the LDPE matrix when introducing 20wt% calcium carbonate, The sample that provided the best creep resistance performance could withstand the maximum temperature before failure, which is 50°C, The tensile strength increased by about 22.222 % when inserting 10% weight fraction of calcium carbonate, which is the highest increase obtained, while the tensile strength increased by 11.111 % when entering 10% weight fraction of alumina. The highest percentage of increase Obtained for Young's modulus was estimated at 53.84 % when inserting 30% weight fraction of alumina, while Young's modulus increased by 38.46 % when inserting 10% weight fraction of calcium carbonate. The impact resistance increased by 48.9 % when introducing 30% weight fraction of alumina, while impact resistance increased by 12.34 % when introducing 30% weight fraction of calcium carbonate. Density and viscosity values increased and the molten flow rate decreased with the increase of the filler content in the low polyethylene density matrix. The SEM images showed the level of dispersion of the filler particles and their proportions in the low-density polyethylene matrix.

Content

List of Abbreviations

Abbreviation	Description
A	Absorbance
AA	Acrylic acid
ASTM	American Society for testing materials
BSE_S	Backscattered electrons
CED	Coherent energy density
FTIR	Fourier transform infrared
GKM	Generalized kelvin-vogite
GM	Generalized Maxwell
HDPE	High-density polyethylene
IR	Infrared spectroscopy

KBR	Potassium bromide
LDPE	Low-density polyethylene
LLDPE	Linear low-density polyethylene
LVE	Linear Viscoelastic
MDPE	Medium-density polyethylene
PP	Polypropylene
PSK	Palm kernel shell
SEM	Scanning electron microscope
SE_S	Secondary electrons
T	Transmittance
UHMWPE	Ultra-high-molecular-weight polyethylene
UV	Ultraviolet
WF	Wood flour
wt.%	Wight fraction

List of Symbols

Symbol	Description	Unit
Tg	Glass transition temperature	^0C
ε(t)	Total creep strain	mm/mm
D(t)	Creep compliance function	MPa^{-1}
б	Tensile strength	MPa
ε′	Creep rate	mm/min
Q	Activation energy	J mol^{-1}
R	The universal gas constant	J/mole K
ε	Strain of materials	mm/mm
E	Elastic modulus	N/m^2
H	Viscosity	$kg \cdot m^{-1} \cdot s^{-1}$
F	Tension force	N
L	Final length	mm
L_o	Initial length	mm
I.S	Impact resistance of material	J/m^2
U_c	Impact energy	Joule
A	Cross-sectional area of sample	m^2
$\Delta\epsilon$	Strain change	mm/mm

Δt	Time change	min
MFR OR MFI	The melt flow rate or melt flow index	g/10min
SiO_2	Silicon dioxide	
AL_2O_3	Aluminum oxide(alumina)	
$Mg(OH)_2$	Magnesium hydroxide	
$CaCO_3$	Carbonate calcium	
H_2O	Water molecule	
$\eta, \delta, \gamma, \kappa, \theta, \rho$	Types from crystalline structures of alumina	
Na_2O	Sodium oxide	
CO_2	Carbon dioxide	
PCC	Precipitated calcium carbonates	
Ca(NO3)Z	Cobalt Nitrate	
CaO	Calcium oxide	
$Ca(OH)_2$	Calcium hydroxide	
KBR	Potassium bromide	

List of Figures

List of Tables

Chapter One

Introduction

1.1 Introduction

Two specific types of ideal materials: elastic solid and viscous liquid usually discuss the performance of materials with relatively low relative molecular mass. The first has a definite shape and is distorted in new equilibrium by external forces; It immediately returns to its original shape when these loads are removed. During deformation, the energy is completely stored by the solid, which is obtained by externally applied loads, and this energy works to restore the material to its original form after removing those loads. A viscous liquid, on the contrary, has no apparent shape and flows through external forces irreversibly [1].

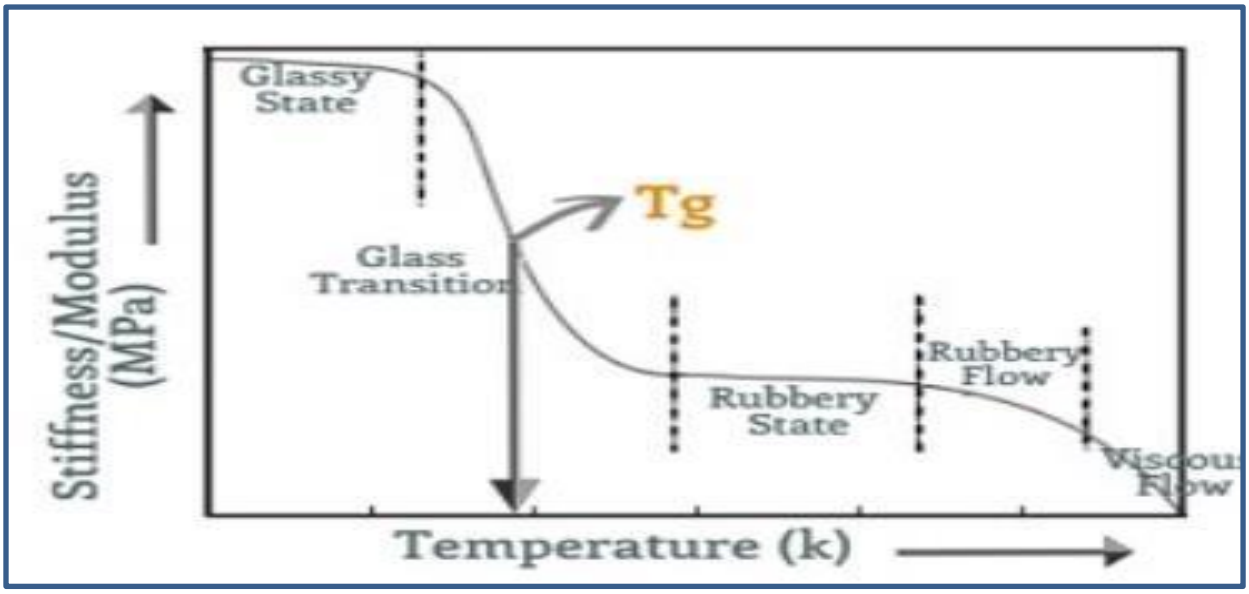

Figure 1.1: Stages of polymer with temperature[1].

The property of materials that display both viscous and elastic qualities when deformed is known as viscoelasticity. Polymers, especially thermoplastics and elastomers, have a temperature of Tm and a transition temperature of Tg. According to these grades, the polymers go through three stages see figure (1.1), the first state before Tg is solid and brittle and is called the glass transition. The second stage begins after Tg, which is viscoelastic where the material possesses

common properties from elastic and viscous and continues to Tm, and after the temperature Tm, the material goes through the third state, which is called the liquid state [2].

Creep and relaxation time are considered among the most important parameters of elastic viscosity. When the material is subjected to a constant load with a specific temperature, and with time, the material is subjected to deformation and its dimensions change as the deformation process accelerates with time until failure occurs. The important thing is that failure occurs at stress less than the design stress values of the material and here, the danger of this behavior lies, and this matter made the engineers pay great attention to this behavior because of its impact on the dimensional stability of products in all applications, whether medical, agricultural, or packaging [3].

The phenomenon of visco-elastic affects the properties of polymers, for example, some important polymers such as polyethylene and polypropylene, which have many applications and have wide uses in all fields, have very low degrees of transformation. Therefore, these polymers are at room temperature in the case of visco-elastic, which negatively affects their properties during work. On the other hand, researchers have invested the influence of viscoelasticity on the polymer manufacturing method, whereby the melt flow index, which is inversely related to viscosity and molecular weight, affects the properties of polymers, through which they determine the manufacturing processes and conditions. Thus the final characteristics of the product are determined. choose extrusion if the melt flow rate is low and injection if the melt flow rate is high [4].

Perhaps the most important way to improve the properties of visco-elastic, especially the creep strain, is the process of strengthening the polymer matrix with particles or fibers, where experiments have proven that it is effective. Deformation occurs as a result of the movement of the polymeric chains. The process of reinforcing with fillings has witnessed significant growth due to the low cost of most fillings, lightness in weight, and some environmental factors. The reinforcing materials restrict the movement of the chains and thus reduce the creep strain and give better thermal stability as it improves the properties of the parts during service due to the improvement of the stiffness values [5].

Particle of fillers are required to generate appropriate properties for most applications. When selecting particle fillers, it is important to first understand the performance needs of the material and then find or produce a material that meets these criteria at a reasonable price. Since there is no ideal polymer or filler, therefore, you may be able to improve a certain property when a certain percentage of the filler is introduced, but other properties may change as well, perhaps in a not-so-good way, even though that was not what we intended. The winner is the person who understands resources better. What important here is that these fillings improve the properties of visco-elastic behaviour significantly by improving the creep resistance at various temperatures in addition to giving it the necessary reinforcement for flexible materials by restricting the movement of polymer chains and has proven successful in this field [6].

1.2 Aim of This Study

Studying the effect of the fillers on the viscoelastic behavior of low-density polyethylene and its composites through its creeping behavior.

Chapter Two

Theoretical Part and Literature Review

2.1 Introduction

This chapter focuses on the viscoelastic properties and relationship of the filler with polymer in addition to the materials used in the research and their definitions, and it also shows mechanical, rheological, and morphological properties of polymers in addition to the tests and their definitions.

2.2 polymers

It is a high molecular weight compound composed of repeating subunits. These materials may be organic, inorganic, or mineral-organic, and may be natural or synthetic in origin. Polymers have become an integral and integral role in everyday life due to their unique properties. They are essential materials in everyday industrial sectors, such as adhesives, building materials, paper, clothing, fibers, plastics, ceramics, concrete, liquid crystals and photoresists, and coatings[7].

2.3 Polymers Structure

In general, polymers consist of long chains that may be organic, inorganic, or semi-organic composed of a small unit, monomer molecules, which are linked by covalent connections with each other. The long chains, therefore, consist of repeating chemical compositions and are represented by the polymerization degree by the number of repeating units. These macromolecular chains are interconnected physically by Van der Waals force or coherent energy density (CED) which is responsible for the outstanding properties of the polymeric material such as physical, mechanical, thermal, and rheological properties. The strength of the Vander Waals depends largely on the chemical formula, the molecular weight of the substance, as well as the polarity, the space organization of the substance, the

tactics of the repeating units of the structure, the presence of heterogeneous atoms in the structure of the repeating units. The units that are repeated within the basic polymer structure determine the identity of the polymer, as shown in the commercial polymers in Table (2.1) [8].

Table 2.1: Chemical Structure of Some Commercial Polymers [8].

Polymer	Chemical structure of the repeating units	Tg (^{o}C)	Tm (^{o}C)	$(CED)^{0.5}$
Polyethylene	$-CH_2-CH_2-$	-125	141	7.9
Polypropylene	$-CH_2-CH-$ | CH3	-20	165	8
Polyvinylchloride	$-CH_2-CH-$ | Cl	87	190	9.5
Polymethyl methacrylate	CH_3 | $-CH_2-C-$ | $CH_3O-C=O$	105	160	9.1

2.4 Mechanical Behavior of Polymers

Polymers cannot be classed as certain types of substances such as glass-based solids or viscous liquids because their mechanical characteristics depend so much on the applied load rating, temperature, and strain value. They are usually described as a viscoelastic material, which has an intermediate position between viscous liquid and elastic solids see figure (2.1) B. A polymer can show all the features of glassy, brittle solid, elastic rubber, or a viscous liquid depending on the temperature and time scale of measurement, The law of Hook has been derived from the basic elasticity theory as in Equation No. (2.1), which deals with mechanical characteristics for elastic substances, see figure (2.1) A, where stress is

directly proportional to strain when deformation is small. The classical theory of Newtonian rheology deals with the properties of viscous liquids from which Newton's Law is obtained, where the stress is always directly proportional to the rate of strain. In the theory of elasticity, the stress is independent of the rate of strain, and in the theory of hydrodynamics, independent of strain. These two theories do not describe the behavior of viscoelastic materials [9].

$$E = \frac{\sigma}{\epsilon} \qquad (2.1)$$

Where:

σ: stress applied.

ϵ: strain.

E: elastic modulus.

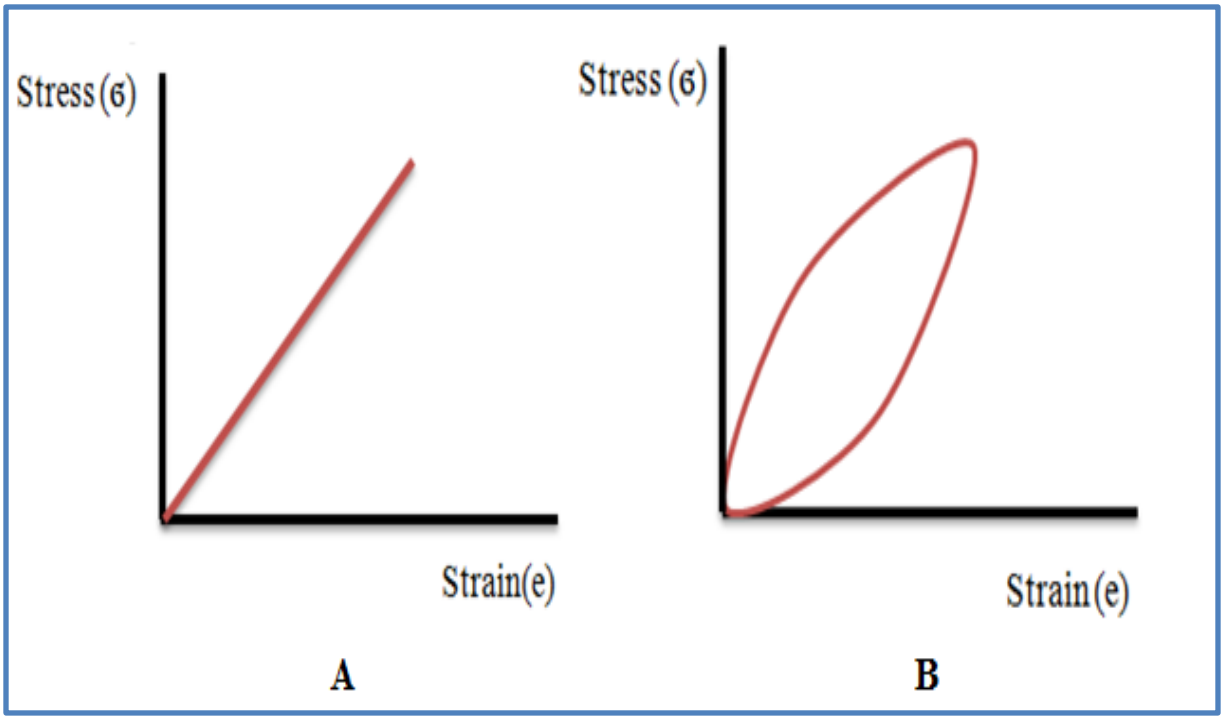

Figure 2.1: Stress-strain curves (A) for a purely elastic material, (B) a viscoelastic material. The area of the loop in curve B represents hysteresis loop [9].

2.5 Viscoelastic Behaviour of polymer

One of the most interesting features of polymers is that a given polymer can display all the intermediate range of properties between an elastic solid and a viscous liquid depending on the temperature and the experimentally chosen timescale. which has great commercial importance and great uses. This type of reaction that combines liquid and solid-like properties is called visco-elastic [10,11].

Viscoelastic materials have elements of both of these properties and, as such, exhibit time-dependent strain showing a 'fading memory'. Such behavior may be linear (stress and strain are proportional) or nonlinear. Whereas elasticity is usually the result of bond stretching along crystallographic planes in an ordered solid, viscoelasticity is the result of the diffusion of atoms or molecules inside an amorphous material [12].

The linear viscoelastic region, see Fig.(2.2), where the isochronous stress-strain curve follows a straight line. Thus the mechanical behavior of polymeric materials can, at least formally, be handled by the theory of linear viscoelasticity, if the stresses (or strains) are sufficiently small. This linear response region, however, is often small or negligible in comparison with the total range available before yielding or fracture. The advantage of the linear theory is that it is a simple and a good mathematical tool that makes it possible to deal with rather complicated deformation problems in time-dependent materials and to obtain at least approximate results and trends, provided that the stresses are not too large [13].

The nonlinear viscoelastic region where the isochronous stress-strain curves show a deviation from the straight line towards the strain axis with increasing

stress, see Fig.(2.2). The deviation occurs beyond a certain strain level, which varies for different polymers depending on the nature of such polymers, time, and temperature. This lies between (0.2-0.5 %). Thus for stresses of larger magnitudes, the linear theories fail, necessitating the use of nonlinear ones. The extent of creep in polymers can be significant depending on temperature, time, and applied load. To reduce creep, the application of polymers should be at a temperature below the glass transition. However using polymers only below Tg could prove uneconomical, for instance in the case of polypropylene (Tg= -20°C). Therefore the use of polymers for engineering purposes necessitates further research into ways of measuring creep and reducing its extent [14,15].

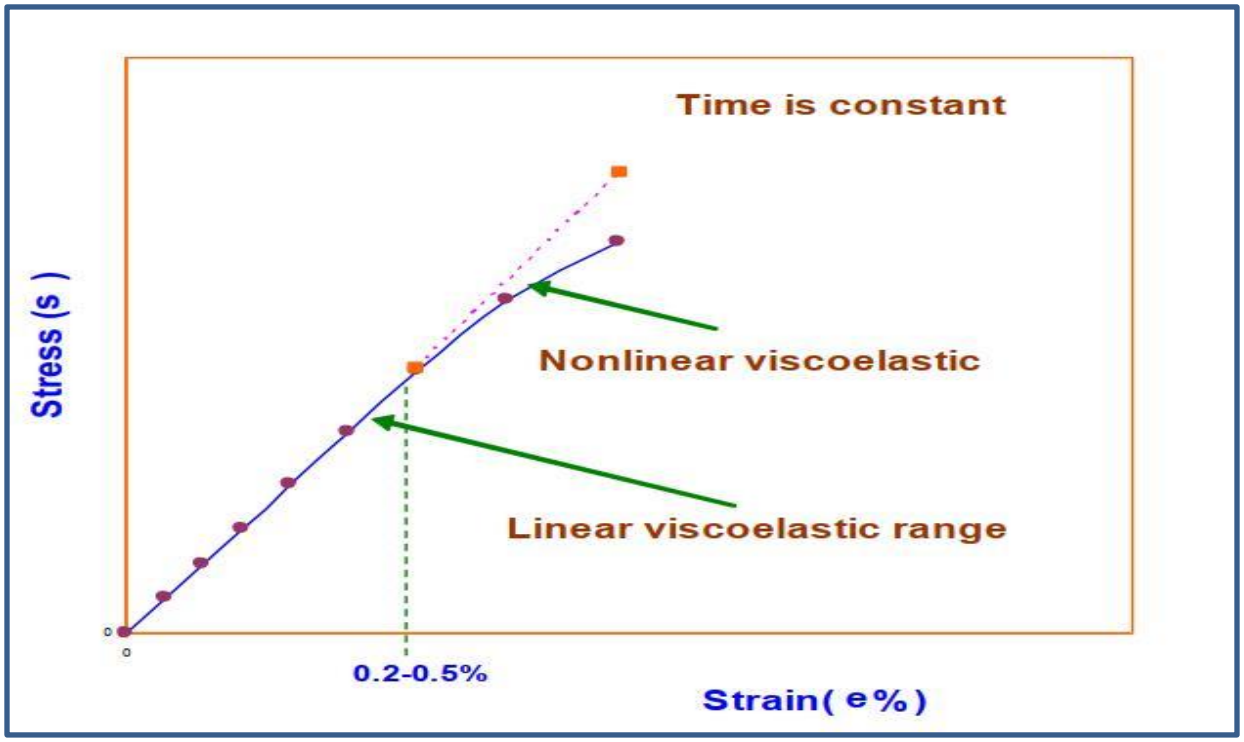

Figure 2.2: Isochronous stress-strain curve [15].

2.6 Linear Viscoelastic

Commonly, the LVE limit is defined as a level of stress or strain above which actual behavior deviates from the behavior predicted based on linearity assumption. However, stress and strain are interrelated time-dependent functions strongly influenced by test type and action of external factors. The concept of an energy threshold as a criterion of LVE limit has the advantage of combining the effects of both stress and strain into one physical function initiating nonlinear behavior [16].

Viscoelastic materials are characterized by their ability to display both viscous and elastic behavior. Most real-life solids demonstrate some viscoelastic properties, and these effects may be particularly important when considering synthetic polymers, The established theory for linear elasticity provides a sound starting point for the study of linear viscoelasticity, Theories of linear viscosity are inferred through the use of well-known models to characterize the behavior of viscoelastic [17].

However, most polymers exhibit nonlinear viscoelastic behavior and the use of known LVE models for the description of their deformability becomes invalid in this case. To choose an appropriate model for characterization of a material time-dependent behavior it is important to know when the contribution of nonlinear components to a general viscoelastic behavior becomes essential. Then, more complicated models of nonlinear viscoelasticity have to be used for further analysis [18].

A valid estimation of limits of LVE has an important role in the analysis of the long-term behavior of composites, in particular, in calculations of their effective characteristics of viscoelasticity and evaluation of stresses in their

components. The use of nonlinear models for characterizing the behavior of the components often requires passage to more complicated numerical approaches. The action of external factors, such as temperature or moisture, accelerates relaxation processes and leads to a reduction of service life of polymers [19,20].

2.6.1 Creep

Creep is the progressive deformation of material at constant stress and temperature. It is used to describe the slow plastic deformation that occurs under prolonged loading, usually at high temperatures. Creep in its simplest form is the progressive accumulation of plastic strain in a specimen or machine part under stress at elevated temperatures over a period of time [21].

polymeric materials can exhibit the phenomenon known as a creep; following an initial, instantaneous linear elastic response the material continues to accumulate strain over time, even when the applied load is held constant. Figure (2.3) shows the stress and typical creep strain response to illustrate this concept[22].

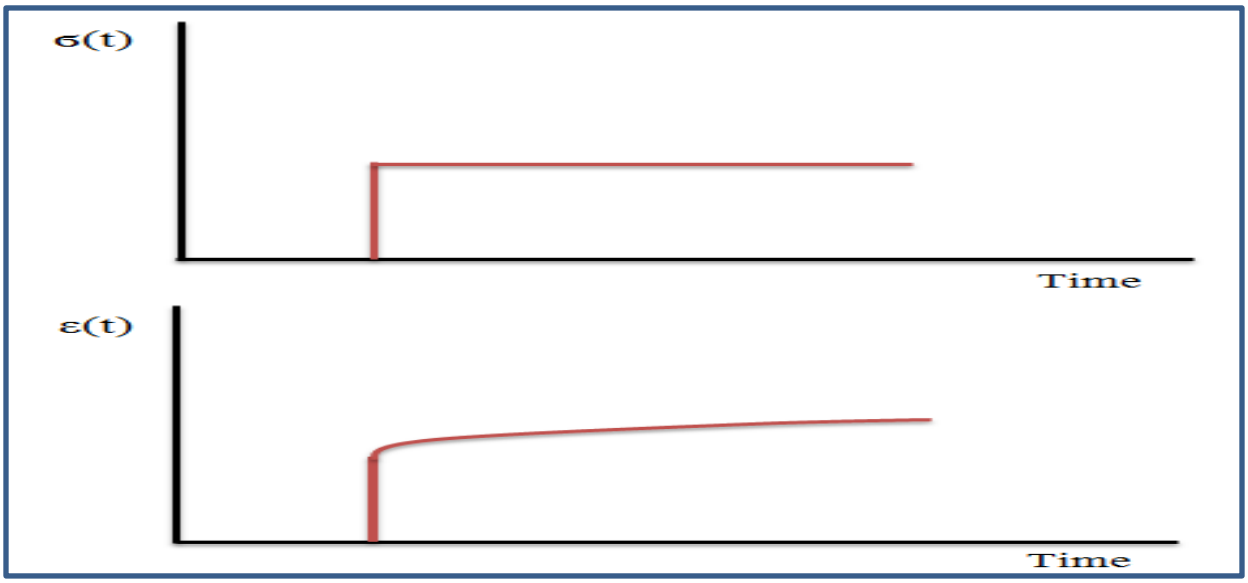

Figure 2.3: Typical creep behavior [22].

the creep strain response to constant applied stress For a viscoelastic material is given by:

$$\varepsilon(t) = D(t)\sigma \qquad (2.2)$$

where D(t) is the creep compliance function, ε(t) is the total creep strain, and σ is the constant applied stress. Understanding the creep behavior of materials is important in design and manufacturing because it can lead to dimensional instability of the final product and failure under constant stress that is significantly lower than the ultimate tensile strength [23].

In general, creep can be described in three stages: primary, secondary, and tertiary. In the first stage, the material undergoes deformation at a decreasing rate, followed by a region where it proceeds at a nearly constant rate. In the third or tertiary stage, it occurs at an increasing rate and ends with fracture see Figure(2.4) [24,25].

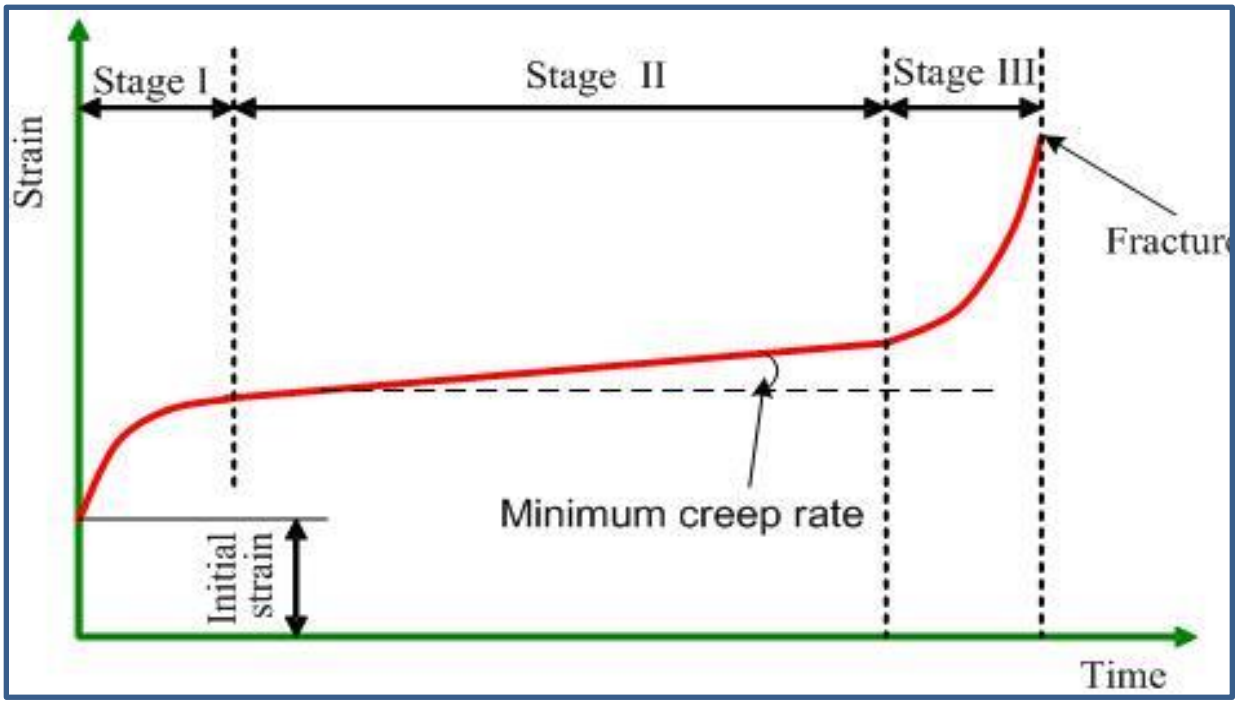

Figure 2.4: Creep stages [26].

The equation governing the rate of steady-state creep is:

$$Creep\ rate\ =\ \varepsilon' = A\sigma^n\ exp(\frac{-Q}{RT}) \qquad (2.3)$$

Q = activation energy (J/mol).

n = stress exponent.

A = constant.

σ = is the applied stress (MPa).

R= is the universal constant of gases (J/mole K).

T= the temperature at which creep test was performed (K)

This can be rearranged into the form:

$$\ln \varepsilon' = \ln A + n \ln \sigma - \frac{Q}{RT} \qquad (2.4)$$

The activation energy Q can be determined experimentally, by plotting the natural log of creep rate against the reciprocal of temperature [27].

2.6.2 Stress Relaxation

A typical material in terms of elasticity and rigidly may be subjected to an immediate strain that affects it, then fixed and limited stress is recorded. concerning elastic solid materials that are subjected to strain, The initial stress is directly proportional to the effective strain. Then Gradually decreasing with time, see figure (2.5), this elapsed time is called the relaxation time. This behavior is called stress relaxation. The stress values may reach zero in some polymers that have linear behavior, especially random ones [28, 29].

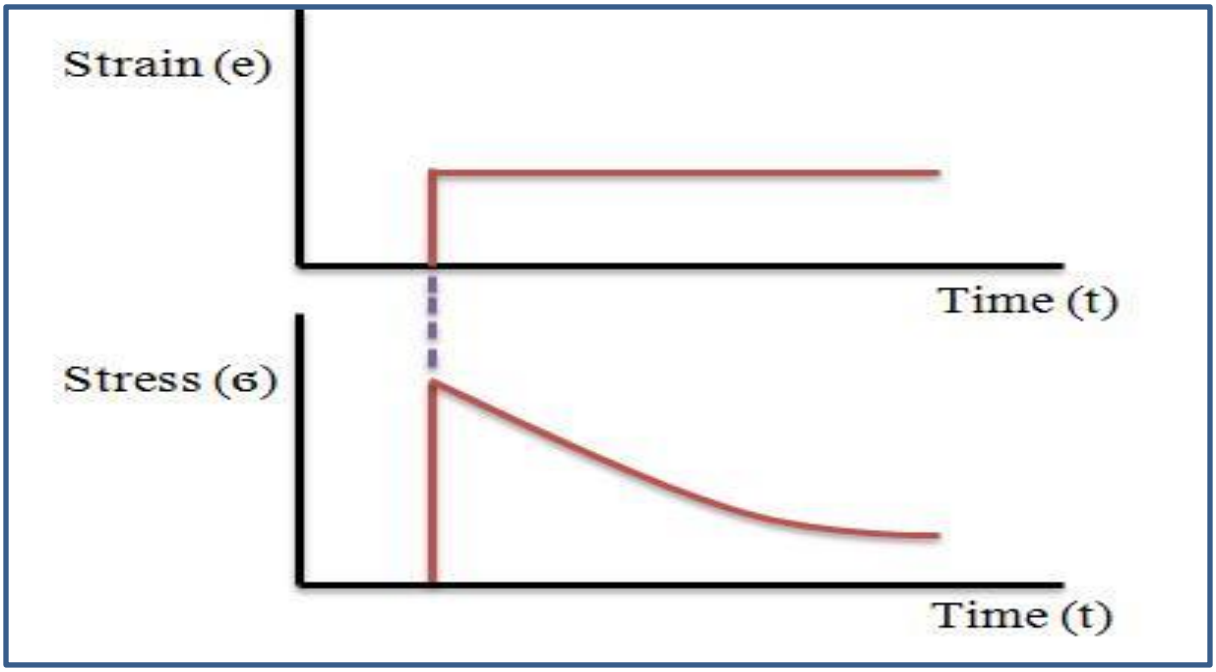

Figure 2.5: Stress relaxation (idealized) [30].

Rheological parameters directly affect the polymer manufacturing process and the properties of the final solid product. Therefore, understanding the rheology of molten polymers is very important in this field. The molten viscosity and relaxation time are among the most important rheological parameters. The amount of elastic energy stored by the molten polymer is related to the relaxation time. Within the backbone of the chain and also outside the chain occurs a variable spectrum of relaxation times related to the relaxation process. The multiplicity of relaxation times usually refers to the interactions that occur in the liquid state between the different polymer chains (i.e. repeats). When the molten polymer undergoes deformation, the entire chain relaxation time is slower than the sub-chain time, and thus the viscoelasticity can be quantified by the relaxation time lengths [31].

2.6.3 Mechanical Models

The mathematical models that characterize the mechanical properties of materials are a continuing issue in engineering research. The simplest and more friendly models for this proposal are the Kelvin–Voigt and Maxwell models because of their linearity. The models are not equivalent: the first can explain creep, but not relaxation phenomena, and the second does the opposite. Both models correspond to materials that show only one characteristic time. To fit a model to materials showing several characteristic times, generalized linear viscoelastic models are used, connecting several Kelvin–Voigt or Maxwell elements. Every generalized Maxwell (GM) model has an equivalent generalized Kelvin–Voigt (GKV) model [32, 33].

I. Maxwell Model

In order to better visualize the stress and stress relation in viscoelastic materials, mechanical models were designed. These models use dashpots and springs to depict the behavior's dual nature. The Maxwell model, shown in figure(2.6), is one of the main mechanical models and represents a series of springs and a dashpot [34].

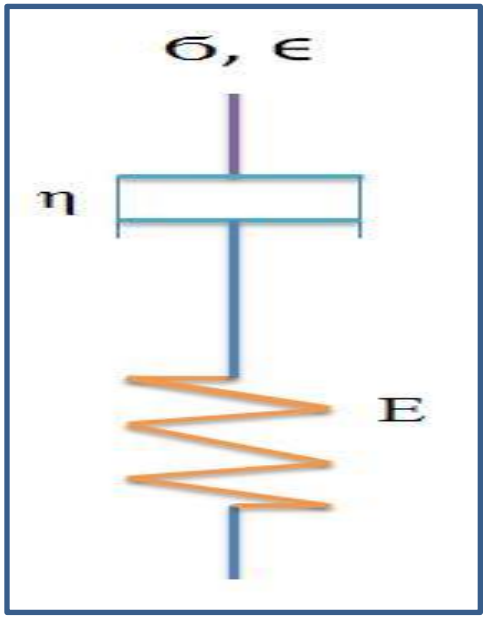

Figure 2.6: The Schematic diagram for the Maxwell model[35].

The linear elastic behavior of a solid is represented by the spring and is typically governed by Hooke's Law:

$$\sigma = E\epsilon \qquad (2.5)$$

where σ is the stress, E is the elastic modulus, and ε is the strain in the material. The viscous behavior of simple fluids represented in the model by the dashpot obeys Newton's Law of Viscosity:

$$\sigma = \eta \frac{d\varepsilon}{dt} \qquad (2.6)$$

where η is the material property known as viscosity. The stress and strain equations representing the two components in this system are combined to give the following equation for the viscoelastic behavior

$$\frac{d\varepsilon}{dt} = \frac{1}{E}\frac{d\sigma}{dt} + \frac{\sigma}{\eta} \qquad (2.7)$$

A problem with this particular approach is that it fails to properly represent the complexity of creep behavior [35].

II. Voigt Model

This model consisting of springs and dashpots are used to describe the viscoelastic properties, provides a more reasonable representation of creep behavior, it does not represent the stress-relaxation behavior adequately more realistic representations of viscoelastic behavior can be developed using these simple mechanical elements by combining many Maxwell elements in parallel, many Voigt elements in series, or even a combination of Maxwell and Voigt. Figure (2.7) shows the Voigt model, which employs a parallel spring and dashpot [36].

This model results in the following equation by combining the spring and dashpots stress and strain equations:

$$\sigma = E\varepsilon + \eta\frac{d\varepsilon}{dt} \qquad (2.8)$$

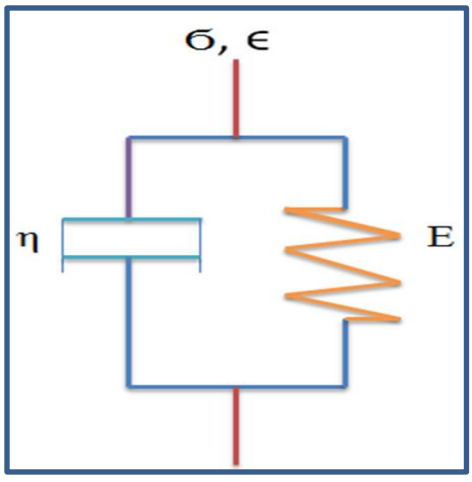

Figure 2.7: The Schematic diagram for the Voigt Model [37].

2.7 Nonlinear Viscoelastic

Linear viscoelastic behavior of materials has been the subject of extensive studies for over a century, but it is only in the last few decades that researchers have started to pay special attention to the more complex subject of nonlinear viscoelasticity. A certain number of nonlinear theories of viscoelasticity have been proposed and applied to a certain class of polymers and polymeric composites. Most of them admit the existence of a threshold that depends on the applied stress level. Beyond this stress-dependent limit, viscoelastic behavior becomes nonlinear. However, existing models for the description of this behavior either determine the transition region from linearity to non-linearity through experimental observations or assume linear response at a low-stress level and then define the threshold as the limit of this response. However, from the experimental point of view, the beginning of nonlinearity may appear either at low or high-stress levels according to time and temperature conditions [38].

A unified theory of nonlinear, large deformation viscoelasticity is created, meaning that nonlinear elastic behavior is combined with time-dependence through a decomposition of the real system into elastic and viscoelastic networks (E and v) [39].

The classical linear theory of viscoelasticity has adequately described the creep, relaxation and loading-rate dependence of polymers. However, is limited to narrow loading rate and temperature regimes, while polymeric materials demonstrate a nonlinear response at relatively small strains. Significant works related more applicable models for nonlinear viscoelasticity have been developed [40].

2.8 Composite Materials

A composite is a structural material that consists of two or more combined constituents that are combined at a macroscopic level and are not soluble in each other. One constituent is called the reinforcing phase and the one in which it is embedded is called the matrix. The reinforcing phase material may be in the form of fibers, particles, or flakes see figure (2.8). The matrix phase materials are generally continuous, in general, the reinforcements are much stronger and stiffer than the matrix. There are many factors to be considered when designing composite materials. The type of reinforcement and matrix, the geometric arrangement and volume fraction of each constituent, the anticipated mechanical loads, the operating environment for the composite, etc., must all be taken into account [41].

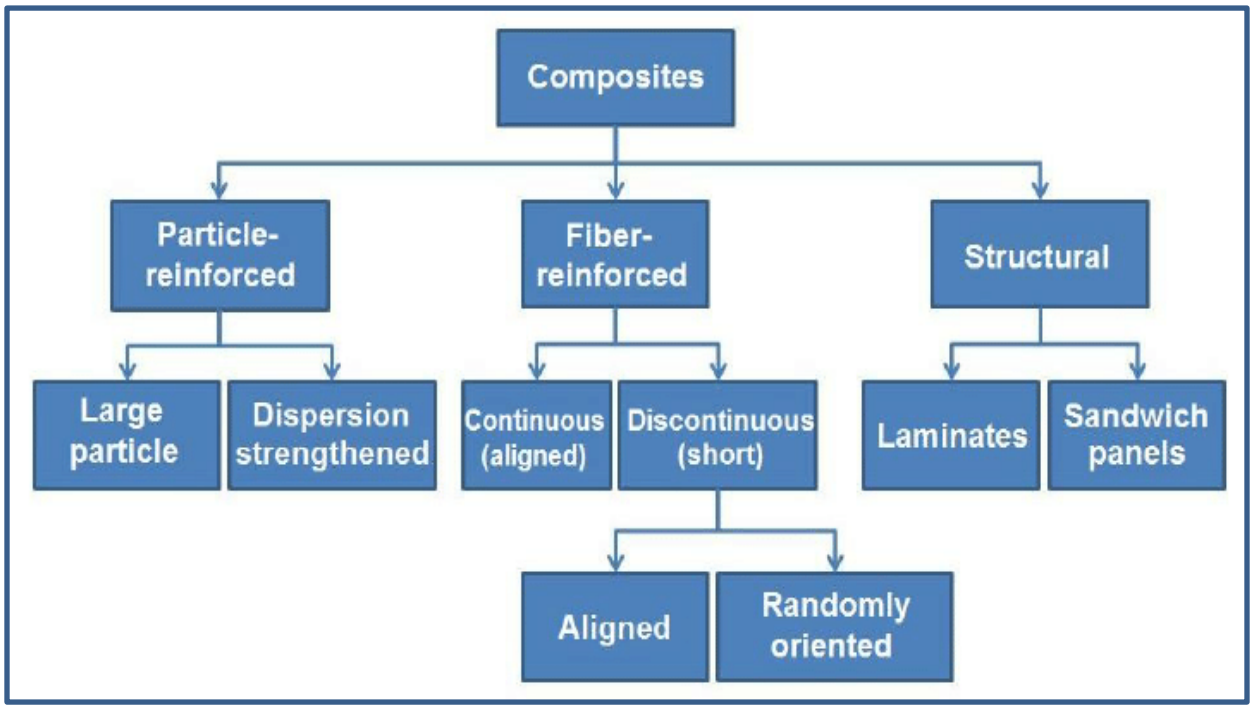

Figure 2.8: A classification scheme for the various composite types [42].

Over the past few years, the development of new materials has been oriented towards polymer composites to obtain materials, which are characterized by specific properties and low manufacturing costs[43].

2.8.1 Polymer Matrix Composite

It is a polymeric material that is chosen to be the base or grounding of the composite material. It protects and contains fillers. Specifically, composites based on polyethylene with inorganic fillers are of great research interest. Properties of the filled composites are determined by properties of the polymer, properties of filler, volume fractions of the constituent phase as well as polymer– filler and filler–filler interactions. Interactions of polymer molecules with inorganic fillers may affect their properties on the microscopic level (conformation, crystallinity, molecular dynamics) and macroscopic level (stiffness, hardness, toughness) [43].

2.8.2 Reinforcement Materials

Composite materials are usually classified according to the type of reinforcement used. Two broad classes of composites are fibrous and particulate. Each has unique properties and application potential and can be subdivided into specific categories as discussed below [44].

I. Fibrous

A fibrous composite consists of either continuous (long) or discontinuous fibers suspended in a matrix material. Both continuous fibers and discontinuous can be identified from a geometric viewpoint [44].

II. Particulate

A particulate composite is characterized as being composed of particles suspended in a matrix. Particles can have virtually any shape, size or configuration. Examples of well-known particulate composites are concrete and particleboard. There are two subclasses of particulates: flake and filled/skeletal [44].

III. Laminate

A laminate is a stack of laminas, oriented in a specific manner to achieve the desired result. The laminate's response depends on the properties of each lamina, as well as the order in which the lamina is stacked [44]**.**

2.8.3 matrix

The matrix is the binder material that supports, separates, and protects the reinforcement materials. The matrix is typically ductile, elastic, or plastic. They can have either linear or nonlinear stress-strain behavior [45].

Thermoplastic polymers and especially polyolefins and polyethylene are produced and consumed today in vast quantities. However, they are seldom used as neat polymers and are usually compounded with mineral fillers. Initially, fillers were used as 'extenders' for polymers to reduce cost but as the polymer price decreased and the requirements of modern applications increased, attention has been more and more focused on functionality enhancement. Nowadays, 'functional fillers' find application in the polymer industry almost exclusively, e.g. to improve stiffness, toughness, dimensional stability, electric-insulation, or to decrease the dielectric loss. A prerequisite for functional fillers is full dispersion (break-up of agglomerates into their primary particles) and uniform spatial distribution in the

polymer matrix because agglomerates entrap air and act as sites for fracture initiation, thus leading to premature material failure [46].

To cope with the obvious limitations of polymers, for example, low stiffness and low strength, and to expand their applications in different sectors, inorganic particulate fillers, such as micro SiO_2, glass, Al_2O_3, $Mg(OH)_2$, and $CaCO_3$ particles to process polymer composites, which normally combine the advantages of their constituent phases. Particulate fillers modify the physical and mechanical properties of polymers in many ways It has been shown that dramatic improvements in mechanical properties can be achieved by incorporation of a few weight percentages (wt%) in polymer Stiffness or Young's modulus can be readily improved by adding microparticles since rigid inorganic particles generally have a much higher stiffness than polymer matrices. However, strength strongly depends on the stress transfer between the particles and the matrix. For well-bonded particles, the applied stress can be effectively transferred to the particles from the matrix [47].

2.8.4 Filler Particles

Is one of the techniques used in reinforcing composite materials. It's principle is similar to the dispersion strengthening they act to cause deformation in matrix material, in addition to that they restrict the movement of matrix material in all directions and share matrix material to bear the loads imposed on it because of their large size, but it differs from the dispersion strengthening in particle size where the particle size is greater than (1μm) and the percentage of volumetric concentrations in which more than (15%) of the volume of composite material [48].

The reinforcing process is when particles work as barriers to the matrix material deformation because they have high hardness and do not deform during loading. They are several types and forms including spherical, cortical, needles, and filamentous where the particles work to increase the rigidity of the material, creep resistance, impact resistance, and improving thermal expansion coefficient of the matrix material. It has been observed that this type of reinforcing includes the participation of particles with the matrix material to bear the stress applied to the composite materials. The fracture occurs when the applied shear stress exceeds the fracture strength of the reinforcing materials. The reinforcing amount depends on the linking force between the matrix material and particles. The particles must be distributed uniformly within the matrix material [49].

This is by itself is of great benefit in some applications that require similar properties for examples alumina, $CaCO_3$ particles, which used in this work.

2.9 Materials

2.9.1 Polyethylene

Polyethylene of different density ranges can be obtained by chain polymerization of ethylene, the simplest olefin monomer. The observed chemical nature and physical properties of the polymer depend largely on the nature of the catalyst used and conditions employed during polymerization. Polyethylene obtained by polymerization of ethylene is mostly branched polymers, the chemical nature, and frequency of braches being largely dependent on reaction condition and the mechanism involved. Thus poly (ethylene) is the linkage of many ethylene units: $H_2C=C_2H \rightarrow \ - (CH_2\text{-}CH_2)_n$- [50].

Factors contributing to the widespread application of polyethylene are low cost, easy processability by a variety of techniques, several types of polyethylene depend on some characteristics in classification, such as density, molecular weight and branches in the polymeric chain .Table(2.2) shows some of these types and their properties [50]

Table 2.2: Some Properties of Various Grades of PE [51].

property	LDPE	LLDPE	MDPE	HDPE	UHMWPE
Tensile strength (MPa)	10–17	20	14	20-35	21
Glass transition temperature (°C)	-110	-110	-118	-110	-118
Melting temperature (°C)	105–120	220–260/105–120 (depends on Branching)	105–120	120–130	123-133
Water absorption, 24 h (%)	0.005–0.015	0.005–0.01	0.01	0.005–0.01	0.005–0.1
Density (g/cm3)	0.917–0.94	0.915–0.95	0.926-0.940	0.95	0.93–0.95

2.9.2Low Density polyethylene (LDPE)

Low density polyethylene (LDPE) is so named because such polymers contain substantial concentrations of branches that hinder the crystallization process, resulting in relatively low densities. The branches primarily consist of ethyl and butyl groups together with some long chain branches. Low density polyethylene

resins typically have densities falling in the range of approximately 0.918–0.935g/cm^3[51].

Due to the nature of the high-pressure polymerization process by which low density polyethylene is produced, the ethyl and butyl branches are frequently clustered together, separated by lengthy runs of unbranched backbone. Long-chain branches occur at random intervals along the length of the main chain [51].

The long-chain branches can themselves in turn be branched. The numerous short-chain branches found in low density polyethylene reduce its degree of crystallinity well below that of high density polyethylene, resulting in a flexible product with a low melting point. Long-chain branches confer desirable processing characteristics, high melt strengths coupled with relatively low viscosities. Such characteristics eminently suit it to the film-blowing process, products of which are its principal outlet, accounting for more than half of all its use. Major applications include low load commercial and retail packaging applications and trash bags [51].

LDPE is a semi-rigid, translucent material, and was the first of the polyethylenes to be developed. It is primarily used at 'normal' operating temperatures. Its qualities include toughness, flexibility, resistance to chemicals and weather, and low water absorption. It is easily processed by most methods and has a low cost. It is also resistant to organic solvents at room temperature. Its use is not advisable in situations where extreme temperatures are found. It is an excellent material where wear resistance is an important factor, but when hardness, high temperature, and structural strength are not important considerations in the application used [51].

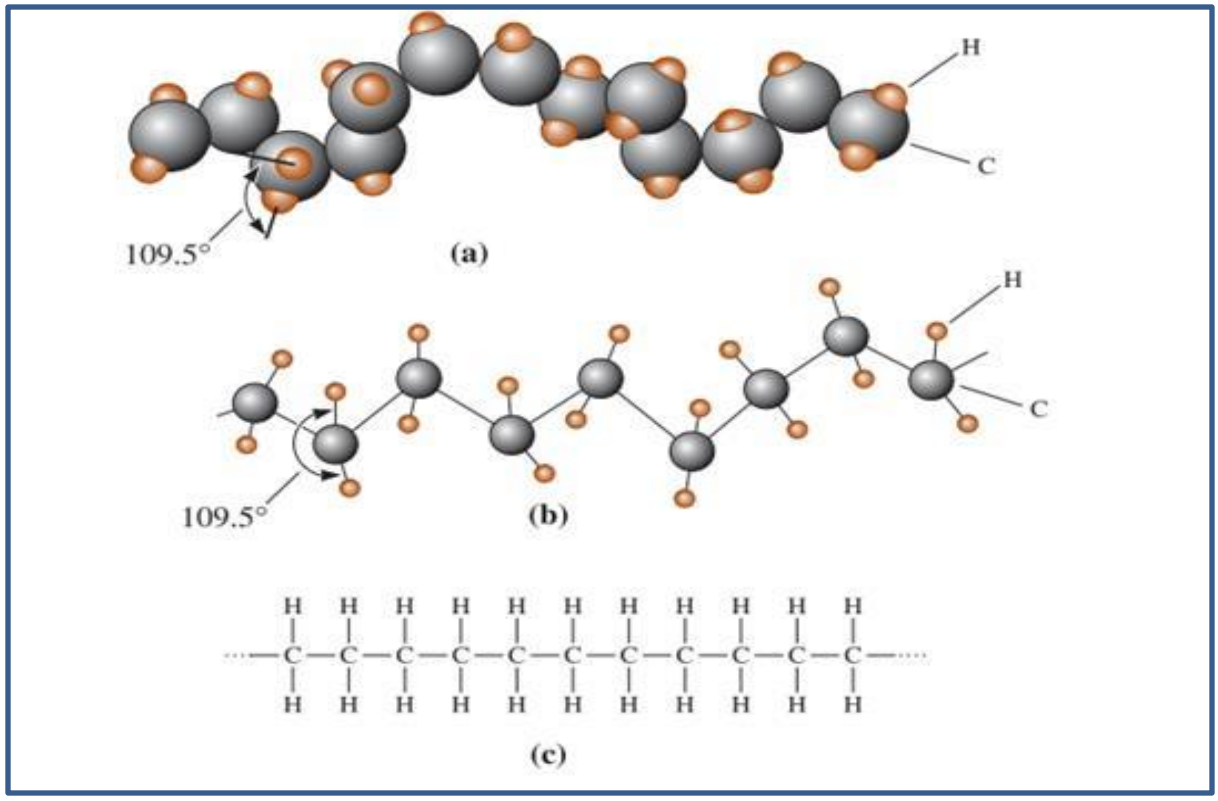

Figure 2.9: Structure of polyethylene: (a) a solid three-dimensional model, (b) a three-dimensional ‘‘space’’ model, and (c) a simple two-dimensional model [52].

LDPE resins are re-emerging as a valuable product family Figure (2.9) shows the repeated chemical structural unit of PE in three forms. combining superior clarity with stiffness and density favored by converters for downgauging. Ease of processing, combined with improved product performance, continues to give cost-competitive solutions to converters in a wide variety of film applications. These range from complex food packaging structures to shopping bags, coated paperboards, liners, overwraps, consumer bags, heavy-duty sacks, clarity shrink and collation films, lamination films, agricultural films, extrusion coatings, caps and closures, and a variety of durable products such as power cables and toys. In packaging applications, UV-stabilised LDPE is used in agricultural/building components and sheeting film[52]

LDPE is more flexible than HDPE and can be prepared by the high-pressure polymerization of ethylene. Its comparatively low density arises from the presence of a small amount of short and long branches in the chain. It is translucent to opaque, robust enough to be virtually unbreakable, and at the same time quite flexible [52].

2.9.3 Alumina

Ceramic materials are the principle reinforcing material for polymer matrix composites and it is crucial to choose an appropriate filler to obtain desired mechanical, thermal, or electrical properties. Alumina whose crystal lattice is shown in figure (2.10) is one of the most studied as a reinforcement material is used in both metal and polymer matrix composites. Synthesis of alumina enables a great number of possibilities to obtain crystal structures that can further determine the mechanical properties of the composite. Alumina (Al_2O_3) or aluminum oxide is an oxide found in nature in many minerals such as corundum (Al_2O_3); diaspora ($Al_2O_3 \bullet H_2O$); gibbsite ($Al_2O_3 \bullet 3H_2O$); and most commonly as bauxite. Alumina has also numerous crystalline structures, such as χ-, η-, δ-, κ-, θ-, γ-, ρ- Al_2O_3 besides the thermodynamically stable α- Al_2O_3 (corundum). Metastable phases, usually called “transition alumina” phases may be irretrievably translated to α - Al_2O_3 by appropriate thermal or hydroxylation treatments [53,54].

The Al_2O_3 is an electrical insulator but it has high thermal conductivity (30 w/mk) for a ceramic material. That Aluminum oxide is unsolvable in water. The crystalline aluminum oxide structure is also named corundum, which is thermodynamically stable in the method, Alumina has a melting temperature of about 2040^0C and an average density (3.75 – 3.95 g/cm^3). The oxygen ions mostly procedure a hexagonal close-packed structure with aluminum [55].

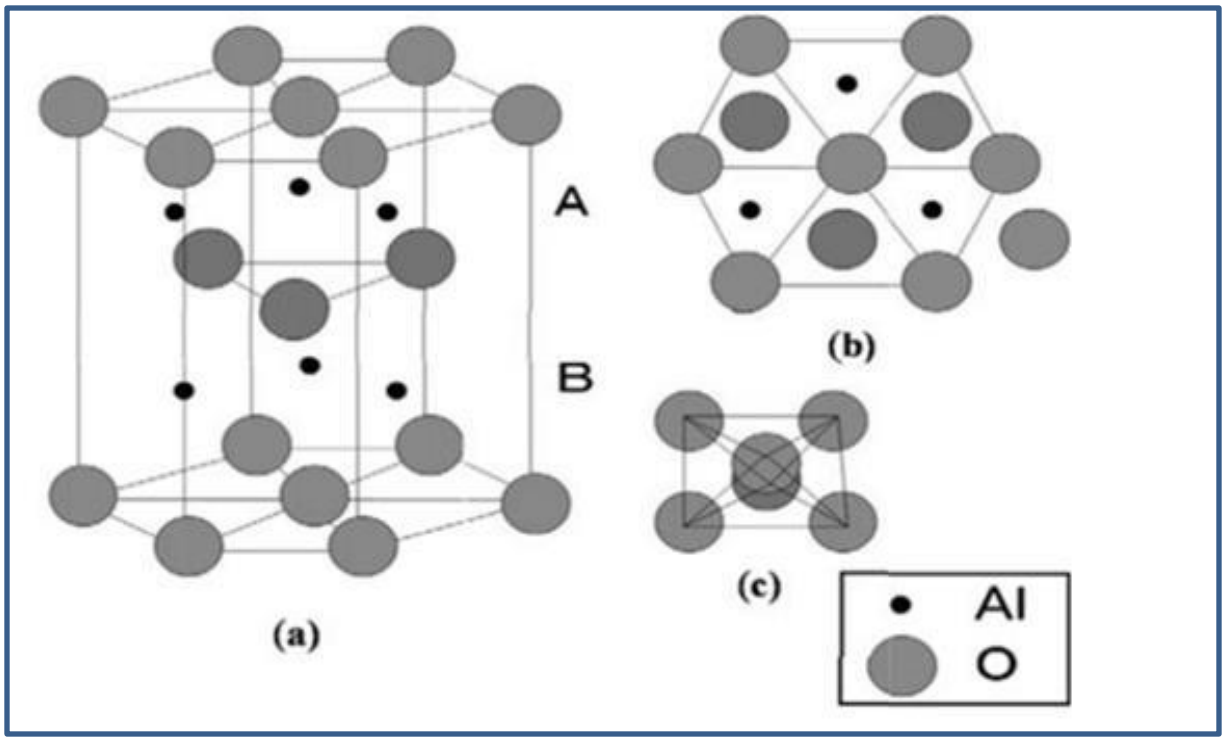

Figure 2.10: Structure of Aluminum Oxide (Al_2O_3) [55].

2.9.3.1 Crystal Structure of α- Al_2O_3

Calcined (fired) alumina for ceramics and refractory materials production, which represents a final product of thermal decomposition of aluminum hydroxides, is One of the most important types of alumina widely used in different applications. The baking process is conducted in drum and tunnel furnaces in a fluidized layer. There is a wide range of technical grades of calcined Al_2O_3 – from pure grade to grades containing large amounts of sodium (so-called -alumina Na2O(11 Al_2O_3). Unlike transition Al_2O_3, the particles of calcined Al_2O_3 are nonporous, so that the specific surface of the material matches the external surface of the particles [56,57].

Technical grade calcined Al_2O_3 is classified based on the particle size, crystallite morphology (angular, rounded, flat), sodium content, and to a lesser extent, other impurities. Depending on the sodium impurity content, the calcined Al_2O_3 has the

following grades: standard grade, containing 0.3 to 0.7 wt.% of Na_2O; intermediate grade, containing 0.1 to 0.3 wt.% of Na_2O; low-sodium grade (0.03 to 0.10 wt.% of Na_2O), and high-purity grade with extremely low sodium content (<0.01 wt.% of Na_2O; such Al_2O_3grade is obtained from aluminum hydroxide using other than the Bayer process technologies). Calcined Al_2O_3 is mostly used as a raw material [58,59].

2.9.4 Calcium Carbonate

Calcium carbonate in which whose crystal lattice is shown in Fig(2.11), is the most abundant mineral in nature, Calcium carbonate has great scientific relevance in biomineralization and geosciences, forming enormous scales of biological (reefs and ocean sediments) and geological origin, which bind a huge amount of CO_2 and affect the chemistry of ocean water[60,61]Worldwide availability of $CaCO_3$ (as limestone), compatibility and nontoxicity Towards the human body makes the composition of this substance a topic attractive and interesting for several of scholars and researchers to delve into it[62]. Precipitated calcium carbonates (PCC) are derived from carbonate rocks. Carbonates are made of particles (composed [50% carbonate minerals) embedded in cement or clast. Most carbonate rocks result from the accumulation of bioclasts created by Calcareous organisms. Carbonate rocks usually are formed in areas favoring biological activity, i.e., in shallow and warm seas, in areas with little to no siliciclastic input [63]. Calcium carbonate has a very low solubility. Calcium carbonate is one of the most widespread vital minerals shells and scales form a variety of deep sea[64] calcium carbonate is usually used as mineral fillers three common forms of calcium carbonate are calcite, Aragonite, and Vaterite , as shown Table(2.3). They frequently coexist, both in natural minerals and both In synthetic preparations. Due to its different crystal structures [65].

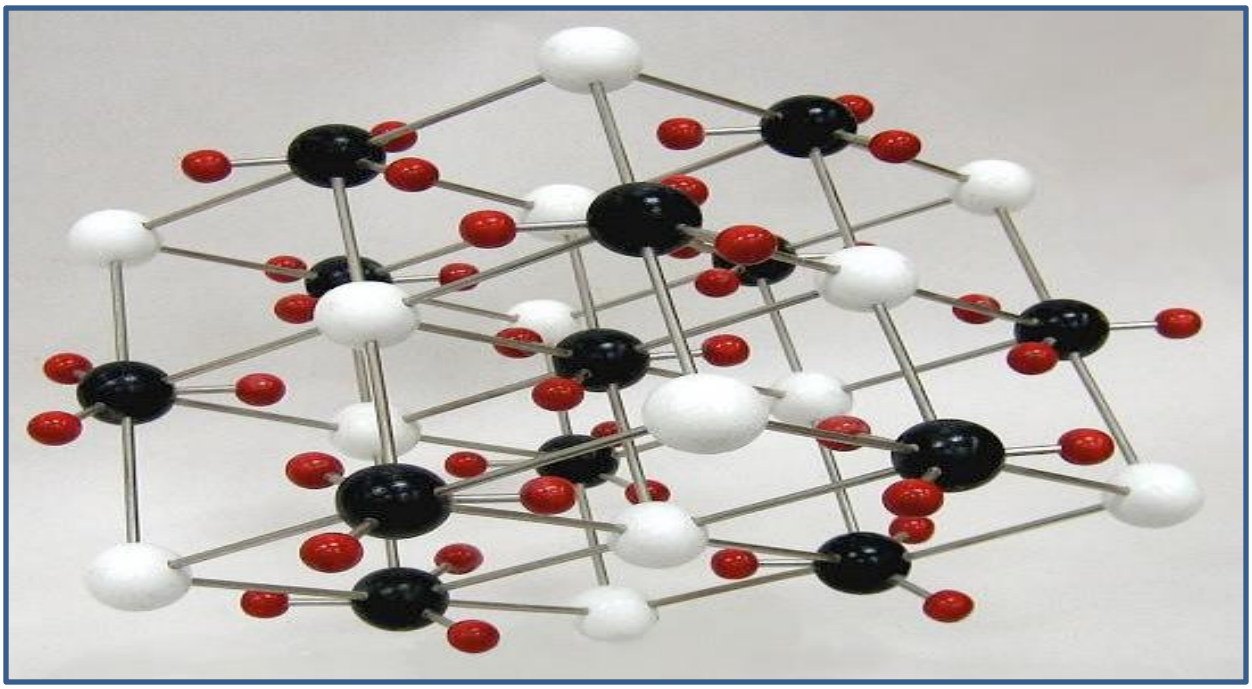

Figure 2.11: Structure of $CaCO_3$ [66].

Table 2.3: Type of $CaCO_3$ [66].

Characteristic	Calcite	Aragonite	Vaterite
Crystal system	Trigonal	Rhomboid	Hexagonal
Crystallographic forms	Hexagonal forms Rhombohedron Scalenohedron	Hexagonal prisms	Hexagonal prisms
Double refraction index	0.172	0.156	0.172
Character of double refraction	Optically negative	Biaxially negative	optically negative
Specific density [g/cm3]	2.72	2.94	2.72
Hardness	3	3.5-4	3
Melting temperature(^{0}C)	842	845	842

2.9.4.1 Calcite

Calcite crystallizes in the rhombohedral system, where the elementary cell of the crystal lattice is a rhombohedral prism. This prism can be regarded as a cube that is pressed together or pulled apart in the direction of a diagonal. All the surfaces are rhombic and identical in width and length. Calcite is one of the most common minerals in the Earth's crust. With its several hundred shapes, it is at all events the one with the largest number of shapes. The individual surfaces of the crystals [66].

2.10 Composite Manufacture Methods

2.10.1 Extrusion

Extrusion is a process for making continuous plastic objects such as tubes, pipes, rods, cables, wires, and a variety of profiles which include filaments, films, and sheets. The process is best described by the very word “extrusion,” which is derived from the Latin words exmeaning and true meaning ‘‘to push.” The polymer powder or pellet is melted or softened in a heated barrel and conveyed forward, plasticated, homogenized, and pressurized by a rotating screw under high shear into a metal die having a shape that is similar to the shape of the desired article. The main operating variables are the frequency of screw rotation and the barrel temperature profile which is controlled by thermocouples placed inside the metal barrel wall[67].

Sections of the barrel are at times cooled to remove excessive heat generated by viscous dissipation. The die continuously shapes the melt into the desired form

and the product is formed which is infinite in one direction. The molten profile produced is cooled either by air-water quench or by running it over chill rolls[67].

I. Single-Screw Extruder

Single-screw extruders operate normally in a flood-fed mode in which the granulate or powder polymeric material is compacted in the solids conveying zone see figure (2.12). These extruders act and operate as a dry friction pump. Therefore, the pressure rises exponentially with the length along the axis. During the material residence time in the solids conveying zone, the boundaries of the material are compressed by hydrostatic pressure. Individual particles of polymeric material are pressed against one another, thus forming agglomerates. There is an increase in the critical shear stress that is needed to break them up during their subsequent residence time in the melting zone and the pumping zone of the extruder[68].

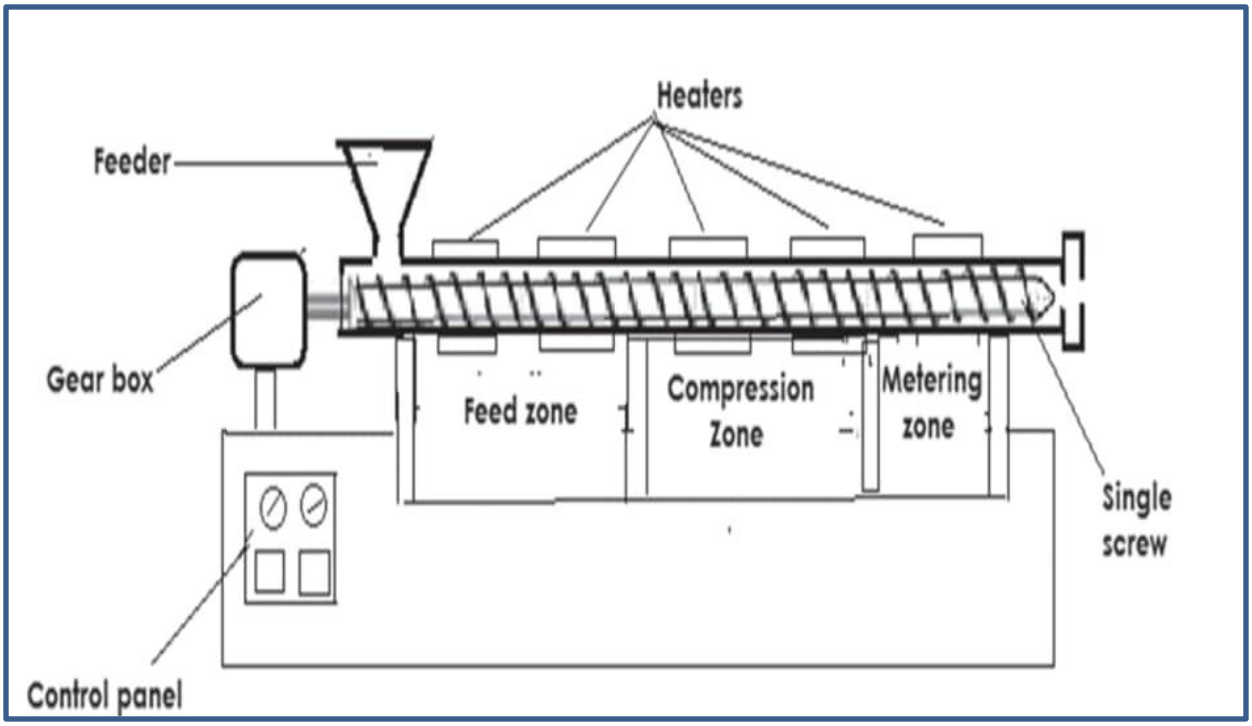

Figure 2.12: Schematic representation of single-screw extruder [68]

II.Twin-Screw Extruder

The twin-screw extruder has been extensively used in the polymer industry, particularly counter-rotating involves in various applications, including melting, pressurization, and mixing, which leads to different end products such as pipe, profile, sheet, and flat film. Twin-screw extruders are usually operated at a specific throughput; therefore, portions of the extruder are filled as in figure(2.13), whereas other locations are partially filled. Filled regions are formed behind restrictive and reverse pumping elements in extrusion screws opposite twin screws dissolve agglomerates better than a single screw [68].

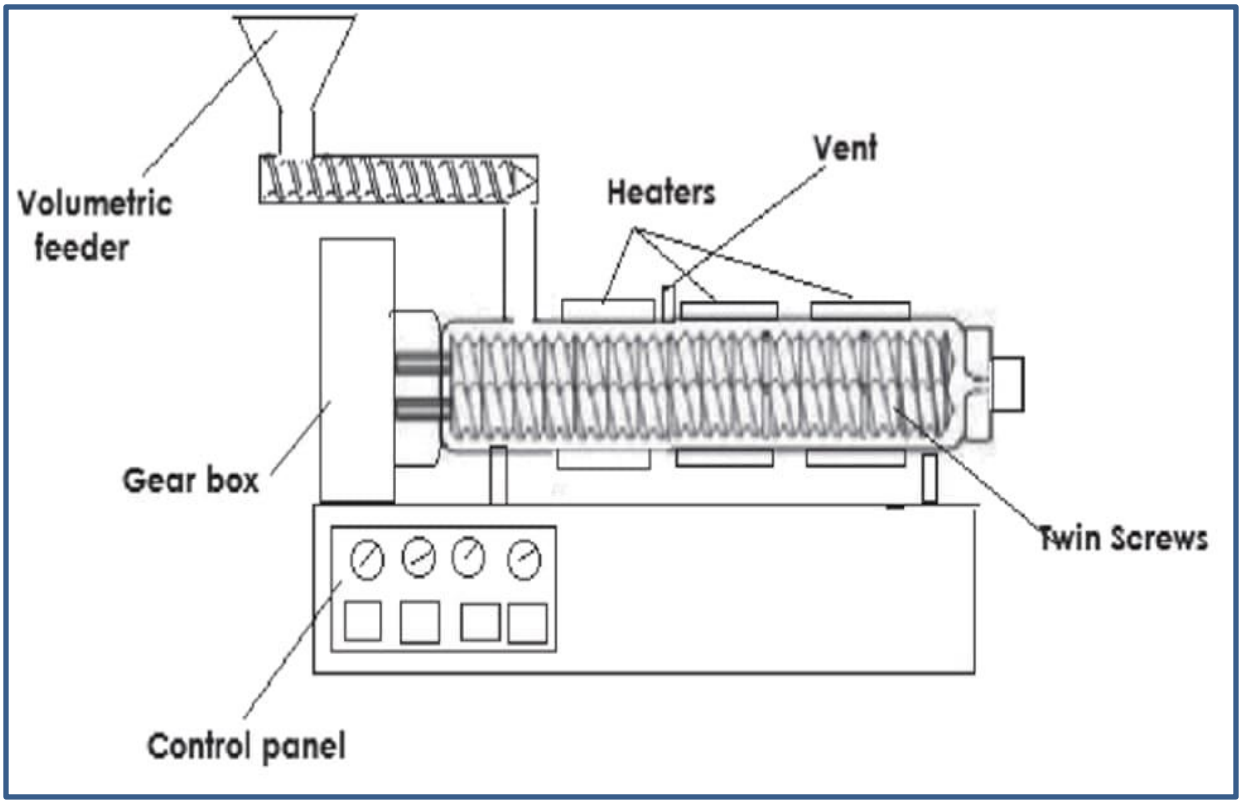

Figure 2.13: Schematic representation of twin-screw extruder [68].

2.11 Rheology of Polymer

Rheology is the study of the flow and deformation of matters. It crops up in all aspects of modern life. From squeezing toothpaste tubes, kneaded dough for bread making, or applying glue for joining purposes, all involve rheology in one way or another. The subject of rheology is extremely important for polymer research that is an important link in the correlation chain from the catalyst over polymerization and chain structure to processing behavior and final properties[69,70].

In all cases, flow is involved in the processing and fabrication of such materials to transform them into useful products. The flow occurs when polymer molecules slide past each other and the ease of flow depends on the mobility of the molecular chains and the forces or entanglements holding the molecules together[70].

On the other hand, rheological behavior also influences the mechanical properties of the finished product significantly. For example, molecular orientation had a dramatic effect on the properties of molded products, films, and fibers. The type and degree of orientation are largely determined by the rheological behavior of the polymer and the nature of the flow in the fabrication process. Such studies can lead to many benefits of which the following are probably the most important[70]:

1. To understand processing faults and defects which are of rheological origin and hence to make logical suggestions for adjusting the processing conditions for either minimizing or completely removing the fault.

2. To make a prior intelligent selection of the best polymer or polymer compound to use under a given set of circumstances.

3. They can lead to qualitative and to some extent quantitative, relationships between such factors as output, power consumption, machine dimensions, material properties, and operational variables such as temperatures and pressure. Since there is so much development in polymer types and grades, in addition to the fact that most of the processing occurs in the molten state, a better understanding of the rheological characteristic of polymer systems is beneficial to the design of polymer processing equipment, with the ability for predicting the energy requirement, optimizing the processing conditions and correlation with the structural development [70].

2.12 Characteristic Tests

2.12.1 Infrared Spectroscopy Test

Infrared (IR) spectroscopy is a popular way to describe polymers, FT-IR standard for (Fourier Transform Infrared), the preferred method of infrared spectroscopy. In infrared spectroscopy, it is passed IR radiation through a sample. Some of the infrared radiation is absorbed by the sample and some of it is passed through (transmitted) [71].

The resulting spectrum represents the molecular absorption and transmission and creates a molecular fingerprint of the sample. Since a fingerprint is a unique property of each material and no two molecular structures produce the same infrared spectrum which makes infrared spectroscopy useful for many types of analysis.FT-IR can identify unknown materials, the amount of components in a mixture, and the quality or consistency of a sample [72].

The basic components of an FTIR spectrometer are shown schematically as in Figure(2.14). The radiation emerging from the source is passed through an interferometer to the sample before reaching a detector. Upon amplification of the

signal, in which high-frequency contributions have been eliminated by a filter, the data are converted to digital form by an analog-to-digital converter and transferred to the computer for Fourier-transformation [73].

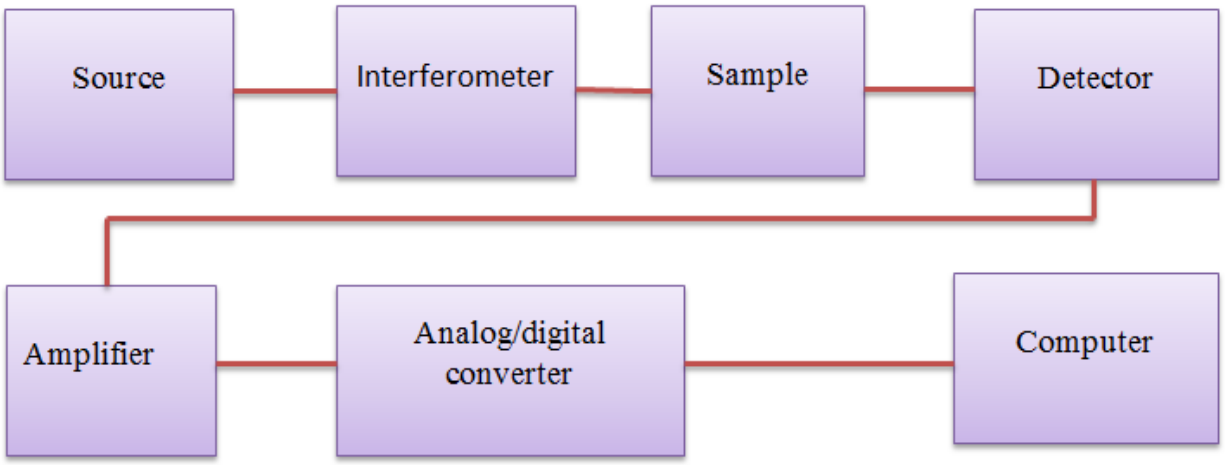

Figure 2.14: Basic components of an FTIR spectrometer [74].

2.12.2 Melt Flow Index or MFI Test Property

The melt flow index (MFI) is defined as the weight of the polymer (in grams) extruded in 10 min through a capillary of specific diameter and length by pressure applied through dead weight under prescribed temperature conditions. The basic principle employed in the MFI test by any of the standards is that of determining the rate of flow of molten polymer through a closely defined extrusion plastometer [75] .

Melt flow rate is commonly used in polyolefins, polyethylene is measured at 190°C and polypropylene at 230°C. The plastics engineer must select a material with a melting index high enough so that the molten polymer can easily be formed in the intended material, but low enough that the mechanical strength of the final material is sufficient for its use [76].

2.12.3 Density Test Property

The method can be used with a sheet, rod, tube, and molded articles, that is the specimen is weighed in the air then weighed when immersed in distilled water at 23°C using a sinker. Density and specific gravity are calculated through the density test device, according to the equations that are fed to the examination device, so that the results appear immediately on a digital screen.

2.12.4 Tensile Test

The tensile test is one of the most important mechanical tests through which many important engineering information can be obtained that determine the mechanical behavior of materials during use, including [77]:

A. Yield stress.

B. Ultimate tensile strength.

C. Modulus of elasticity.

When a particular load is applied to a test sample so that it conforms to its longitudinal axis, it will undergo a certain elongation depending on the amount of force applied. So that gets a geometric curve called the stress-strain curve. The stress can be expressed in terms of the following relationship [77]:

$$\sigma = \frac{F}{A} \qquad (2.9)$$

Where:

σ: the stress and it's unit (MPa).

F: the force applied on the sample to cause elongation along the axis of the sample and it's unit is (N).

A: is a cross-sectional area of the sample and it's unit (m^2).

While strain denoted by ϵ and is expressed in the following relationship [77]:

$$\epsilon = \frac{\Delta L}{\text{Lo}} = \frac{(\text{L}-\text{Lo})}{\text{Lo}} \qquad (2.10)$$

Where:-

L: the elongation (final length of the sample).

Lo: initial length of the sample (primary).

ΔL: the amount of change in length.

Strain is divided into two types (elastic strain and plastic strain), and the ratio between the stress applied on the material and the resulting strain in the elastic zone of the stress-strain curve. It is a constant ratio called modulus of elasticity or young's modulus, which has the symbol (E). It is measured in units of (N/m^2) and is expressed in the following relationship [77]:

$$E = \frac{\sigma}{\epsilon} = \frac{P}{A} / \frac{\Delta L}{\text{Lo}} = \frac{P\text{Lo}}{\Delta L A} \qquad (2.11)$$

2.12.5 Impact Test

When a material is subjected to a sudden load (dynamic load) i.e. high strain rate, it will follow behavior different from its behavior when subjected to static load. The material may follow ductile behavior when exposed to static load (tensile and bending test). But when you expose it to dynamic load(impact test), it will follow brittle behavior. Impact resistance can be obtained from the following relationship [78].

$$I.S = \frac{Uc}{A} \qquad (2.12)$$

Where:-

I.S: impact resistance of the material (J/m^2).

Uc: impact energy (J).

A: cross-sectional area of the sample (m^2).

2.12.6 Creep Test

Creep is the progressive deformation of material at constant stress and temperature. It is used to describe the slow plastic deformation that occurs under prolonged loading, usually at high temperatures. Creep in its simplest form is the progressive accumulation of plastic strain in a specimen or machine part under stress at elevated temperatures over some time [79].

Deformation or strain is measured and plotted as a function of elapsed time up to rupture. Most tests are the constant load type, which yields information about the engineering nature; constant stress tests are employed to provide a better understanding of the mechanisms of creep. Creep often takes place in three stages. In the initial stage, strain occurs at a relatively rapid rate but the rate gradually decreases until it becomes approximately constant during the second stage. This constant creep rate is called the minimum creep rate or steady-state creep rate since it is the slowest creep rate during the test. The slope of the steady-state portion of the creep curve is the creep rate which is calculated from the equation below [80].

$$Creep\ rate\ = \frac{\Delta\epsilon}{\Delta t} \qquad (2.14)$$

$\Delta\epsilon$:is strain change (mm/mm)

Δt:is time change (min)

In the third stage, the strain rate increases, creep necking begins. The stress increases and the specimen deforms at an accelerated rate until failure occurs. The time required for failure to occur is the rupture time [81].

2.12.7 Scanning Electron Microscope (SEM)

The scanning electron microscope (SEM) is one of the most versatile instruments available for the examination and analysis of the microstructure morphology and chemical composition characterizations and is considered a type of electron microscope that produce images of a sample by scanning it with a focused beam of electrons. The electrons interact with atoms in the sample, producing different signals that can be detected and containing information about the sample's surface topography and composition. Samples must be less than 2 cm in diameter. Non-conducting samples are usually coated with a thin layer of carbon or gold in order to prevent electrostatic charging [82].

A major reason for the SEM's usefulness is the high resolution which can be obtained when bulk objects are examined; instrumental resolution on the order of 1-5 nm (10-50A) is now routinely quoted for commercial instruments. Specimens can be observed in high vacuum, low vacuum and in environmental SEM specimens can be observed in wet conditions. The basic components of the SEM are the lens system, the electron gun, the electron collector, the visual and photorecording cathode ray tubes (CRTs), and the associated electronics [83].

2.13 Literature Review

In 2010, Rabeh H. Elleithy et al,[84] studied twin screw extruder for polyethylene (HDPE) high-density pelletizing with micro calcium carbonate ($CaCO_3$) and several ASTM samples were produced by an injection molding machine. The composite morphology was investigated through scanning electron microscopy (SEM) and image analytical software. SEM was used for evaluating the dispersion and interactions of $CaCO_3$ and the polymer matrix. $CaCO_3$ has no major impact on the melting behavior of the composites. (TGA)that thermogravimetric analysis showed superior thermal stability to the virgin HDPE resin. The viscoelastic characteristics of compounds and HDPE were investigated using torsional and rotational techniques. The presence of $CaCO_3$ enhanced the composite shear module at 80 C over the neat, low-frequency resin. The compound's complicated viscosity increased with the addition of CaCO3. On the other hand, the neat resin and the micro compound were equally sensitive to shear stress.

In 2011, Y. Lu et al,[85] Investigate The creep behavior of polypropylene reinforced by calcium carbonate (PP/CaCO3) under various vibration situations. When studying the effect of frequency as well as vibration pressure, used tensile and creep tests were. noticed that at (.72) Herzan, the tensile fracture stress had reached (11 percent), which is its maximum. He also concluded that with increasing vibration amplitude, fracture tensile stress values decrease. Reaching the frequency values to (.72) Note that the (pp/CaCO3) compounds that were prepared at (.48) Hertz have higher tensile creep than other frequencies samples. With

increasing pressure level, the tensile creep of compounds decreases(pp /CaCO3) prepared at (.48)

In 2012 H Salmah et al,[86] Investigated the melting flow of low density polyethylene reinforced with palm kernel shells (pks). The palm kernel material that was used as filler in this study was treated with acrylic acid (AA) to chemically modify it. they investigated the effect of the filler by adding acrylic acid and without acid on the behavior of melt flowforLDPE Reinforced by pks , the melt flow of composite decreased with the increase of the filler loading. It was observed that the viscosity affected the reciprocal temperature and they were in a linear relationship. The filler increased the thermal stability of the composite. The bond between the matrix and the filler containing the modified acid was observed. For these compounds, the rate of activation energy of the compoundLDPE inclusion of the acid AA increased the activation energy of the compound LDPE reinforced with PKS when a similar filler was introduced.

In 2013, Martin M. Riara et al, [87] study Polyethylene compounds with various cellulose loading ratios create by pressure molding and then underwent tests creep at (30 , 40 , 50 and 60 ^{0}C). Temperature, time, and cellulose content influence Polymer composite creep behaviour. Creep performance deteriorated with a rise in temperature and improved with cellulose content, but with a rise in time and temperature, declined the creep modulus . Timing overlay has been used to predict the creeping behavior of the samples over long periods of time (up to 106 s).Use the William Land Ferry model to predict the long-term behavior of the material, use the free volume for the action of deformation.

In 2013, Fangwei Qi et al,[88] Investigated the change that might happen by adding calcium carbonate particles as a filler in terms of size and diffusion in

LLDPE (Low Density Polyethylene). Note that the long polymer chains have restricted their movement by particles of the filler material ($CaCO_3$). Also, the entry of these particles between the polymer chains has increased The amount of transformation temperature and melting temperature. Through the results obtained, The compounds showed a decrease in viscosity when the shear stress was increased. In addition, improved elongation at fracture significantly to some extent at the acceptable dispersion and reasonable size for the filler.

In 2016, Randa K. Hussain et al,[89] studied The creep test was conducted to find out the behavior of pure polypropylene and polypropylene reinforced with different percentages of calcium carbonate in an ocean of different temperatures. The soaking method was adopted in mixing polypropylene samples with calcium carbonate, and when compared to the original solution after it was soaked, the results of (FTIR) changed clearly For THE (FTIR) virgin polypropylene. obtained results that the creep resistance improved. Also, The Creep behavior of the polymer formed was observed to increase with the increase in temperature and stress, Calcium carbonate enhanced creep rate and rapture time. This novel method provides the capability to treat the material with any engineering shape and even post-polymerization.

In 2016, M. Tazi et al,[90] studied the evaluation of numerical analysis of the viscoelastic, mechanical and thermophysical properties of a compound consisting of high-density polyethylene (HDPE) reinforced with softwood particles, whereby compounds composed of different proportions of wood particles need a better understanding of the behaviors of materials according to the temperature and contents of the wood particles. The results indicate that the rheological and thermal properties of the compounds differ according to the wood filling content and temperature. Composites' behavior became more elastic than

viscous while wood particles' percentage increases. This allowed us to predict the thermophysical behavior of composite at temperatures and wood fillers where it is difficult to measure experimentally.

in 2018, Maher Al-Ibrahim et al,[91] investigated The effect of adding carbon black and calcium carbonate as fillers on the properties of high-density polyethylene, especially the fluidity of the material in order to determine the change of the fluidity of the high-density polyethylene while increasing the percentage of these materials. The carbon black was added in increasing percentages from 2.5% to 15% and the fluidity decreased from 23.5 g/10min to 15.5 g/10min. The calcium carbonate was added in increasing percentages from 5% to 20% and the fluidity decreased from 23 g/10min to 12 g/10min.

In 2019, Xiaolong Hao et al,[92] investigated the mechanical properties and creep values that are expected to be affected by the content of filled wood in the casing, the basic fill layers, and the dimensional stability of the model for high-density polyethylene extruded with wood particles. Test (SEM) revealed the existence of an association between the two basic layers and the shell, Impact resistance and flexing stress are greater than the basic control elements despite their lower values, creep stress was greatly reduced when hardwood flour (WF) was introduced into the shell and substrate, model (Co-WPCs) with 70٪ WF In the base layer and 20٪ WFin the shell had a change in creep values of an amount equal to those of the basic control only, but the impact resistance and bending stress were clearly better.

In 2019, Harun Sepet et al,[93]investigated of the influence interfacial area and the particle size of $CaCO_3$ filler particles on the mechanical and thermal properties of high-density polyethylene (HDPE) was studied in this work. The

HDPE-based microcomposites were manufactured by using an industrial compounder system. The tensile, impact, creep, flexural and hardness properties of the filled and unfilled HDPE samples were investigated. The experiment revealed that the addition of microparticles increased the tensile and flexural modulus of unfilled HDPE. However, it was observed that the addition of these particles did not have a significant effect on the tensile and flexural strength of unfilled HDPE. On the other hand, the presence of these particles decreased the elongation of the break of unfilled HDPE. The impact strength of filled HDPE composites decreased slightly with micro-and particle contents. microparticles were found to be more effective at low-stress levels (8 and 12 MPa) unfilled HDPE. It was found that the particle size has a profound effect on the thermal and physical properties of unfilled HDPE, such as density, melt flow index. The results showed that the size of filler particles has a significant effect on the mechanical and thermal properties of the unfilled HDPE. Therefore, the size selection of constituent materials of micro composites is an important consideration because it directly affects the functional performance of particle-filled HDPE micro composites.

In 2020, Kenechi Nwosu-Obieogu, et al,[94] investigated The creep and stress relaxation behavior of rice husk reinforced low density polyethylene composite. The exponential and power model was used to study the creep while the stress relaxation assessed the time required for the composites to maintain a certain strain level. The creep strain increased with increase in time, at various temperatures, with its highest creep at 70^0C while the lowest is at 30^0C, the power model provided an excellent fit than other models with a coefficient of determination of 0.9977 at 30^0C, the neat low density polyethylene had a good stress relaxation behavior with 4.95 seconds for it to decay and subsequently decreased with increase in filler concentration.

Chapter Three

Experimental Part

3.1 Introduction

This chapter focuses on the practical side of the topic, which includes the raw materials used in preparing samples of composite materials and their general characteristics in addition to the methods used in preparing these samples and all mechanical and physical tests, which are (Ftir ,melt flow rate, density, tensile, impact , creep ,and SEM test).

3.2 material

The materials used in the preparation of the samples consist of a polymer matrix material (low-density polyethylene) and a reinforcing material consisting of two types of fillers (alumina, calcium carbonate,) and they were used separately for each type.

3.2.1 Matrix material

LDPE was obtained as pellets from Company of Amir Kabir Petrochemical ,in Iran. Some characteristic of LDPE are shown table (3.1) according to produced compony.

Table 3.1: Properties of LDPE[95].

Properties	**Units**	**Values**
Density	g/cm^3	0.923
Hardness	Shore D	41-46
strength Tensile	MPa	8
Melting point	°C	110

3.2.2 Reinforced Materials

Tow types of powders were used in this work as reinforcing materials with the matrix (LDPE). The following is a summary of the materials used:

I. Alumina Filler

The reinforcing material is The alumina (Al_2O_3) powder provided by the Thomas Baker Mumbai company, India, the average diameter of about (14 µm) as Measured by FESEM. Was used as filler to obtain the new modified composite material (LDPE/ Al_2O_3), table (3.2) shows properties of alumina powder according to produced company:

Table 3.2: Properties of Alumina Powder[96].

The Properties	**Units**	**Values**
The Density	g/cm^3	4
Melting point	°C	2000
Solubility in water[%w]		Insoluble in water

II. Calcium Carbonate Filler

The reinforcing material is the carbonate calcium ($CaCO_3$) powder provided by the company Thomas Baker Mumbai, India, with an average diameter of about (6 µm) as Measured by FESEM. Was used as a filler to obtain the new modified composite material (LDPE/$CaCO_3$), Table (3.3) shows the properties of carbonate calcium powder according to produced company.

Table 3.3: Properties of Carbonate Calcium Powder[96].

Properties	Unit	Value
Density	g/cm^3	2.81
Melting point	°C	825
Solubility in water[%w]		weakly soluble in water

3-3 Preparation of Composite polymer

3.3.1 Weighing and Preparation

1. The low-density polyethylene(LDPE) material is mixed through different weight ratios (90, 80, 70, and 60%) of weight fraction of the composite polymer, with the reinforcing material, which is (alumina or calcium carbonate) through different weight ratios as well (10, 20, 30 and 40%) of weight fraction of the composite polymer in respectively as shown in Table(3.4), and to obtain Composite materials (LDPE/AL_2O_3) and (LDPE/$CaCO_3$) in respectively.

2. Sensitive balance with an accuracy of 0.0001g type (TE 214S)-Sartorius, was used to weigh the mixture of composite polymer (LDPE/AL_2O_3),(LDPE/$CaCO_3$)

Table 3.4: Polymeric Composite Percentages.

Samples notation		Concentrations (%)	
LDPE/AL_2O_3	LDPE/$CaCO_3$	LDPE	AL_2O_3 or $CaCO_3$
P100A0	P100C0	100	0
P90A10	P90C10	90	10
P80A20	P80C20	80	20
P70A30	P70C30	70	30
P60A40	P60C40	60	40

3.3.2 premixing:

The mixing process was used the first is dry mixing mechanical the (ball mill) by using Electrical, rolling mixer type (STGQM-1/5-2) as shown in figure (3.1), to mix granules of the (LDPE) with the powder of reinforcing material(AL_2O_3 or $CaCO_3$), to obtain Composite materials (LDPE/AL_2O_3) and (LDPE/$CaCO_3$). The time used for the mixing process was an average of one hour for each sample and at a rotational speed of 40 revolutions per minute.

Figure 3.1: Mechanical dry mixer (ball mill).

3.3.3 Mixing and Extrusion

Extrusion operation was achieved by a twin extruder (SLJ-30A) located in the College of Materials Engineering - University of Babylon Figure (3.2). The dry mixtures are entered into the cylindrical chamber of the extruder, which heats the polymeric material through heaters spread along the cavity at a rate of (145-150°C) The screw inside the extruder is set at a rate of (40 rpm) revolutions per minute. The screw works to mix the resin and break up agglomerates. The material is pressed at the end of the screw through a narrow neck and then goes through a rolling process after leaving the extruder to form into sheets.

Figure 3.2: The twin-screw extruder

3.3.4 Rolling

When the resin comes out of the extruder, it goes through a rolling process through steel rollers that rotate in an opposite way that presses on the material, causing it to expand, reducing the spaces, and giving a product in the form of regular sheets as figure (3.3).

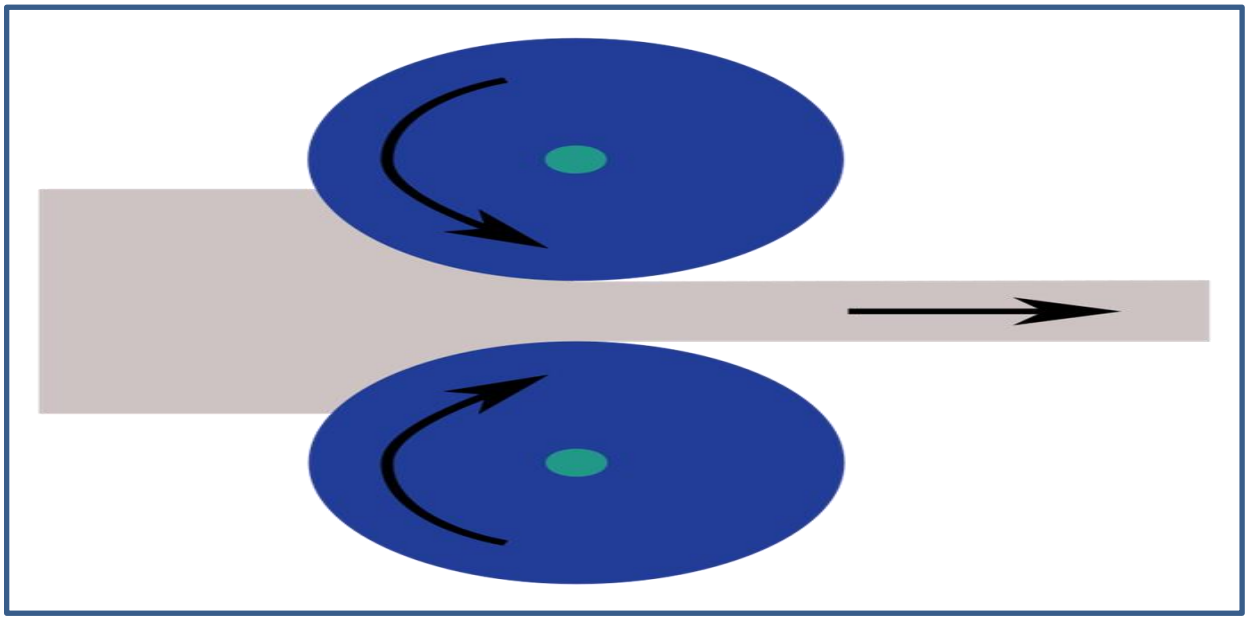

Figure 3.3: Rolling process.

3.3.5 Samples Cutting

The samples are carefully cut to avoid the occurrence of operating defects. The cutting is carried out according to the American society for testing and materials (ASTM) as shown in Table(3.5). about the impact and creep test, an electric saw with very soft teeth was used, while the tensile test is carried out using a special standard mold.

Table 3.5: Standard Dimensions of the Test Sample[97,98,99]

No.	Property	Sample	ASTM
1	Creep	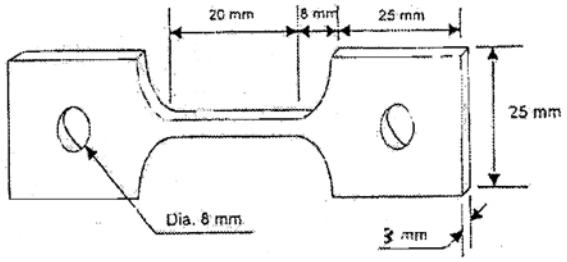	D2990
2	Tensile	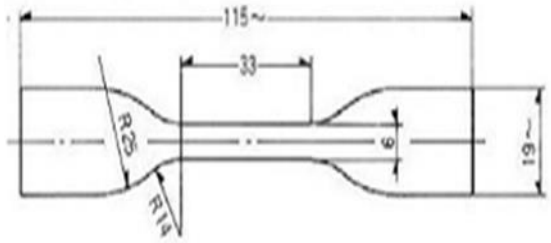	D638IV
3	Impacte	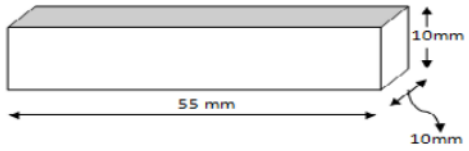	D-6110

3.4 Testes

3.4.1 Fourier Transforms Infrared Spectroscopy Analysis (FTIR)

Samples are characterized using the Fourier transform infrared spectra methodology. This was accomplished using an IR Affinity-1 (manufactured in Japan), figure (3.4) which is an available instrument from the Materials Engineering college laboratory/University of Babylon's. In Fourier transform infrared (FTIR) spectroscopy, IR radiations are passed through a sample, where some of the infrared radiations are absorbed by the sample. When the radiant

energy matches the energy of specific molecular vibration, absorption occurs. In the IR spectrum, the wavenumber is plotted on the x-axis and is proportional to the energy. The band Intensity can be expressed as absorbance (A) or percentage transmittance (%T) as plotted on the y-axis (zero transmittance corresponds to 100% absorption of light at that wave number). Absorbance (A) is logarithms, to the base 10, of the reciprocal to the transmittance (T).

$$A = \log_{10} (1/T) \qquad (3\text{-}1)$$

The absorbance of transmittance with the corresponding wavenumber as a peak in spectra gives information about the molecule to the analyst, by matching it with a spectrum of a known compound, peak by peak correlation. The spectrum represents a fingerprint of a sample, a unique characteristic, as no two different molecular structures can produce the same spectra. This makes infrared spectroscopy useful for several types of analysis as each different material is a unique combination of atoms. Therefore, infrared spectroscopy results are used in molecular identification (qualitative analysis) of every different kind of material, and the size of a peak in the spectrum is a direct indication of the amount of material present (i.e., purity) in the sample to Analyzing the sample, a calibration of the device is carried out and a powder KBr is used, the sample is converted into a fine powder and mixed with a powder KBr in a ratio of 99 %from KBr.To ensure the radiation transmittance, the disc used to put the mixture is semi-transparent.

Figure 3.4: FTIR analysis device

3.4.2 Melt flow index (MFI)Test

Figure (3.5) Demonstrates melt flow index device type (shi jia zhuanc zhong shi testing machine co., ltd). The use of the MFI machine of the international standard (ISO 1133:2005) to measure the MFI of the molten polymer by adding ratios of 0 wt%,10 wt%, 20 wt% 30 wt% and 40 wt% of AL_2O_3, $CaCO_3$ Respectively particles to the virgin LDPE under different temperatures and constant load. The procedure for determining MFI is as follows:-

1- Preparation of 6 g from material which consists of an LDPE pure and LDPE composites

2-Determination of the parameters includes temperature, load, cutting time, and cutting interval as(185°C, 195 °C),(2.16 Kg), (10 sec), and (3)respectively.

3- Waiting for the temperature to rise until it reaches the required test temperature, then adding the compounds consisting of (LDPE / Al_2O_3), (LDPE / $CaCO_3$) to the barrel and putting the load on it.

4-As a result the extruded molten from capillary die to down, MFI determined within the region on the piston of the device represented by two lines where molten polymer reaches the first line automatically cutting three pieces.

5- Finally, we entered the average weight value into the device to determine the MFI value of the sample using the following equation.:

MFR = t ref * w /t (3.2)

Which:-

t ref=10 min /600 s.

t=time.

W=average weight of cutting time of the sample.

6- repeated steps for all ratios of composites at varied temperatures and constant load (185 °C, and 195 °C) and 2.16 kg. The capillary diameter is 2.0955, The die length to capillary diameter ratio is 8/2.095.

The equation below was used to compute the shear rate at the wall of molten exits from capillary dies at varied ratios and temperatures with constant load.:

$\gamma = (1840/\rho) * MFR$ (3.3)

γ: the shear rate at the wall (S^{-1}).

ρ:density of polyethylene g/cm^3.

MFR: melt flow rate 10/min.

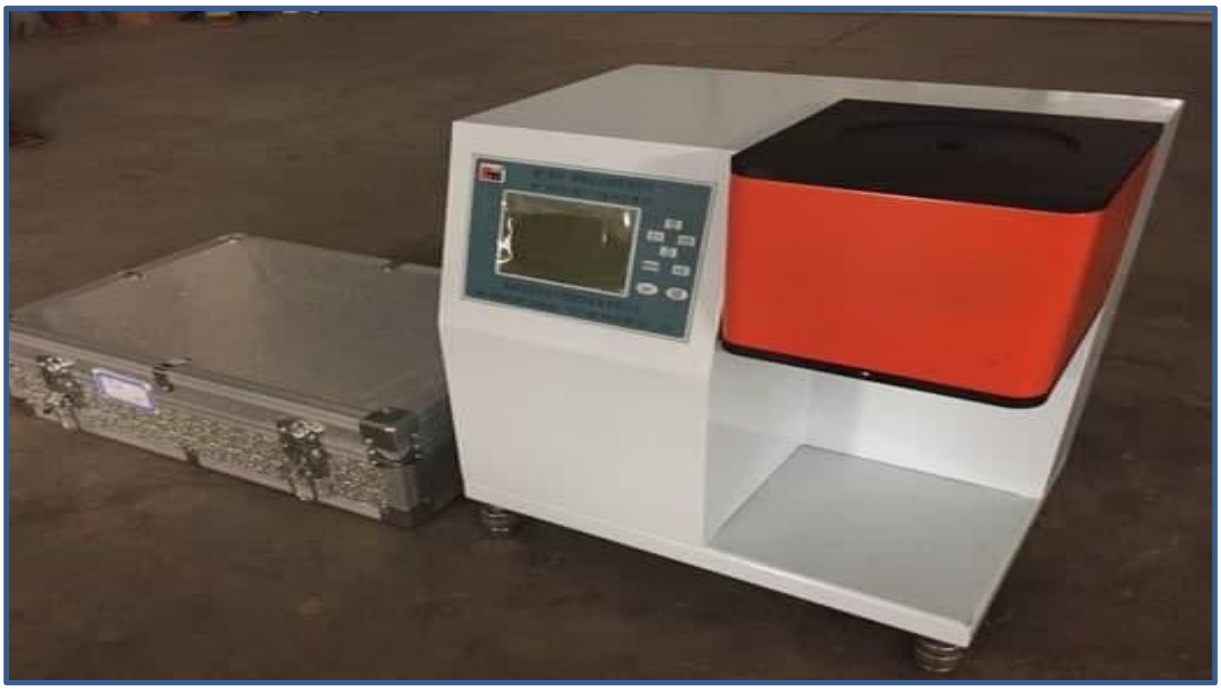

Figure 3.5: Melt Flow Rate Testing Machine.

3.4.3 The Density

Figure (3.6) shows a High Precision Density Testing Machine (GP-120S), this device has a digital accuracy (0.0001 g/cm^3). The series (matsu haku) is the one who provided this equipment. This test was done according to ASTM D -792.

In this test, samples from any previously performed test have been measured their density, this method can be used with the sheet, rod, tube, and molded articles the specimen is weighed in the air then weighed when immersed in distilled water at 23°C using a sinker and wire to keep the specimen completely submerged as required. It utilized polymer material where distilled water was used for testing.

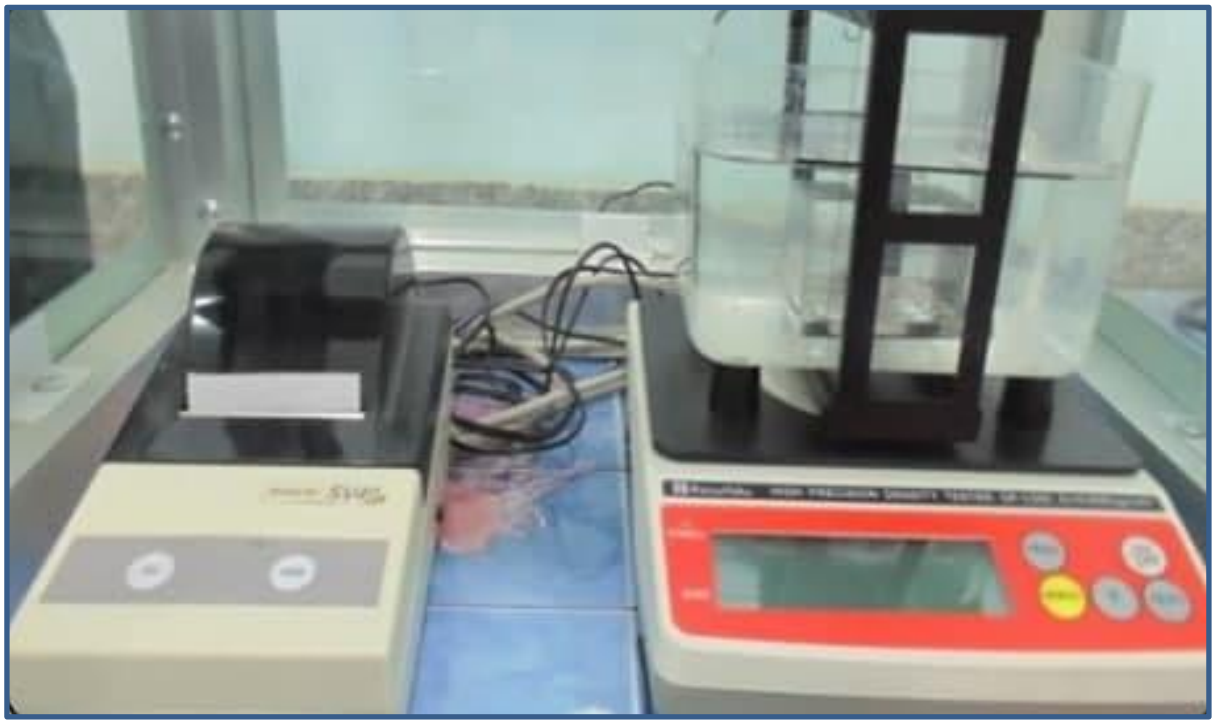

Figure 3.6: Density test machine.

3.4.4 Tensile Test

specimens were cut according to ASTM (D638-03), Microcomputer Controlled Universal Electronic Testing Machine Model is the used for Tensile Traits Testing (WDW-5E), Supplied from the People's Republic of China, Made in China, Found in Laboratory of College of the Materials Engineering / University of Babylon shown in Figure (3-7). The test was performed at room temperature with a load of 5 kN and a speed of 10 mm/min for all samples. The axial force is applied to the sample until the sample detaches, the computer attached to the machine records a stress-strain relationship.

Figure 3.7: Tensile test machine.

3.4.5 Impact Test

Figure (3.8) shows the WP 400 pendulum impact testing machine. Charpy tester (DIN EN 10045 / DIN), type (pendelschlagwerk (gunt hamburg), according to ASTM D-6110 made in Germany.

Is highly preferred in practice as quality control or for evaluating susceptibility to brittle fractures since the test is simple to set up and easy to run.

It consists of a standard test piece that will be broken with one blow of a swinging hammer, the hummer provides an impact of(15N.M- 25N.M) can be reached by adding weight disks. The test piece is supported at both its ends in a way that the hammer strikes it at the middle. The testing method of this instrument includes lifting the pendulum to its maximum height and fixing it firmly. The specimen is fixed in its pertaining place, and then the energy gauge is initialized

(on zero position) after that, the pendulum is freed where its potential energy would be changed to kinetic energy. Some of this kinetic energy is utilized to fracture the specimen, while the energy gauge reads the value of fracture energy (Uc) for the sample under test. Impact strength (I.S.) is calculated by applying the equation (2.12).

Figure 3.8: The machine of Impact test.

3.4.6 Creep test

The WP 600 Kriechtester creep test machine was used to perform basic experiments demonstrating the behavior of polymeric materials under constant load and providing a clear idea of the suitability of polymeric materials for a particular application. Figure (3.9) shows the creep test equipment found in the laboratories of the College of Materials Engineering at the University of Babylon

to perform this test under constant load and different temperatures. The dimensions of the samples in this test are within Specification ASTM D 2990, and this test method was used to know creep behavior plastics reinforced and non-reinforced.

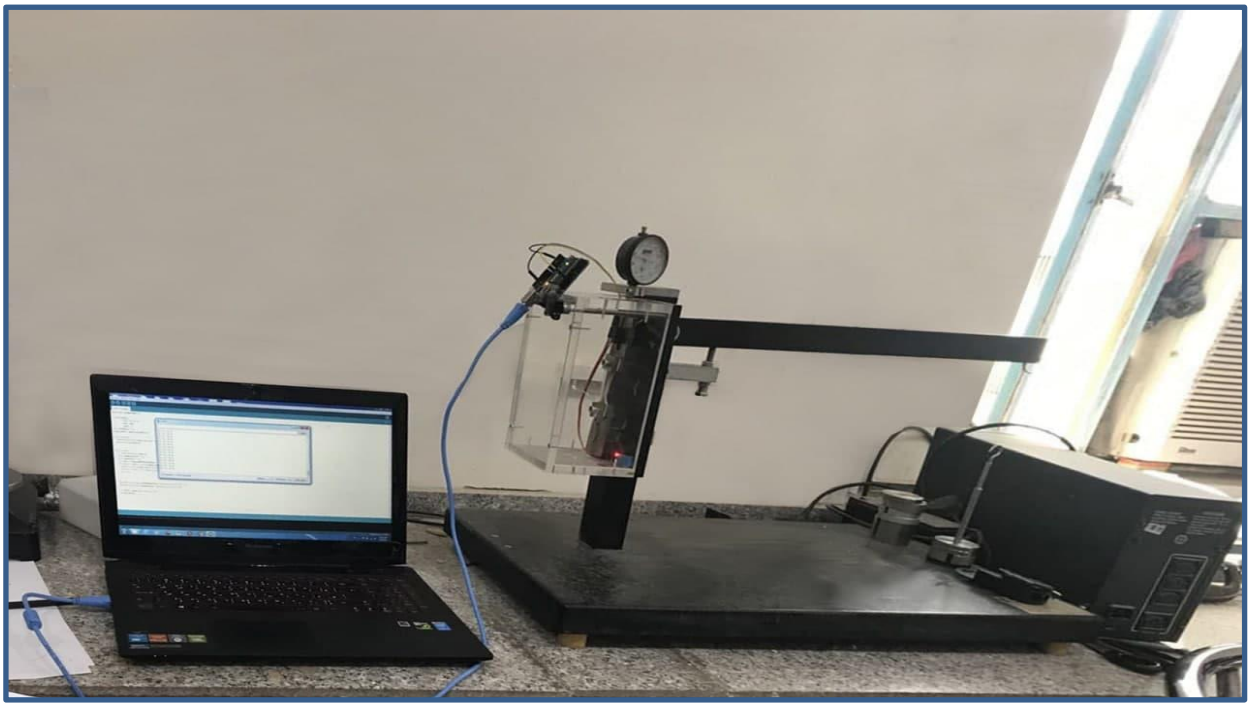

Figure 3.9: The machine of creep test

3.4.7 Scanning Electron Microscopy Test

Figure (3.10), Analytical Scanning Electron Microscope (SEM), (TESCAN MIRA3) model at Danish Bunyan Arya Iran/Tehran used to examine the morphology of composite polymers. The sample used in the testing was cut into small pieces (1x1 cm) to fit into the device. The magnification powers of all samples were (100x ,200x,500x,1000x).The principal electron signals that are used are backscattered electrons (BSEs) and secondary electrons (SEs). Differences in specimen composition and surface topography affect the generation, transport, and escape of these signals. Images formed in an SEM result from variations in electron signal intensity collected at each point (pixel) as the electron beam briefly

dwells within the scanned area. In addition to the strong interactions of electrons with the matter, their mass and charge make it easy to direct them to where we want them, using electromagnetic fields to act as lenses and mirrors, rather like glass lenses and deflectors are used in a light microscope For modern SEM, the maximum resolution is better than 1 nm. This is mainly limited by the physics of electron–specimen interactions.

Figure 3.10: Scanning Electron Microscopy device

Chapter Four

Results and Discussion

4.1 Introduction

In this chapter, we present a complete analysis of the results and calculations related to Mechanical properties including (tensile test, and impact test, creep test) And rheological behavior such as the MFI (or MFR) test. And Physical properties include density and Fourier transform spectroscopy (FTIR) and SEM Test. Where it includes a discussion of the effect of each of the reinforcing materials on the visco-elastic properties that represent creep, in addition to its effect on the physical and mechanical properties of the Composite Materials. Includes current work the samples is the consistent as follows:

1. Matrix polymer (LDPE) with different weight fractions (10wt%, 20% wt, 30% wt, and 40% wt) of alumina particles were prepared and tested.

2. Matrix, polymer (LDPE) with different weight fractions (10wt%, 20% wt, 30% wt, and 40% wt) of Calcium carbonate particles were prepared and tested.

All the tests are discussed with their results in this chapter, starting with the FTIR test for verification e of materials used in this work, and occurrence of any reaction between reinforcement filler and polymers matrix understudy and then touched to discuss the results.

4.2 FTIR Result

FTIR test was used for LDPE pure and LDPE Reinforced with 10wt% alumina powder and LDPE Reinforced with 10wt% calcium carbonate powder prepared by method extrusion to verify and occurrence of any reaction between reinforcement filler and polymers matrix for LDPE composite, The band values and the changing in intensity or shifting of peaks for composites recorded by FTIR are shown in table (4-1), which were derived from the figures (4.1),(4.2), and (4.3) respectively.

FTIR for LDPE virgin shows many bands at distinct peaks such as bands at 2916 and 2854 cm^{-1} for (C-H stretching), the band at 1465 cm^{-1} for(CH_2 scissoring), The band at 717 cm^{-1} for (CH_2 rocking)as in figure (4.1).

for LDPE Reinforced by10wt% alumina the bands at 2916 cm^{-1} shifted to 2924 cm^{-1} while the others band don't change, while LDPE Reinforced by 10wt% calcium carbonate the bands at 2916 $cm^{-1}$and 1465 cm^{-1} shifted to at 2924 $cm^{-1}$and 1442 cm^{-1} respectively a for the other bonds, they remain unchanged as in figures (4.2),(4.3) respectively.

These results indicate that there is no change or chemical bonding in the structure of the polymer because there is no new bond that appears or disappears. we also note that the permeability decreased after adding alumina particles or calcium carbonate particles, respectively, because these particles increased the absorption of the polymer due to its optical properties, and also in some areas that the permeability e decreased compared to the pure polymer which means that the polymer chain extends after adding AL_2O_3 and $CaCo_3$ particles where are these particles filled the holes between the polymer structure.

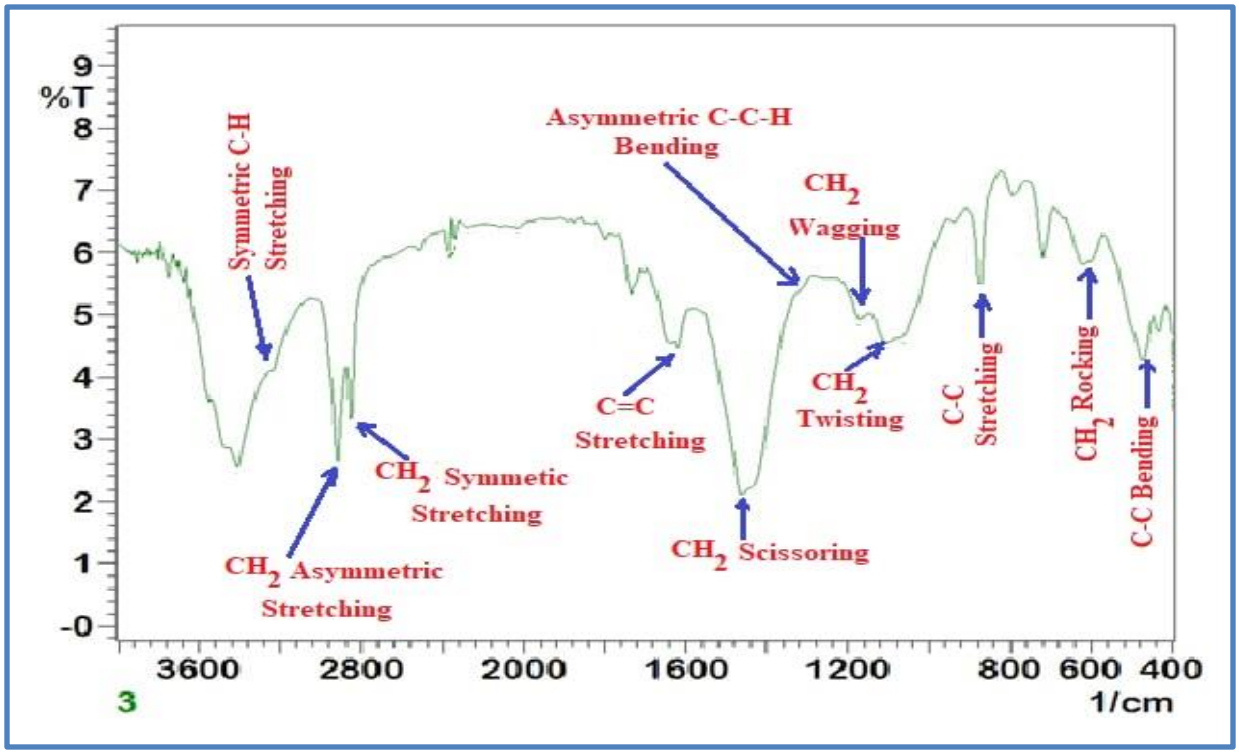

Figure 4.1: FTIR spectrum for pure LDPE.

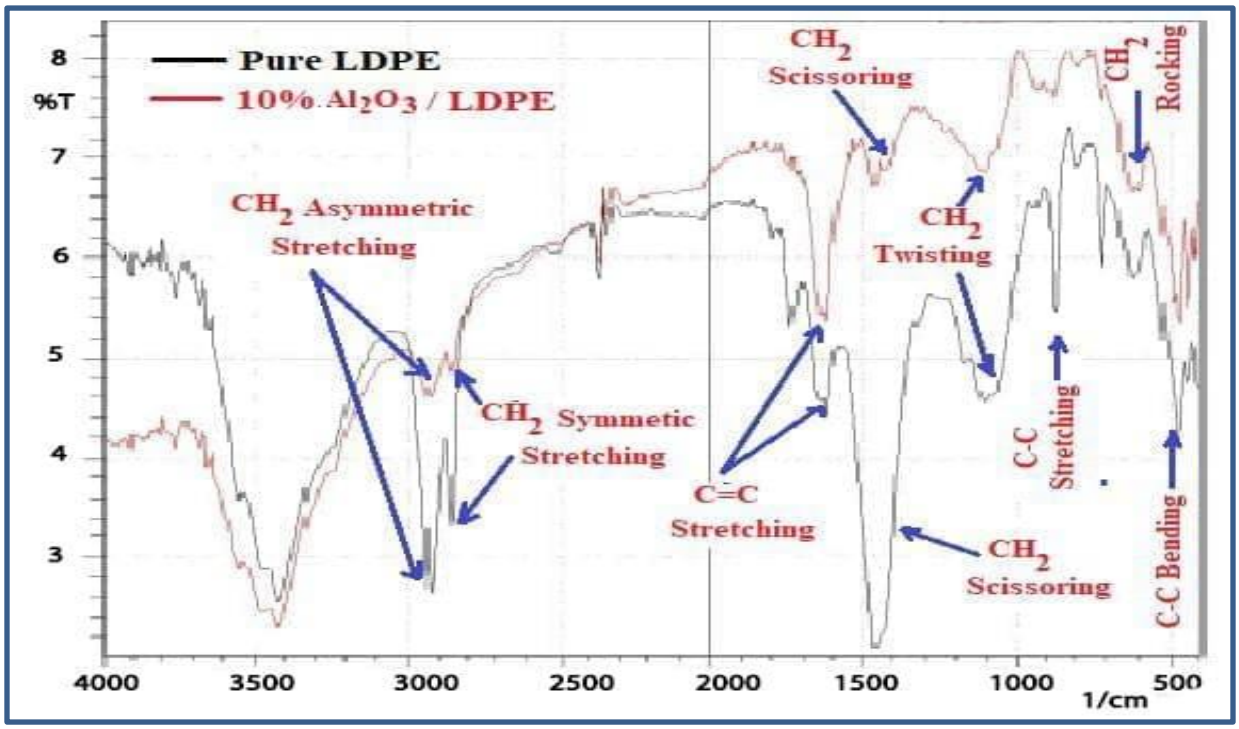

Figure 4.2: FTIR spectrum for LDPE reinforced by 10 wt % Al_2O_3.

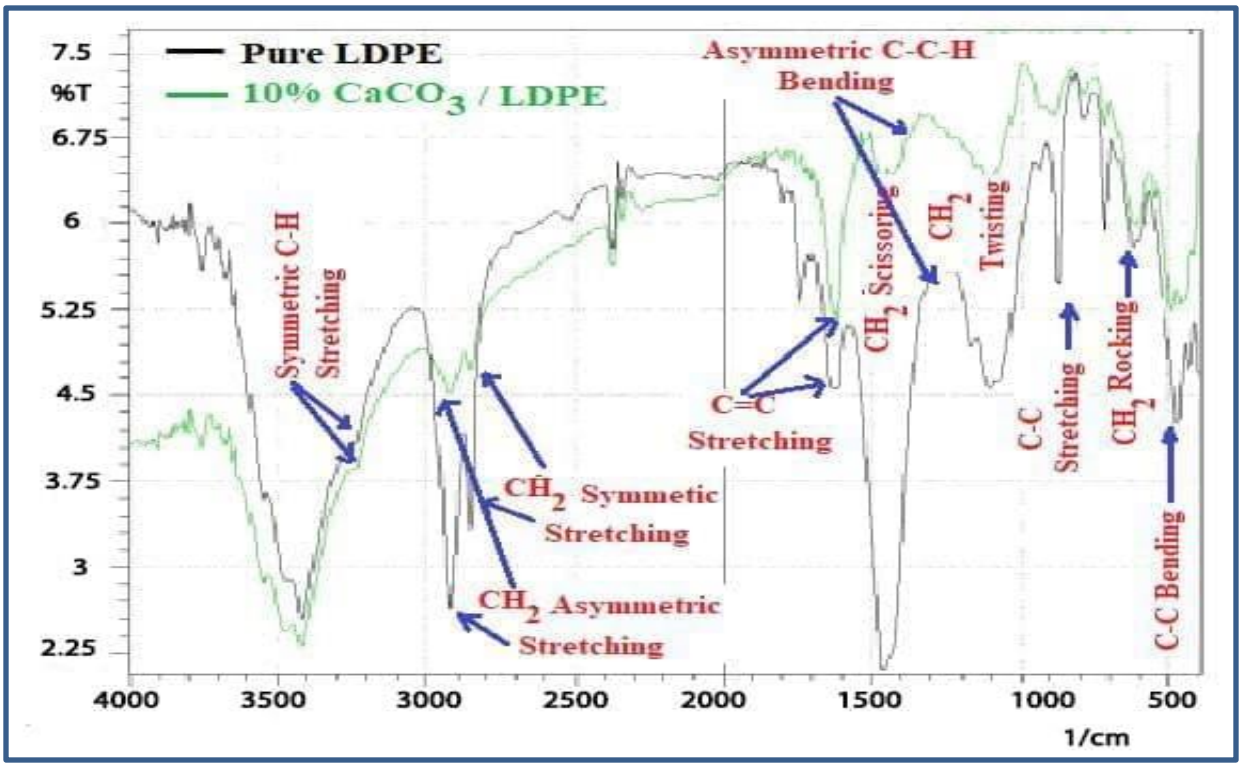

Figure 4.3: FTIR spectrum for LDPE reinforced by 10 wt % $CaCO_3$.

Table 4.1: The Absorption Bands of IR Spectrum Characteristic of LDPE and LDPE Composite.

Type of bond	LDPE standard[100]	LDPE exp.	LDPE/10% AL_2O_3	LDPE/10% $CaCO_3$
CH_2 stretching	2918 2849	2916 2854	2924 2854	2924 2854
CH_2 scissoring	1463	1465	1465	1442
CH_2 rocking	719	717	717	717

4.3 Melt flow Index Results

the figure (4.4) which is showing melt flow rate for pure LDPE and LDPE reinforced by Varying (10, 20, 30, 40) % weight fraction of AL_2O_3, melt flow rate value under the following conditions is temperature 185°C,195°C, and applied load is2.16 Kg, MFI test was implemented to indicate the relation between alumina wt % and its influences on the viscosity of the LDPE/ AL_2O_3 composite To assess the flow of the polymer. from this figure can be seen the MFR it is very clear that the MFR value is decreasing with increasing the AL_2O_3 content at 185°C and 195 °C due to increasing viscosity in the LDPE composite.

The viscosity is affected by several factors, which play an important role in the polymer flow rate. The physical reactions between the filler and the polymer, as well as the type of polymer, the type and size of the filler, its distribution within the polymer matrix, and the temperature, are all elements that determine the shape of the flow.

At 185 °C and 10% and 20% alumina, it is possible to observe a relatively small decrease in the flow rate compared to 30% and 40% alumina as it decreases further. The reason for this may be that the lower weight ratios of the filler tend to have relatively good dispersion and distribution and thus the filler resistance to polymer flow decreases. In comparison with the higher ratios, which decrease the dispersion process of the particles inside the LDPE matrix, which leads to the proximity of the particles to each other due to the increase in concentration and the occurrence of clusters and thus an increase in the filler resistance to the flow process.

At 195 °C, we notice that linear or marginal changes occurred at 10% alumina due to the effect of the test temperature, which contributed to the decrease

in the viscosity values compared to the same ratio at 185 °C, the change is almost linear in the rest of the ratios at 195 °C and with lower viscosity rates than their counterparts From the filler ratios at 185 ° C, the temperature affects the behavior of LDPE as it loosens the entanglement between the polymeric chains and thus reduces the friction, which causes a decrease in the viscosity.

The MFR is affected by the molecular weight and viscosity inversely, while the viscosity values increase with the increase in the filler concentrations and their values decrease with the increase in temperatures [101,102].

The most common quality control test on materials to be extruded is the melt flow index The high-flow polymer is made by injection molding, while the low-flow polymer is used in the extrusion and blow-molding process. Molecular weight, the availability of co-monomers, the level of chain branching, and crystalline size all influence flow behavior and heat transmission in the processing of polymer.

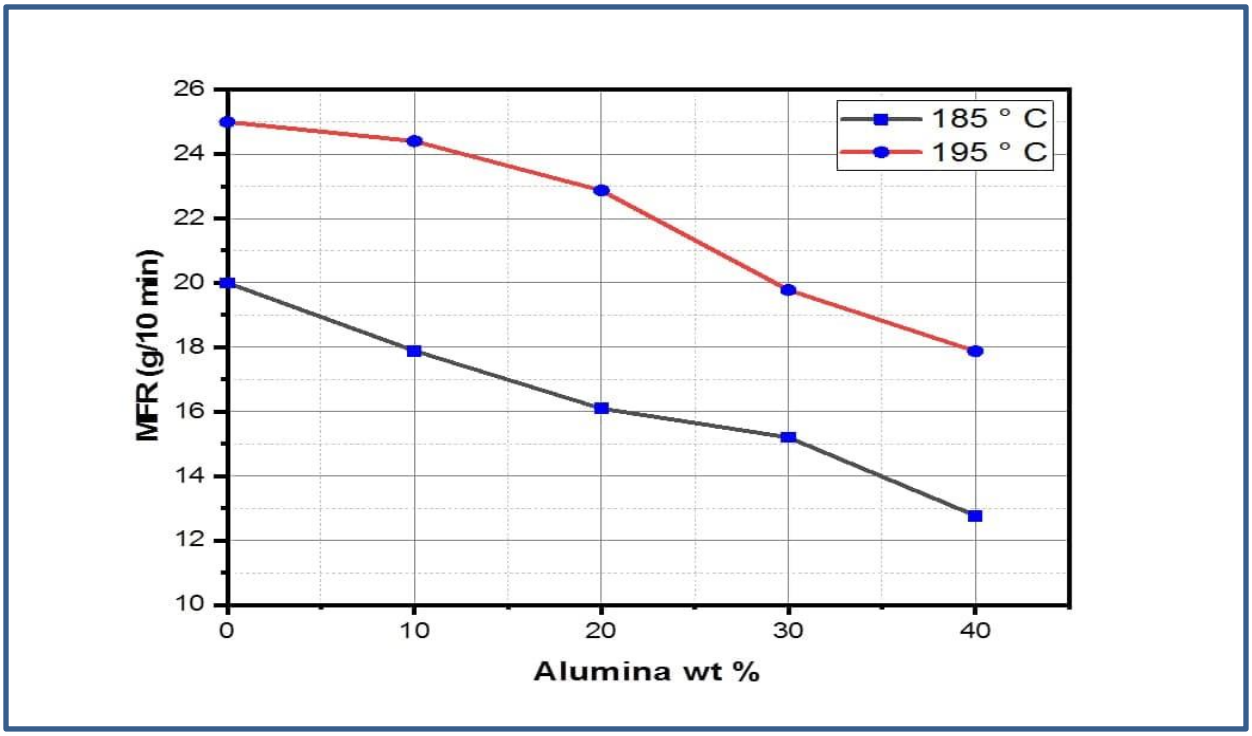

Figure 4.4: Melt flow rate versus the percentage of alumina filler.

Figure (4.5) is showing the melt flow rate for LDPE reinforced by 10%,20%,30%, and 40% weight fraction of $CaCO_3$, melt flow rate test was under the following conditions is the temperature at 185 °C and 195 °C, and applied load is2.16 Kg, MFI test was implemented to indicate the relation between the content of $CaCO_3$ and its influences on the viscosity of the LDPE/$CaCO_3$ composite to assess the flow of the polymer at the same conditions from temperatures and content of fillers. The explanation for the behavior of alumina applies in fig(4.4) with the behavior of calcium carbonate in reducing the flow rate of low-density polyethylene composites When the filler content increases and the flow rate increases with the High temperatures, but it differs from it in two points, we note at 20% $CaCO_3$ There is a decrease in the flow rate that was not within the normal behavior, which may be due to the presence of agglomeration during the manufacturing process . The other thing is that the flow values of calcium carbonate composite are higher than the flow values of alumina compounds at the same proportions which may be due to the high stiffness of the alumina particle and the difference is in particle size, as the larger filler size further impedes the flow [103].

The decrease in the liquidity of LDPE will affect its manufacturing parameters. Therefore, this decrease in the liquidity value must be taken into consideration when manufacturing plastics with added calcium carbonate or alumina; manufacturing temperature varies for the virgin polyethylene from the grade of manufacturing polyethylene mixed with additives. Therefore, the manufacturing temperature must be raised the higher the percentage of the additive[103].

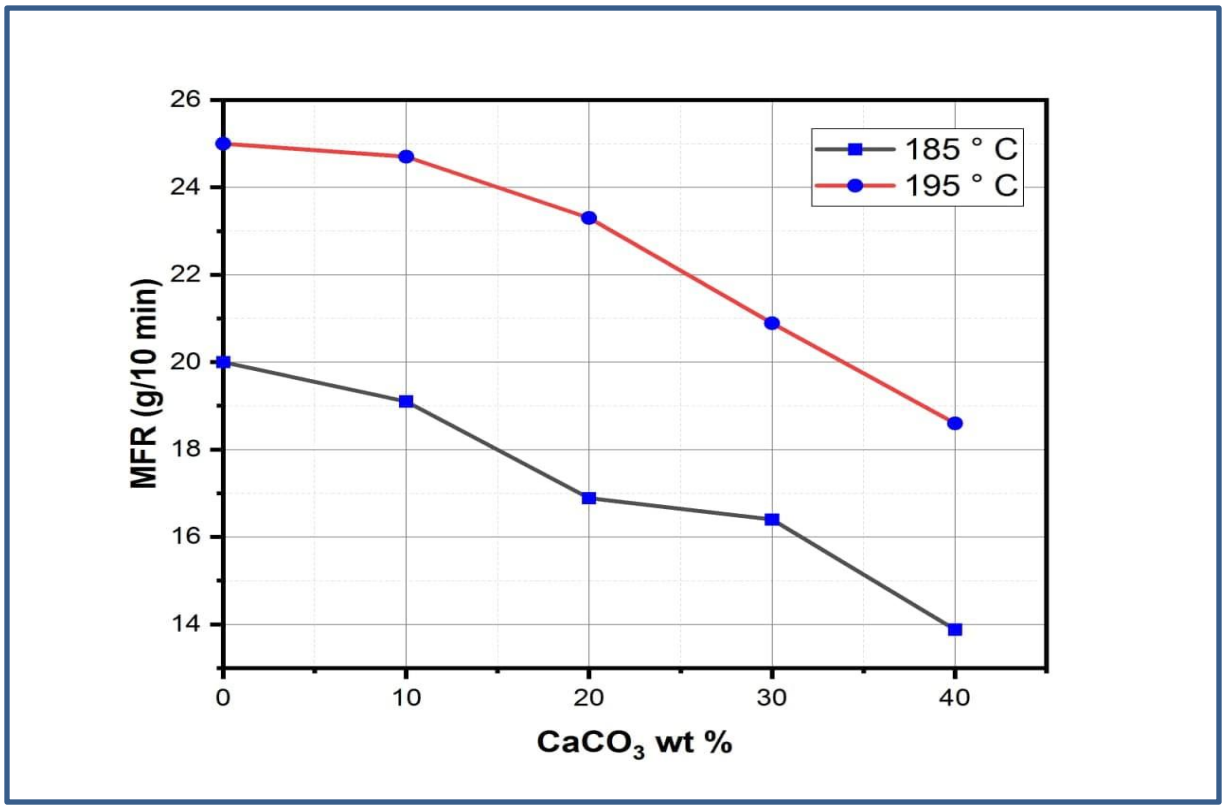

Figure 4.5: Melt flow rate versus the percentage of $CaCO_3$ filler.

The amount of shear on the wall is proportional to the melt flow rate, as we note that decreasing the melt flow rate leads to a decrease in the shear rate values and as shown in Figures (4.6) and (4.7). The critical shear stress value affects the quality of the final polymer product.

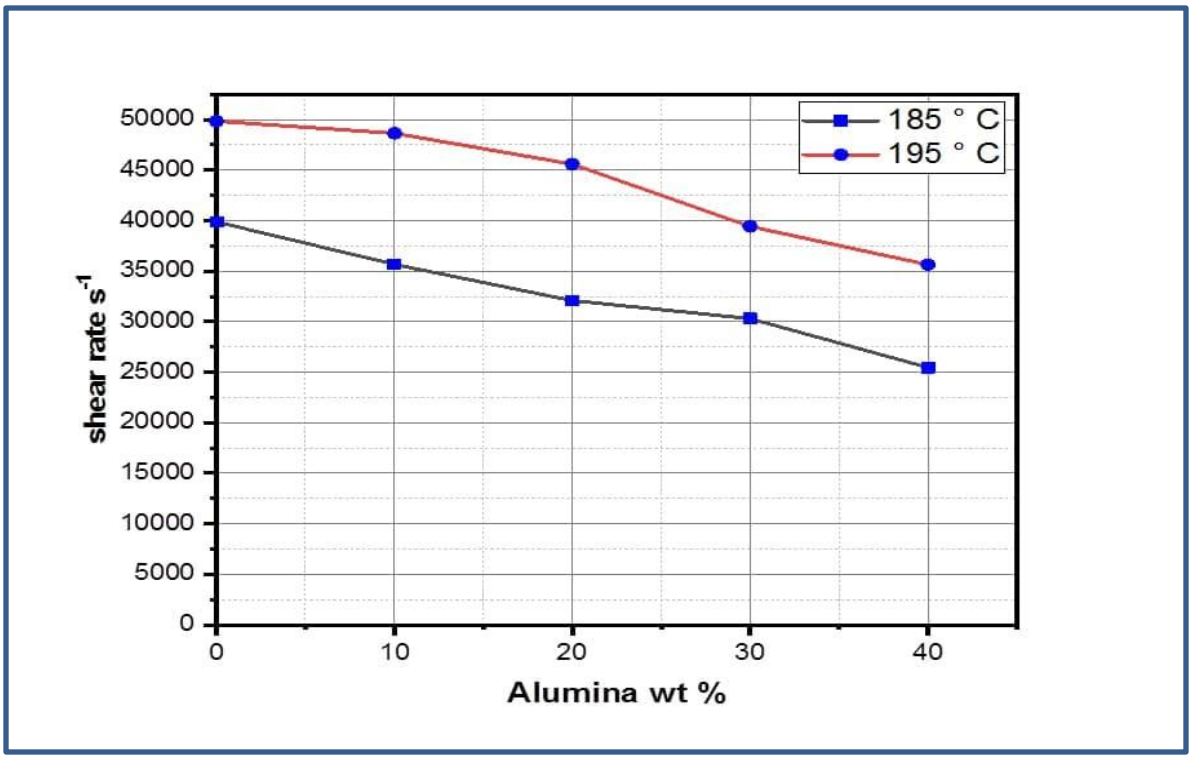

Figure 4.6: Shear rate versus the percentage of alumina filler.

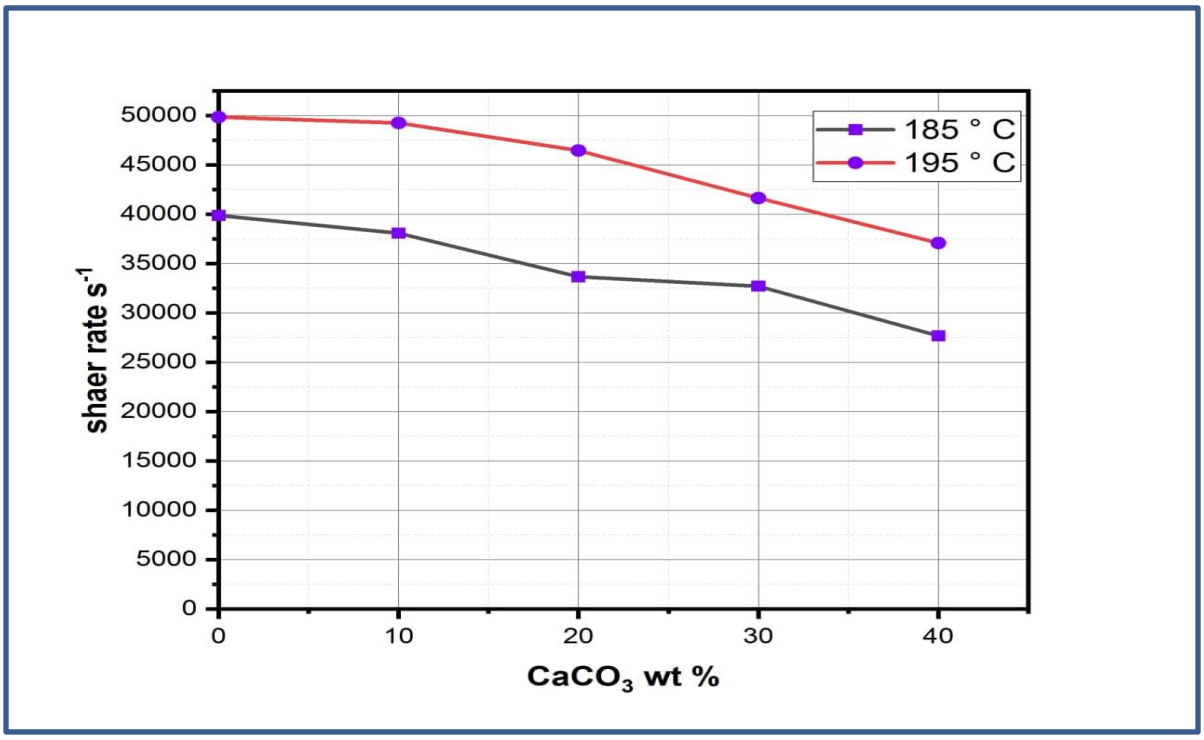

Figure 4.7: Shear rate versus the percentage of $CaCO_3$ filler.

4.4 Density Test

Figures (4.8) and (4.9), showed the density behavior of composites of (LDPE/Al_2O_3, and LDPE/$CaCO_3$) respectively. From the data shown in the two figures, it can be seen that the density of the obtained extruded mixture increases with the increase of both types of fillers which was most likely due to the weak bonding between the fillers and LDPE, as the particles interfere between the polymeric chains during the mixing process to occupy the voids in those chains. On the other hand, this weak interface is believed to provide channels for gas loss that caused the shrinkage of the composite.

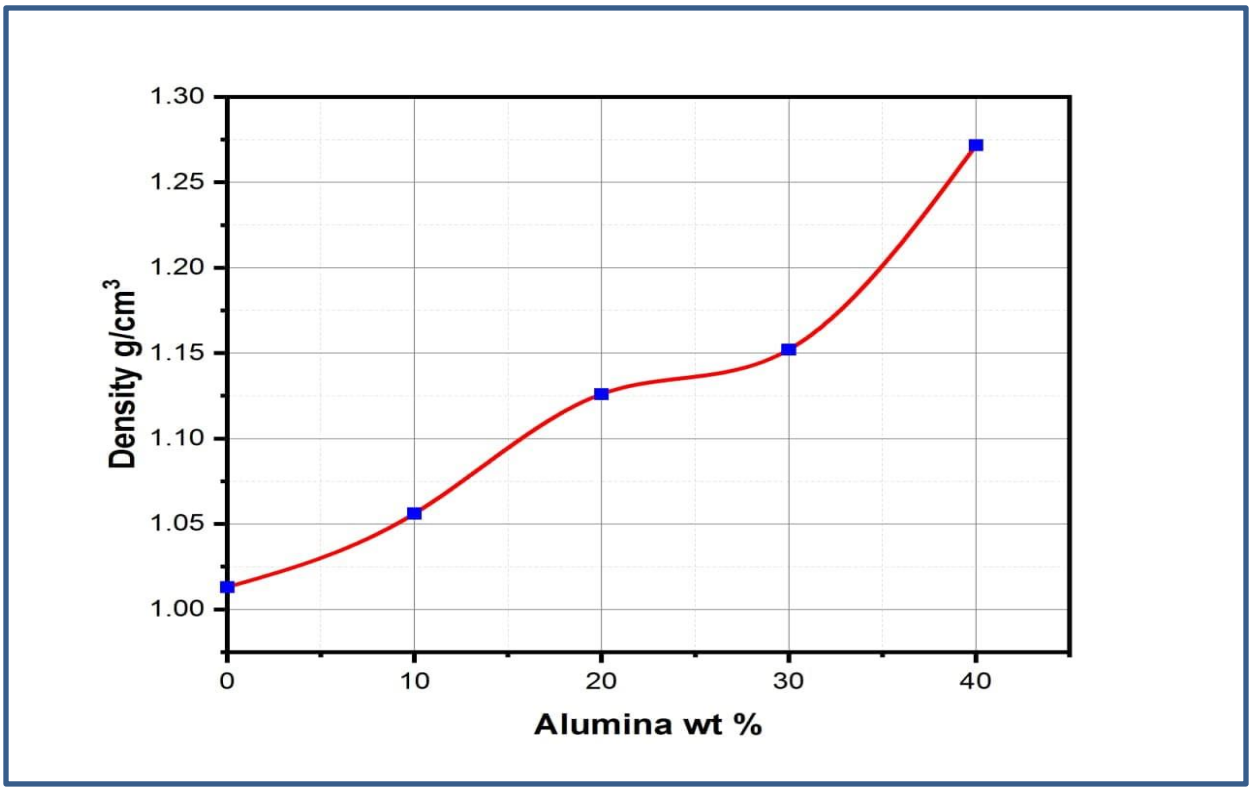

Figure 4.8: Density versus the percentage of AL_2O_3 filler.

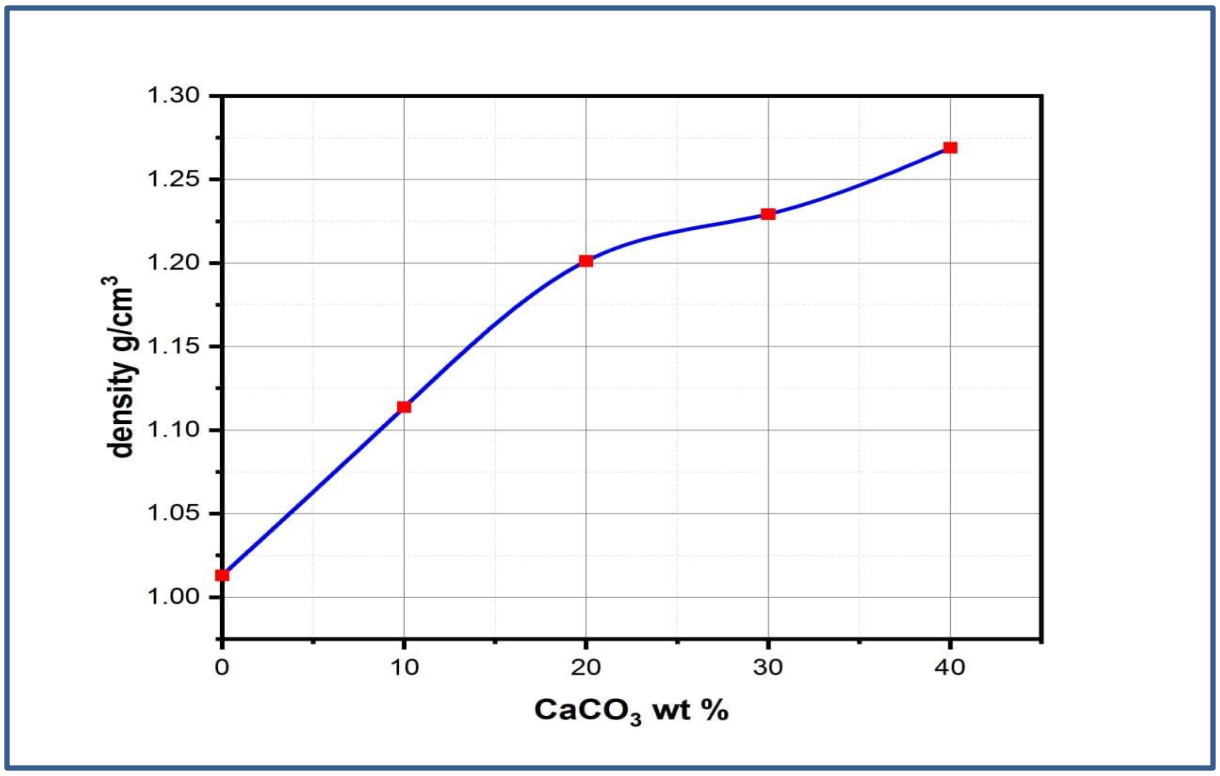

Figure 4.9: Density versus the percentage of $CaCO_3$ filler.

4.5 Tensile Result

When the as-prepared samples are mounted in the tensile testing machine and the test is performed, the graph between the stress (σ) and the sample strain (ε) was obtained from the graph of the tensile testing machine. Through this scheme, the values of stress and strain were calculated using equations (2.9) and (2.10), respectively.

The stress-strain curves were drawn for all the prepared samples and numbers showing the mechanical behavior of these curves were for two types of composite materials, the first (LDPE) with reinforcing materials (alumina microparticles) and the second (LDPE) with reinforcing materials (calcium carbonate microparticles) as in Figures (4.10) and (4.13) respectively. The behavior of these curves depends on the nature of both the matrix and the

reinforcement material as well as on the adhesion strength between the matrix and the reinforcing material.

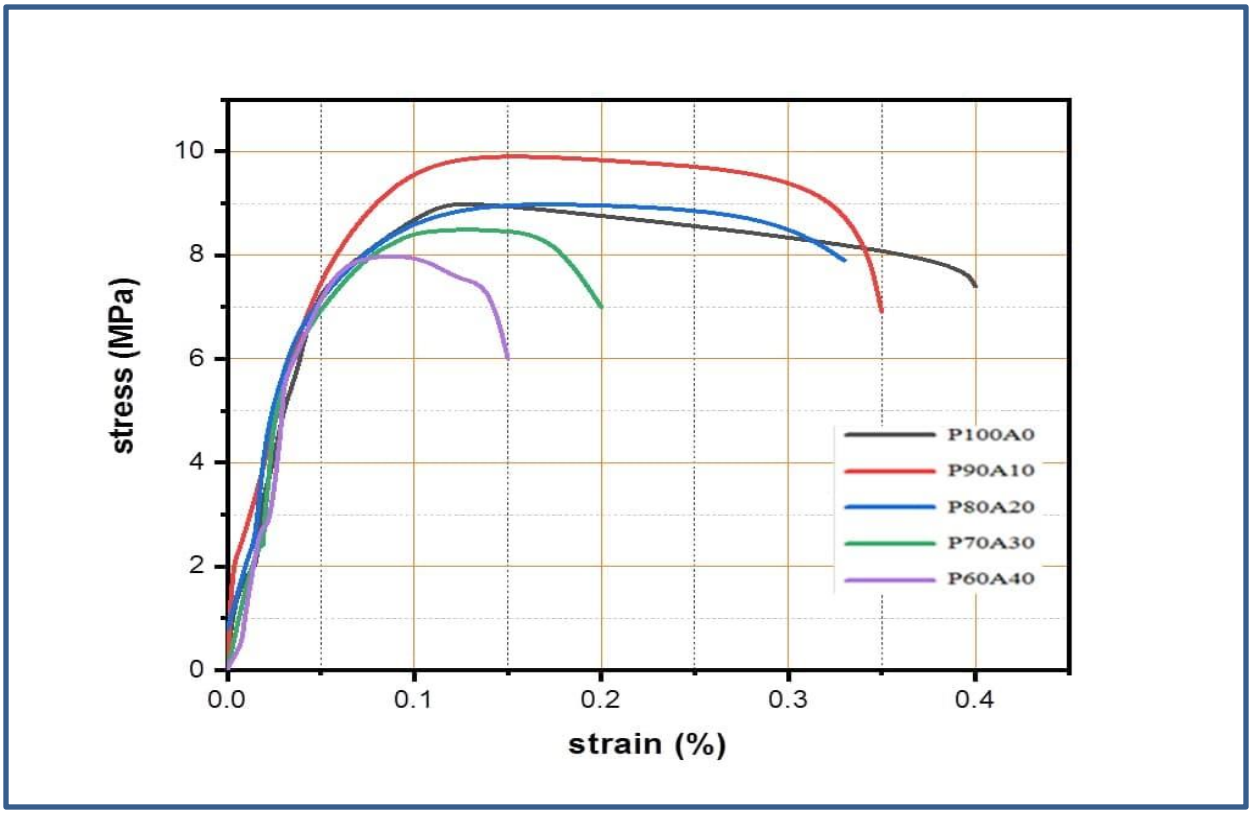

Figure 4.10: Stress-strain curve for LDPE pure and reinforcement by (10, 20, 30, and 40) wt % of AL_2O_3.

Figure (4.11) which is showing the relation between the tensile strength for LDPE reinforced by Varying (10, 20, 30, 40) % weight fraction of AL_2O_3. Dispersion and interfacial adhesion between the matrix and the filler play a crucial role in improving the tensile strength of the composite [104]. There is usually no chemical reaction between AL_2O_3 and LDPE, but the SEM images indicate a good dispersion that reduces voids and supports the load in the matrix and which explain tensile strength reinforcement for the LDPE composite at 10 wt% AL_2O_3 To the highest value, and which is estimated (10MPa), which is approximately 1.11 times compared to pure LDPE, Then the tensile strength begins to decrease with the

increase of the filler ratio above10 wt% AL_2O_3, this decrease of the tensile strength from the value (10MPa to 8MPa) with increase percentage loading alumina from(10-40)wt%, respectively, may be due to the weak surface adhesion and low dispersion of the raw alumina filler affects the LDPE matrix. The presence of voids in the interfaces and aggregates of the filler particles reduces the tension values because it increases the distances between the particles and works to centralize the stresses in the loading operations. Aggregations available the defects that can develop rapidly and lead to failures [105].

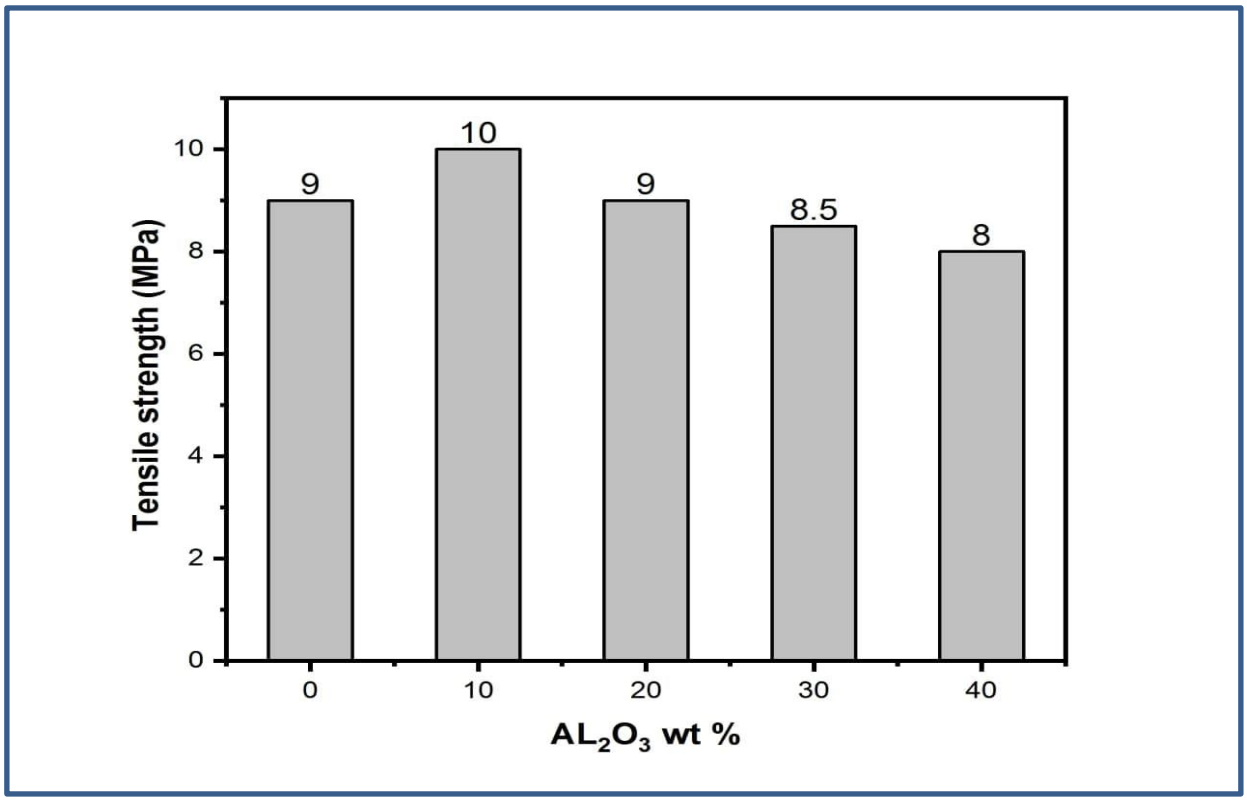

Figure 4.11: Tensile Strength versus the percentage of alumina filler.

Figure (4.12) shows Young's modulus of LDPE reinforced by varying weight fraction of AL_2O_3, which is defined as the ratio of stress to the strain of solids only, The Young's modulus is the slope of the initial stress-strain curve, which represents the stiffness. All specimens of LDPE composite are higher than

the LDPE virgin and their values increased with the increase in the content of aluminum oxide. There was a significant improvement in Young's modulus of the composites which recorded the values (170, 150, and 200 GPa) with 10, 20, and 30 wt% of alumina, respectively as compared to that of neat LDPE which recorded the value of its 130 GPa. However, the value of elastic modulus at 40 wt% alumina content reduces to 170 GPa, although it is still higher than pure LDPE is an indication of increased agglomeration, which increased the stiffness values and increases the brittleness of the composite as in [105]. there is a good possibility that what happened is that the motion of the chains in the array was closed by an interlocking mechanism, which was further strengthened by the presence of aluminum oxide particles. In addition to the high stiffness of alumina, It becomes self-evident that Young's modulus values in LDPE / alumina composite increase when loading the filler material is increased [106].

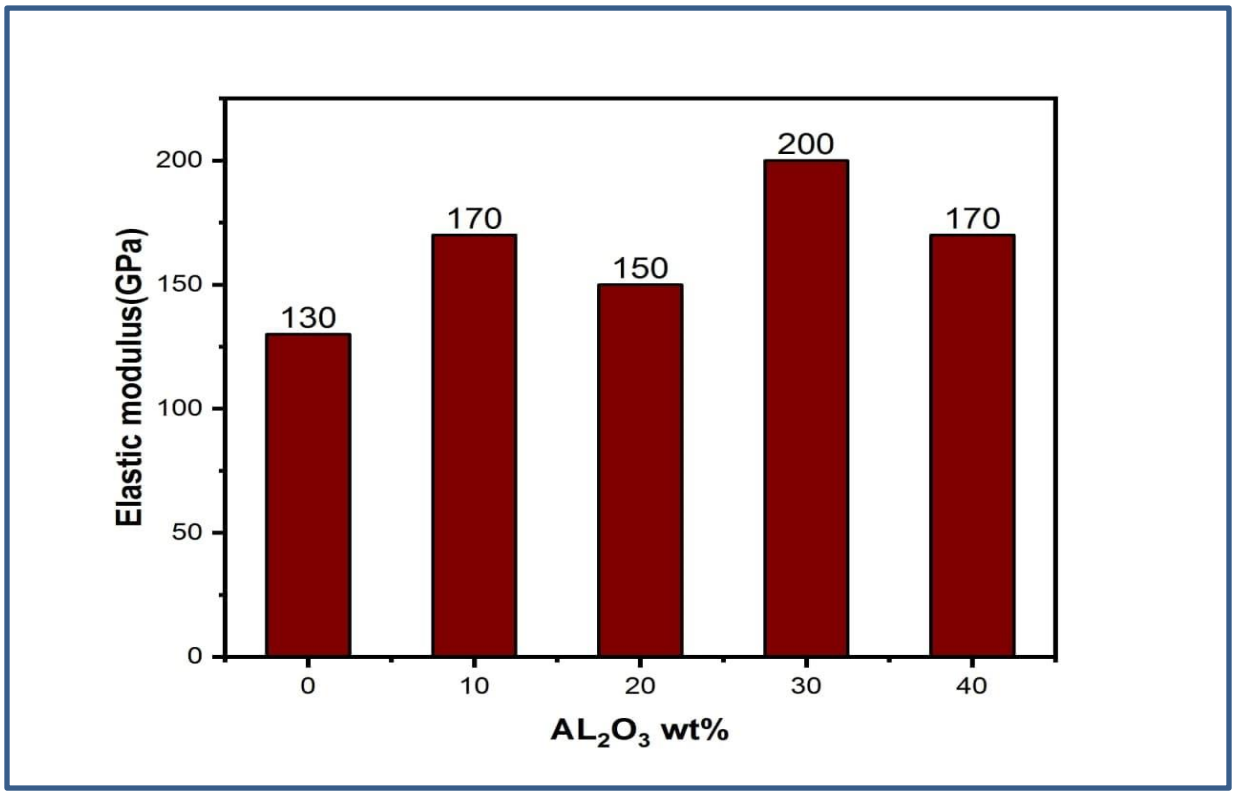

Figure 4.12: Elastic modulus versus the percentage of alumina filler.

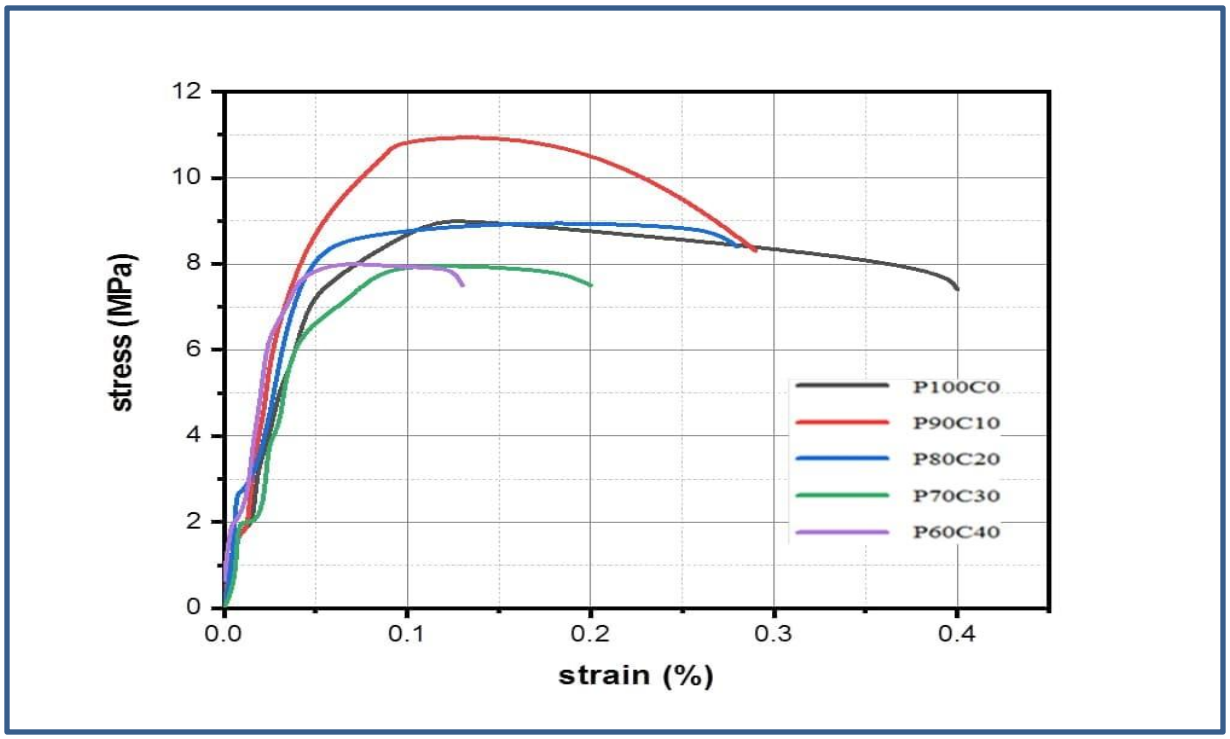

Figure 4.13: stress-strain curve for LDPE pure and reinforcement by (10, 20, 30, and 40) wt % of $CaCO_3$.

Figure (4.14) shows the tensile strength of for LDPE reinforced by Varying (10, 20, 30, and 40%) weight fraction of $CaCO_3$, The tensile strength depends largely on the interaction of the polymer matrix and adhesion with the material filler and the degree of dispersion of the filler and its homogeneous distribution within the matrix [107]. There is no chemical reaction and this was reported by FTIER assay Figure (4.3). But there is a homogeneous distribution and best distribution of filler material inside the polymeric matrix at the ratio of 10% W Calcium Carbonate, which is shown in SEM images Fig (4.23), which may explain the high tensile strength at that ratio which amounted to(11MPa). Which is the highest tensile strength of all LDPE composites It appears that the poor homogeneity at 20wt% $CaCO_3$ due to the defect in the manufacturing process also contributed to the reduction in tensile rates to the value (9MPa) in addition to the increase in the content of the filler. When a greater amount of calcium carbonate

content is introduced into the LDPE matrix, the tensile values begin to decrease. This may be due to poor adhesion between the filler and matrix as we explained previously in addition to an increase in the concentration of calcium carbonate which makes the dispersion and homogenization process somewhat difficult. Which gives undesirable mechanical properties, which explains the low tensile values at 30 and 40wt% at value (8MPa) for each all, as in reference [108].

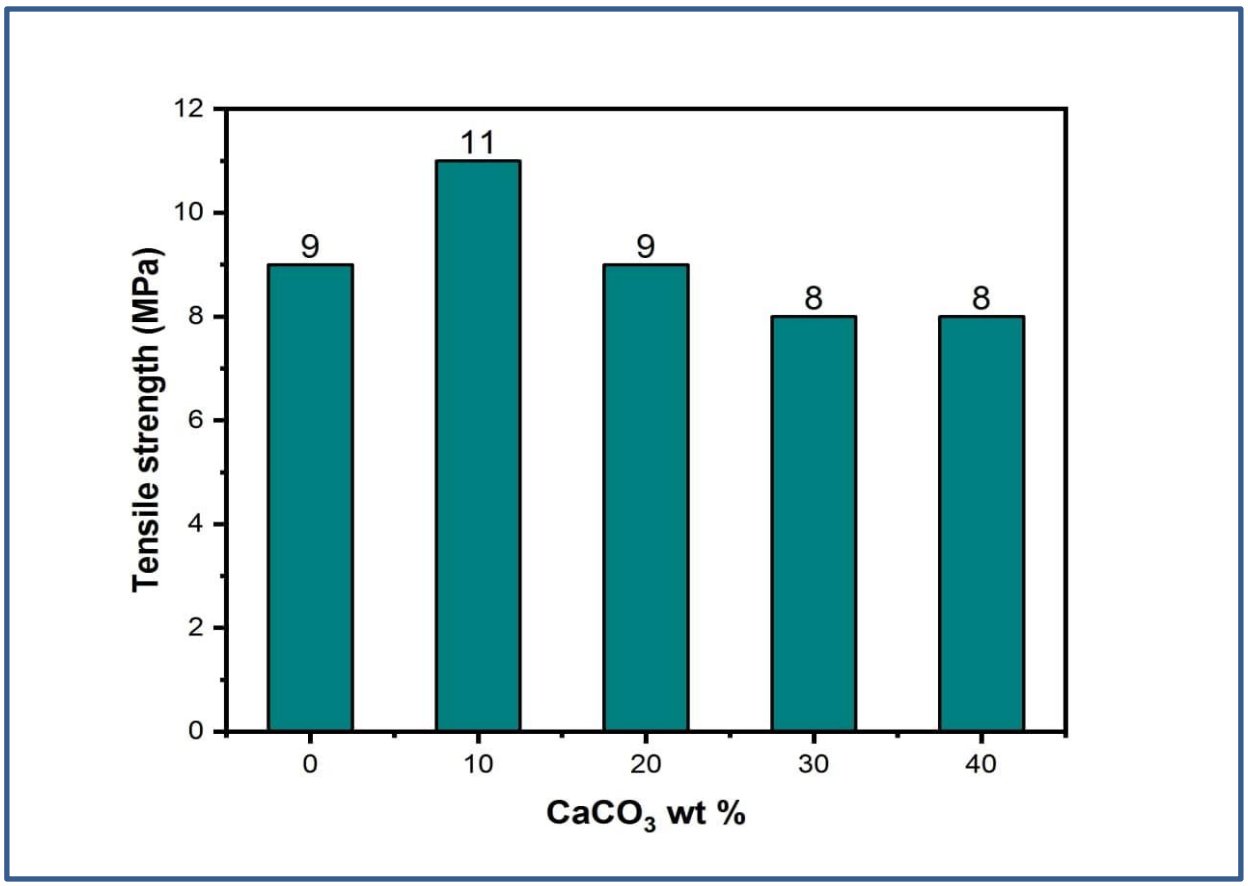

Figure 4.14: Tensile Strength versus the percentage of $CaCO_3$ filler.

Figure (4.15) shows the Elastic modulus of LDPE reinforced by (10, 20, 30, 40) % weight fraction of calcium carbonate. From this chart, we note the increase of Calcium carbonate content led to an increase in the tensile modulus of all LDPE

composites comparison with LDPE virgin. These increases were probably due to the stiffness of the calcium carbonate particles compared to the stiffness of the matrix. In addition to supporting $CaCO_3$ molecules in the polymer matrix, calcium carbonate may also contribute to increasing the level crystallinity of LDPE compounds, and this would raise the stiffness of the compounds. We note that the effect of dispersion and increasing content of calcium carbonate is a factor affecting the stiffness. When entering 20 wt%, The dispersal process was not up to the required level due to the appearance of agglomeration in the matrix, which was due to the manufacturing processes, although the preparation and manufacture of LDPE compounds were under the same conditions, this agglomeration contributed to the reduce values of Young's modulus in this test sample compared with the other values for the LDPE compounds even though they are still higher than the pure LDPE. We also note that the increase in the insert of the filler material at 30% and 40% by weight means an increase in the concentration of the solid material in the low-density polyethylene matrix, thus reducing the chances of dispersal of the filler and increasing the chances of agglomeration. However, the values of the elastic modulus are maintained above the original due to the stiffness of the filler material. this result partially agrees with Kantima Chaochanchaikul. , et al. 2009 in ref [109].

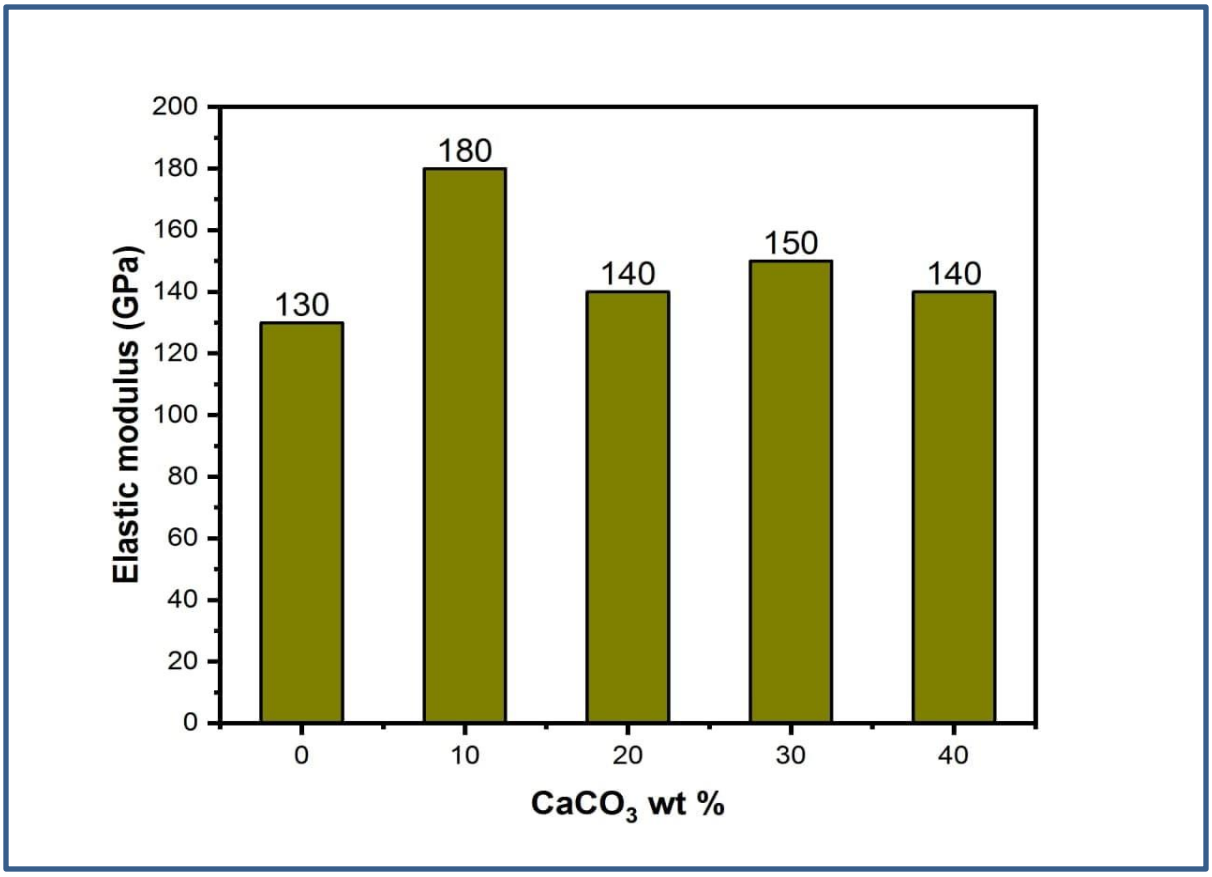

Figure 4.15: Elastic modulus versus the percentage of $CaCO_3$ filler

Alumina has a high hardness characteristic as it can withstand high loads before facing failure compared to calcium carbonate $CaCO_3$, which explains the higher stiffness values represented by Young's modulus for LDPE composite reinforced by alumina compared to calcium carbonate. As for the tensile strength, we explain its increase in LDPE composite reinforced by calcium carbonate compared to alumina Because of the small size of the calcium carbonate particles compared to alumina, which works to fill the voids and improve the tensile strength.

4.6 Impact Result

Figure (4.16) shows impact resistance of LDPE reinforced by Varying weight fraction of AL_2O_3 The strengthening efficiencies of aluminum oxide particles vary greatly, where we can observe a relatively low impact resistance was amounted to (14.36 KJ/m²)at the content (10wt% alumina), Then we notice an improvement in the resistance was value amounted to (16.835 KJ/m²) when the content is (20% alumina), then the impact resistance begins to rise to its highest value which equals (23.825 KJ/m²), at the content (30wt% alumina)which is equivalent to (1.48)% of pure LDPE, which is the percentage in which the bond between the filler and the matrix is in the best direction of the impact resistance, while there was a sharp decrease in the impact values, its value amount(10.434 KJ/m²) Because of the appearance of agglomerations. There are several mechanisms for toughening of polymer. For the inorganic particles toughening polymer, at least three factors are necessary: inherent ductility of the matrix, weak interphase supporting the filler/matrix debonding, and suitable interparticle distance. The stress concentration first leads to debonding of the filler particles and voids formation. The particle content affects the interparticle distance and the stress state of the matrix polymer surrounding the voids. At low alumina content, the interparticle distance is long and the interparticle matrix ligament lies in a plane strain state which is hard to yield, as a result, the impact strength cannot be improved. When the alumina content increases and the interparticle distance reach a suitable range, the interparticle matrix ligament lies in plane press state, which can be plastic yield easily and the impact strength can be improved. But when the alumina content is too high, the interparticle distance becomes too small and even

leads to large size agglomerates, which provide convenient triggers for brittle behavior. As in [110].

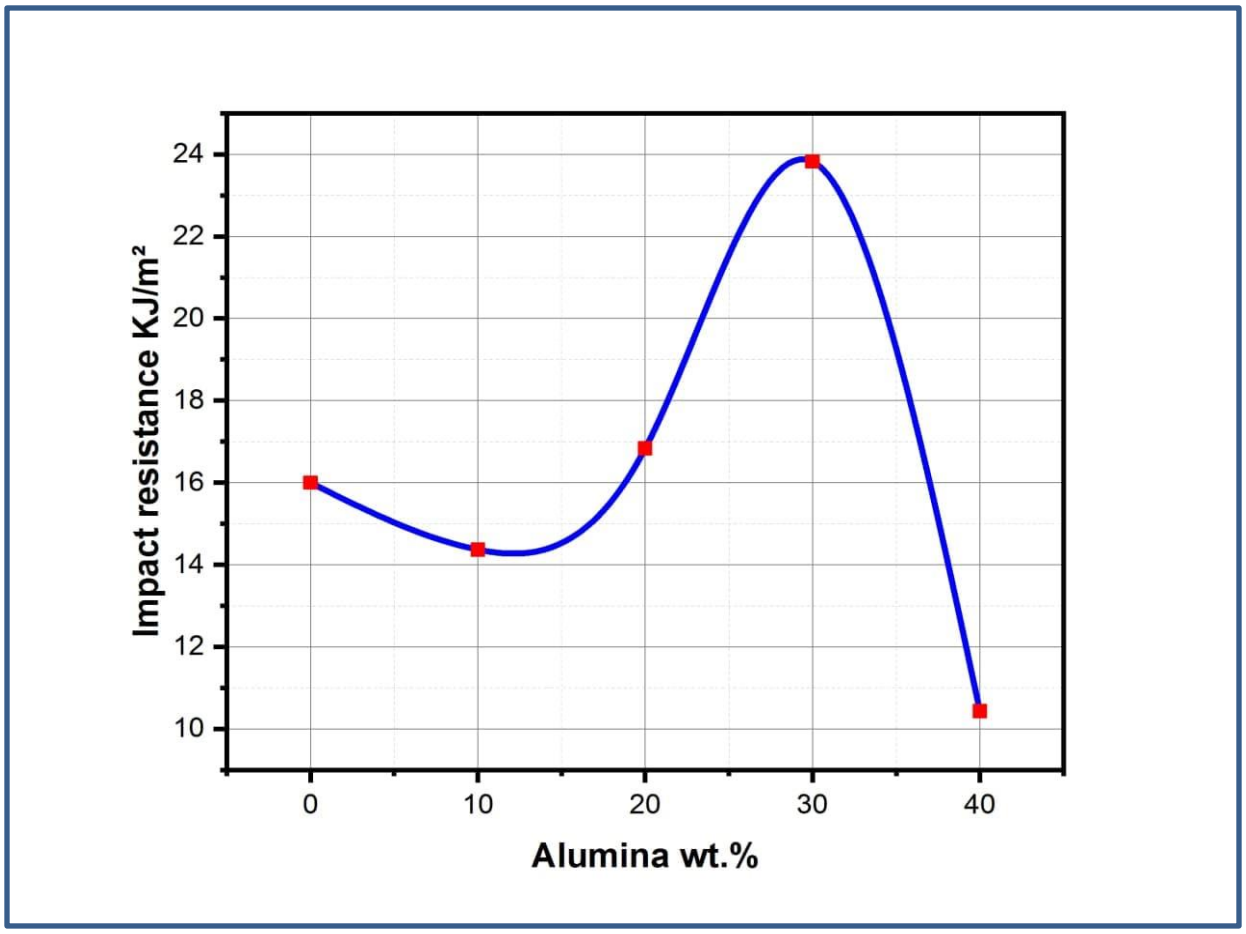

Figure 4.16: Impact resistance versus the percentage of alumina filler.

Fig (4.17), shows impact resistance of LDPE reinforced by Varying weight fraction of $CaCO_3$ The strengthening efficiencies of carbonate calcium particles vary greatly, where we can observe a low impact resistance amounted to (7.213 KJ/m²)at the content (10wt% $CaCO_3$), Then we notice an improvement in the resistance was value amounted to (14.78 KJ/m²)at when the content is (20% $CaCO_3$)but is still less virgin LDPE this may be due to the agglomeration effect,

which is clearly shown in Figure (4.22), which is a defect that reduces the mechanical properties, then the impact resistance begins to rise to its highest value which equals (17.975 KJ/m²), at the content (30wt% $CaCO_3$)which is equivalent to (1.1) of pure LDPE which is a slight improvement, but it remains the only reinforcement that has improved impact resistance compared to pure LDPE, at 40 wt % $CaCO_3$, impact value is decreasing at the amount(8.4KJ/m²). The effect of calcium carbonate added as a filler on the behavior of LDPE composites is explained in the same way as discussed in Figure (4.15), which is in part in agreement with S. Zhang et al 2011 in reference [110].

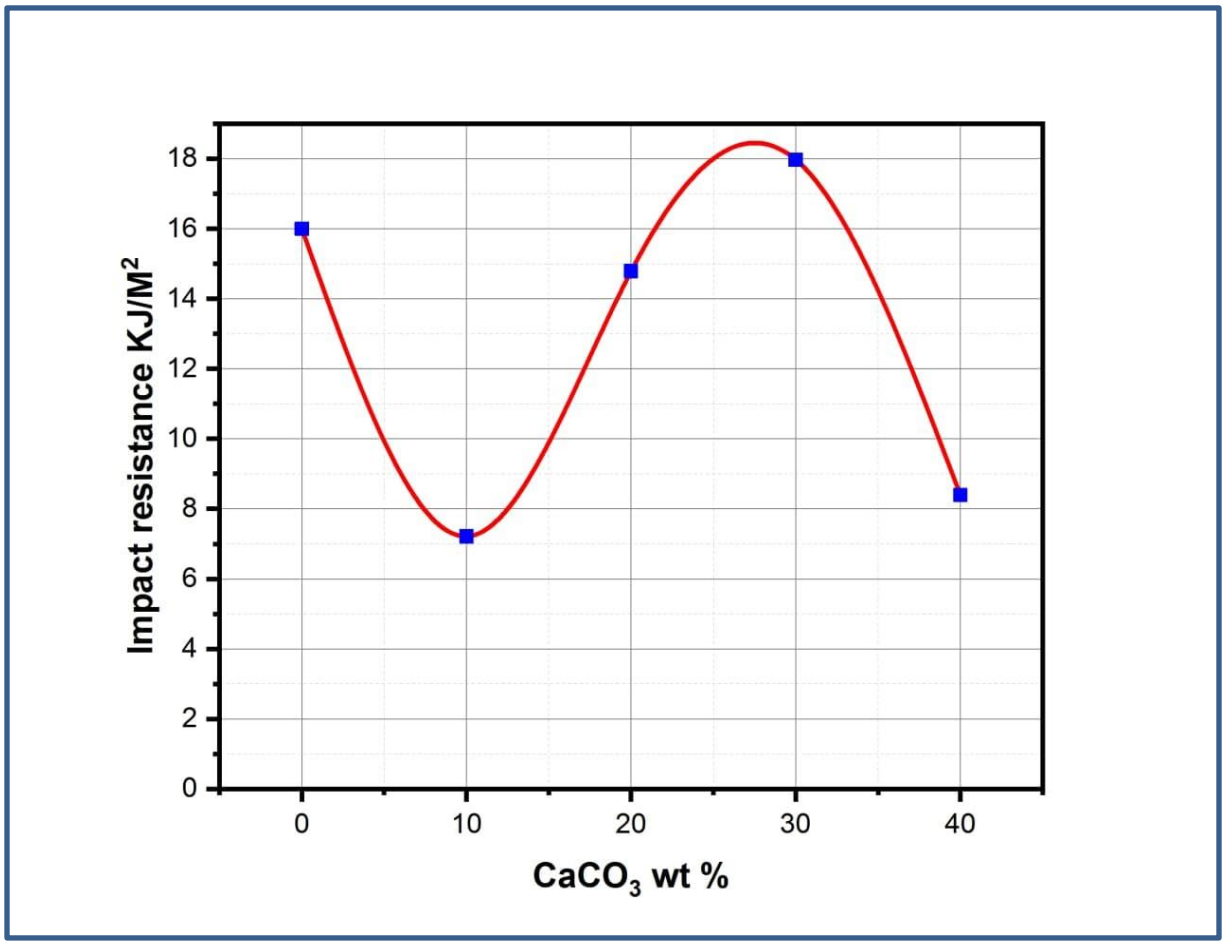

Figure 4.17: Impact resistance versus the percentage of $CaCO_3$ filler.

By comparing the figures (4.16) and (4.17), we notice the high impact values of alumina despite its high stiffness compared to calcium carbonate. This may be due to the well-known needle-like shape of alumina particles, which, upon contact and closeness, are connected forming chains like fibers that cause high impact strength.

4.7 Creep Test Result

Figure(4.18) shows the relation between the creep behavior for LDPE reinforced by Varying (10,20,30 and 40,)% weight fraction of AL_2O_3, The creep test was carried out under the following conditions, a temperature of 20 ^{0}c and an applied load of 5KN. from this chart can be seen the creep strain it very clear that the creep strain for LDPE pure is higher than the creep strain value for the LDPE composites and its behavior increasing with time, To clarify the effect the filler on behavior creep of polymer, need to know the mechanism by which creep performance is affected when fillers are inserted, the creep characteristics are modified by the presence of stiff particulate of alumina, which in effect will not deform throughout the test. It should also be noted that the same applied loads were used for all composite materials, therefore, the greater stiffness of the composites meant that the elastic strains were lower and so the true stresses were also lower. This effect will reduce the creep strain. Figure (4.18) shows that the sample (P90A10) exhibits the best performance in creep resistance, beyond what would be expected based on its higher stiffness. This is consistent with the expected load transfer to the particles (and also with the concept of the particles remaining well-bonded to the matrix). On the other hand, the improvement is not a dramatic one when compared with the other LDPE composites, which might have been expected from the limited nature of the load transfer (and indeed of the stiffening effect) [111]. The SEM images also showed that the dispersion is

reduced and the roughness is increasing as the filler content increases, Which may be the reason for the relatively good performance at 10 wt% alumina.

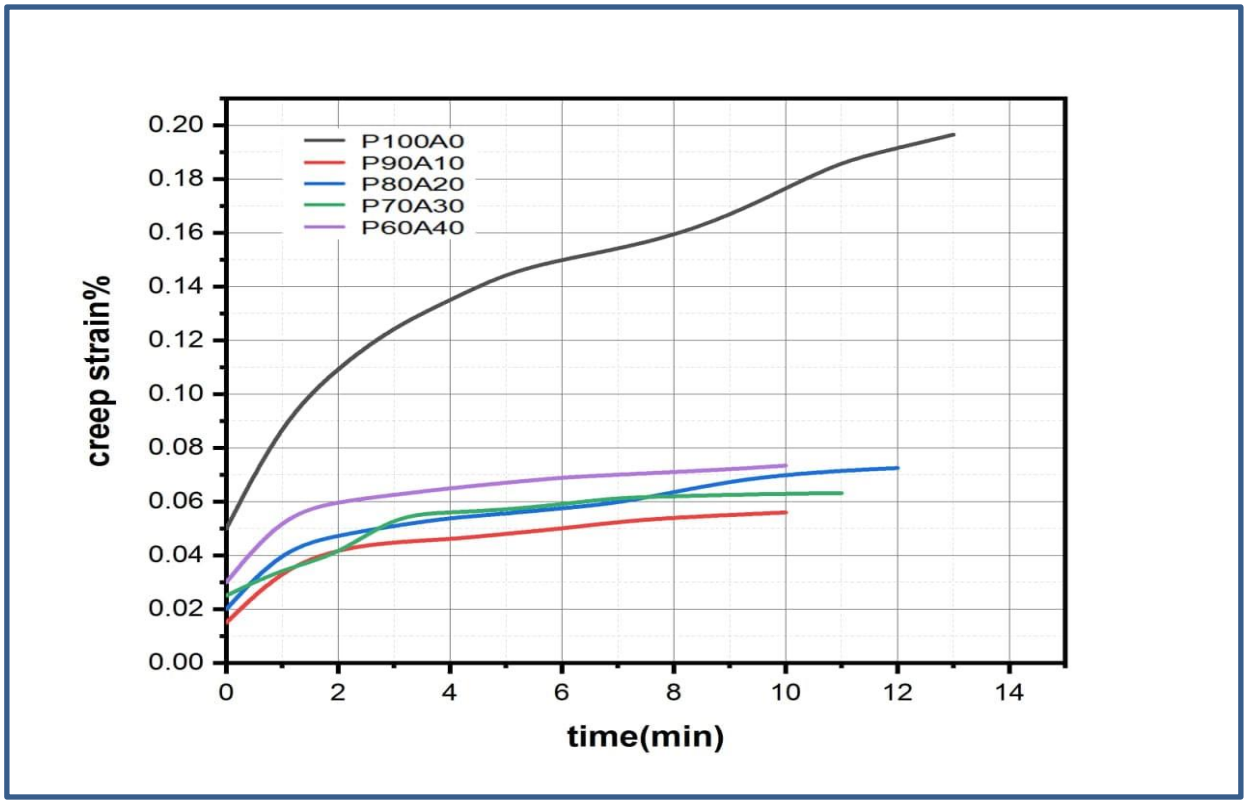

Figure 4.18: Percentage creep strain for LDPE /Alumina composite.

Figure (4.19) shows the Creep test achieved at room temperature with constant load (5 KN) for LDPE reinforced by Varying (10,20,30,40,)% weight fraction of $CaCO_3$, This graph indicate that the creep strain for LDPE pure is higher than the creep strain value for the LDPE composites and its behavior increasing with time, The behavior is due to the effect of Calcium Carbonate particles between the chains that prevention chains from sliding one on the other which increase the creep resistance under load as shown. With an increase in the filler content, the creep performance getting better up to 20% calcium carbonate, were The sample (P80C20) was Presented the good resistance in this creep test, It showed the best performance off all the other composites including the virgin

LDPE matrix, When the calcium carbonate content is increased from 20% to 40%, the creep performance begins to decrease gradually over time. The creep performance depends on the physical properties of LDPE composites, where interference at moderate proportions of the filler allows to provide support for the polymer matrix, which causes the impedance of chain movement, which improves the performance of the creep strain. the SEM images show a change in the surface shape where the solid concentration increased in the low-density polyethylene matrix, thus reducing the chances of the filler dispersal and increasing the chances of agglomeration, especially at high percentages (40% wt), which contributed to a relative decrease in the creep strength and on Nevertheless, the values of LDPE composites remain close to each other in their creep resistance due to the interference of the filler between the polymer chains. Test results agree with the opinion of the scientist Sivarao, et al 2011.in reference [112].

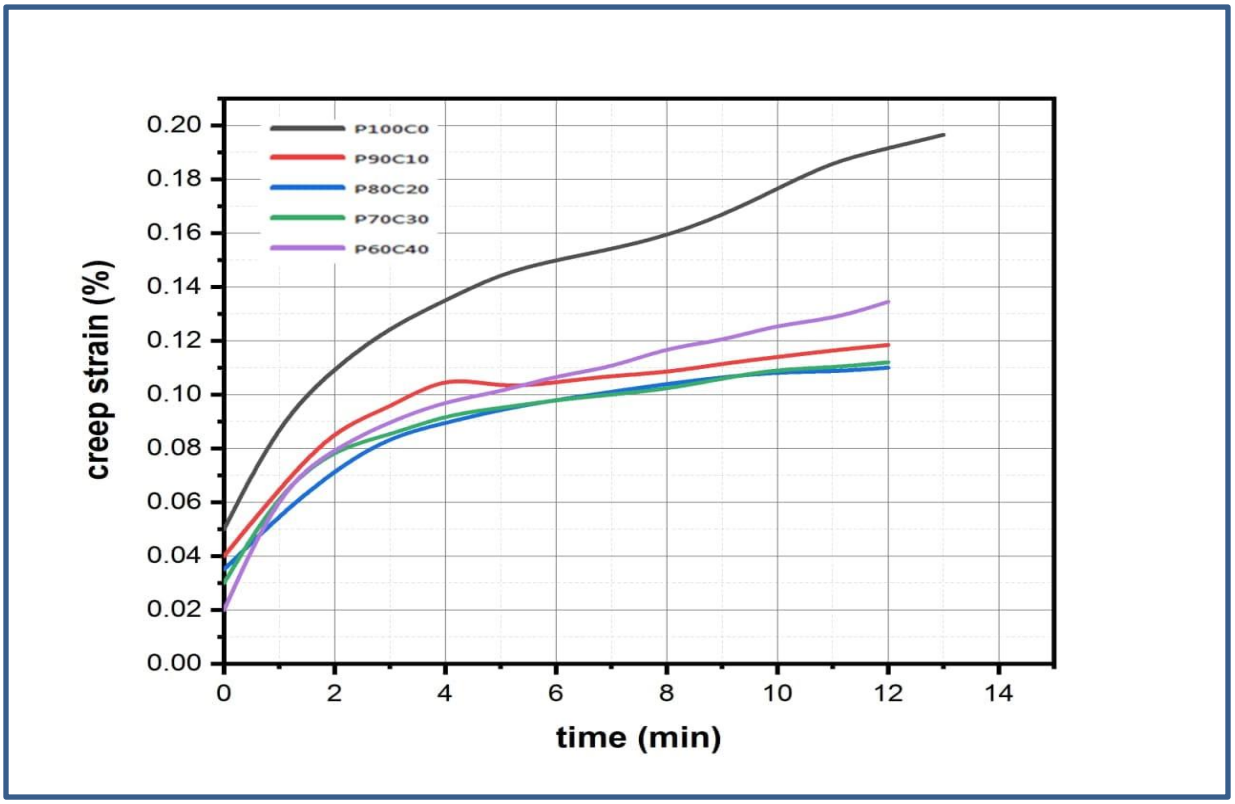

Figure 4.19: Percentage creep strain for LDPE /$CaCO_3$ composites.

The high creep resistance at alumina compared to the values of creep resistance for calcium carbonate may be due to the high stiffness and the needle-like shape of the alumina particles compared to the ball-like form of calcium carbonate, which contributed to rising rates the creep resistance even at low percentages of alumina.

Figure (4.20) shows the creep behavior for sample LDPE composite (P90A10). Creep measurements were at 5 KN and temperatures of 20, 30,40, and 50^0C.from this graph and as expected, increased the creep strain with increasing temperature in the LDPE sample (P90A10), and thus the creep values are very sensitive to the direction of temperature increases. From 20 to 40 ^{0}C, and as expected, increased deformation of composite is, but it maintained its stability during the test period, while at 50 ^{0}C, the deformation increased by a greater percentage compared to previous temperatures, although the sample remained also steadfast during the test period. can say that 50 ^{0}C is the maximum temperature the sample can handle before it fails and the reason for this is because the activation barrier for the breakdown of molecular bonds decreases with increasing temperature which allows the partial chains to untangle, re-orient and slide more easily with the temperature as in reference [87].

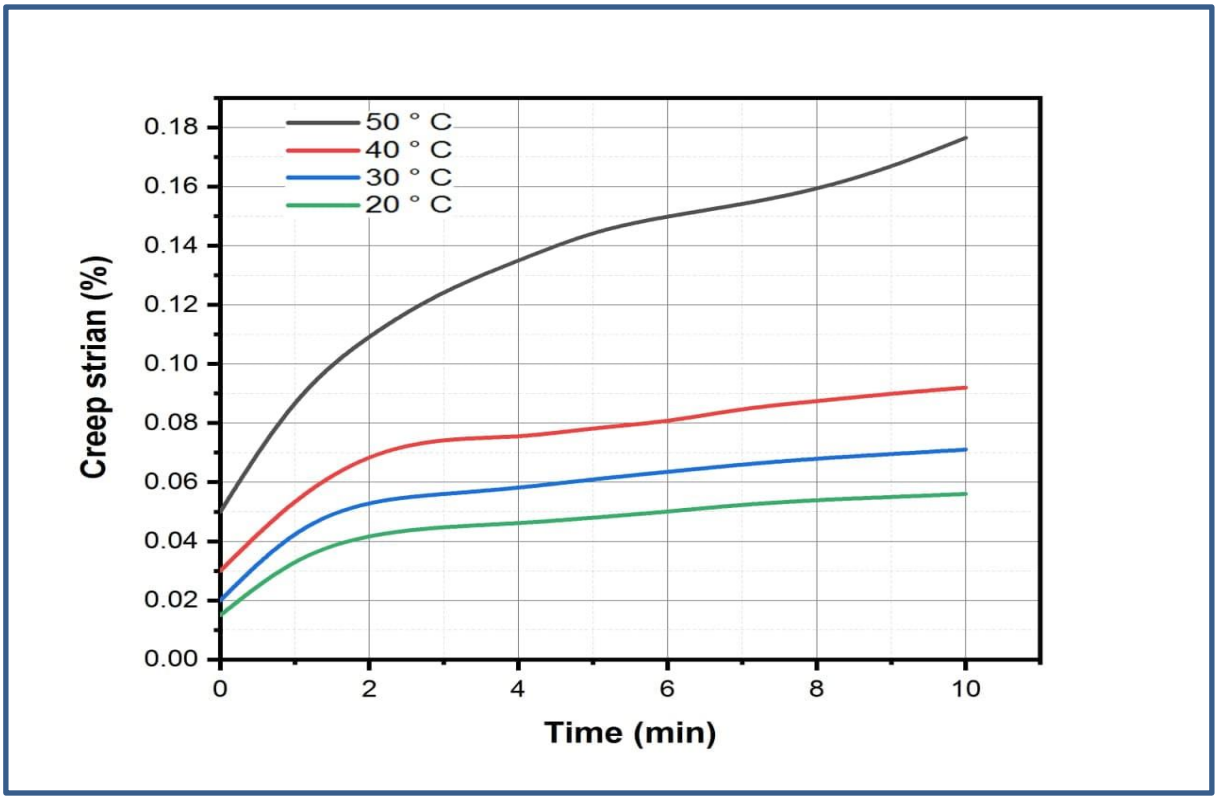

Figure 4.20: Creep strain for (P90A10) in varying Temperatures 20 ^{0}C, 30 ^{0}C,40 ^{0}C, and 50 ^{0}C.

4.8 (SEM) Result

The morphology of the surface of the specimen was examined by scanning electron microscope (FESEM) to obtain additional useful information and ideas on the effect of increasing the weight ratios of the filler on the viscoelastic behavior and its relationship to the mechanical properties of the composite of LDPE and knowing the level of filler distribution and homogeneity within the LDPE matrix.

Figures (4.21) from (A) to (C) represent the SEM micrographs of surface samples for LDPE reinforced by Varying (10,20,30,40,)% weight fraction of AL_2O_3 at magnifications(200X).in the micrograph (A)The picture SEM shows that the aluminum oxide particles are well distributed, and there are particles attached

to the surface of the LDPE also there is no obvious defect during casting, we also see a suitable bonding between the polymer matrix and the particles filler, which justifies the good properties of this composite matrix. the micrograph (B)Illustrates There are no defects in casting and the increase in the percentage of alumina resulted in a relatively increased surface roughness. The surface morphology was not bad which explains its acceptable mechanical properties. Micrographs (C, D) show the LDPE composite with an additional (30,40) wt% content of alumina. An increase in the concentration of solids reduces the chances of fillings dispersal within the polymeric matrix and increases the chances of agglomeration, some of which appear in the picture. This agglomeration is the area of stress concentration and the beginning of crack formation and failure that is reflected in the mechanical properties.

A **B**

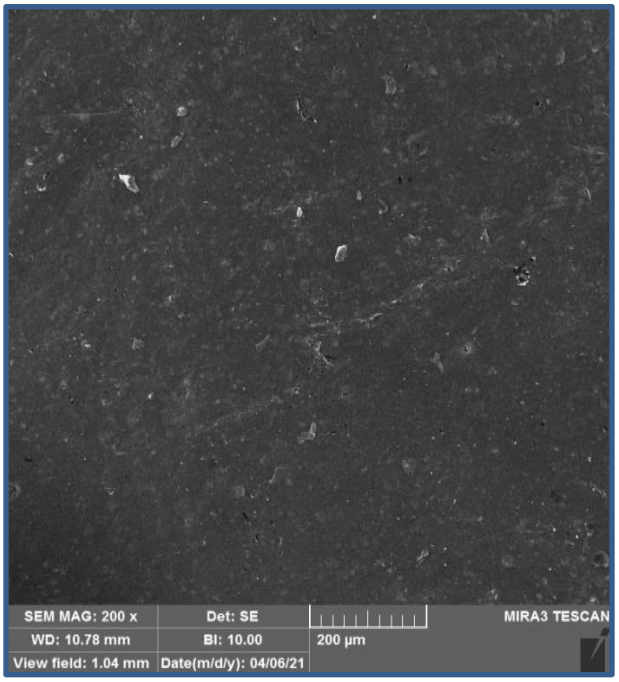

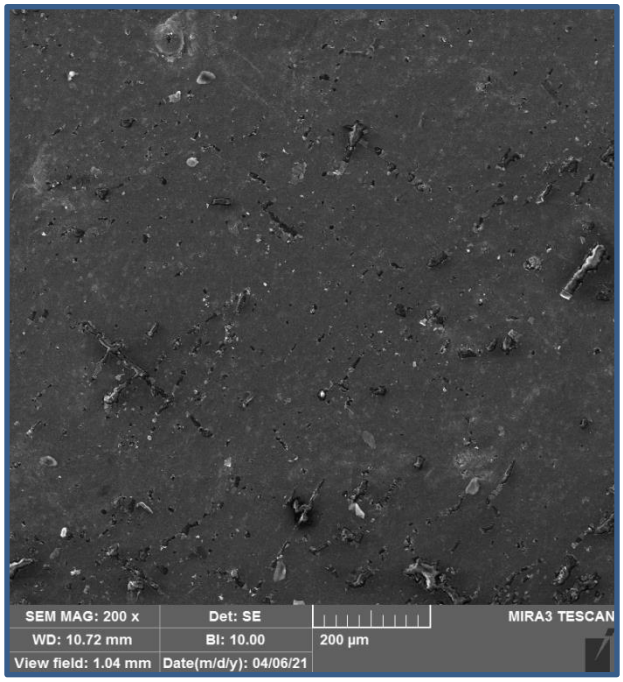

C **D**

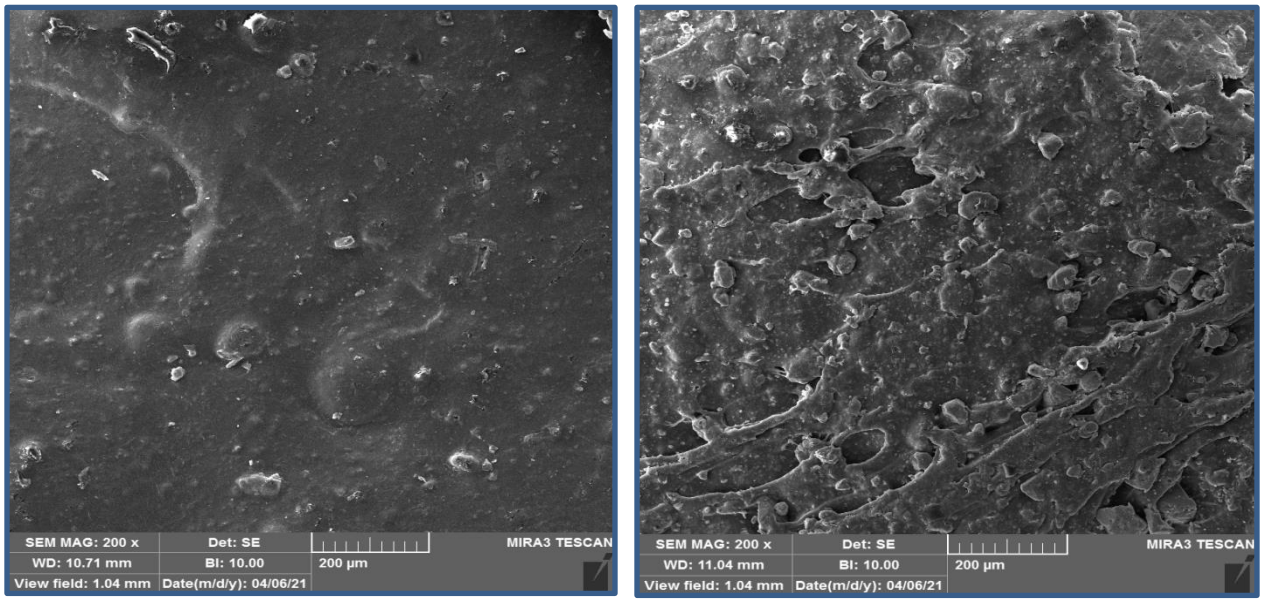

Figure 4.21: FESEM for (a) 90% LDPE/10% AL_2O_3 (b) 80% LDPE/20% AL_2O_3 (c) 70% LDPE/30% AL_2O_3 (d) 60% LDPE/40% AL_2O_3.

Figure (4.22) shows the sample (LDPE + 30wt% Alumina) that was tested by the FESEM device to detect the presence of alumina. The (EDX) results indicated the presence of alumina in percentages (53.20w%)

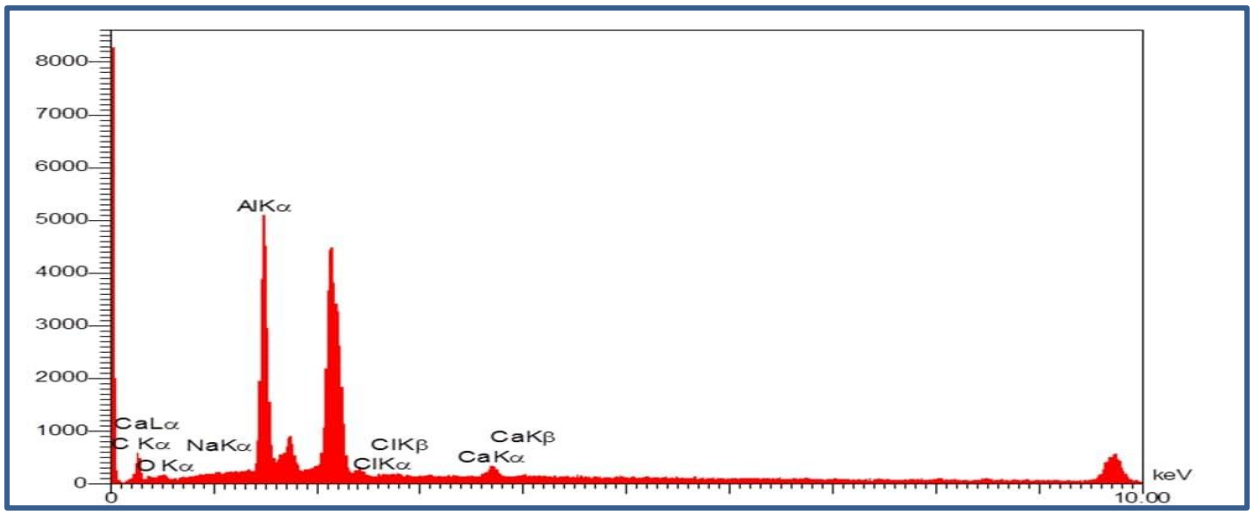

Figure 4.22: EDX for LDPE+30wt % AL_2O_3

Figure (4.23) shows from (A) to (C SEM micrographs of surface samples of LDPE reinforced by (10,20,30 and 40%) represent the weight fraction of calcium carbonate at magnification (200X). (A) shows a regular and smooth surface, and no obvious agglomeration, which indicates a good dispersion of $CaCO_3$ in the LDPE matrix, which played a prominent role in improving the tensile performance at this ratio. Micrograph (B), agglomeration was identified in a portion of the sample due to the manufacturing process even though the working conditions were the same. This agglomeration may affect the mechanical and rheological properties as the flow values were lower than expected with relatively low Young's modulus values. Micrographs (C, D) As it is known, when overloading, the concentration of the filler in the matrix increases, which serves to reduce the interfacial distances between the filler particles within the polymeric matrix, Reducing the distances contributes to the formation of agglomerates, which negatively affects the rheological and mechanical properties, especially after 30% wt, these high concentrations contributed to a relatively low modulus of elastic modulus and tensile strength.

A **B**

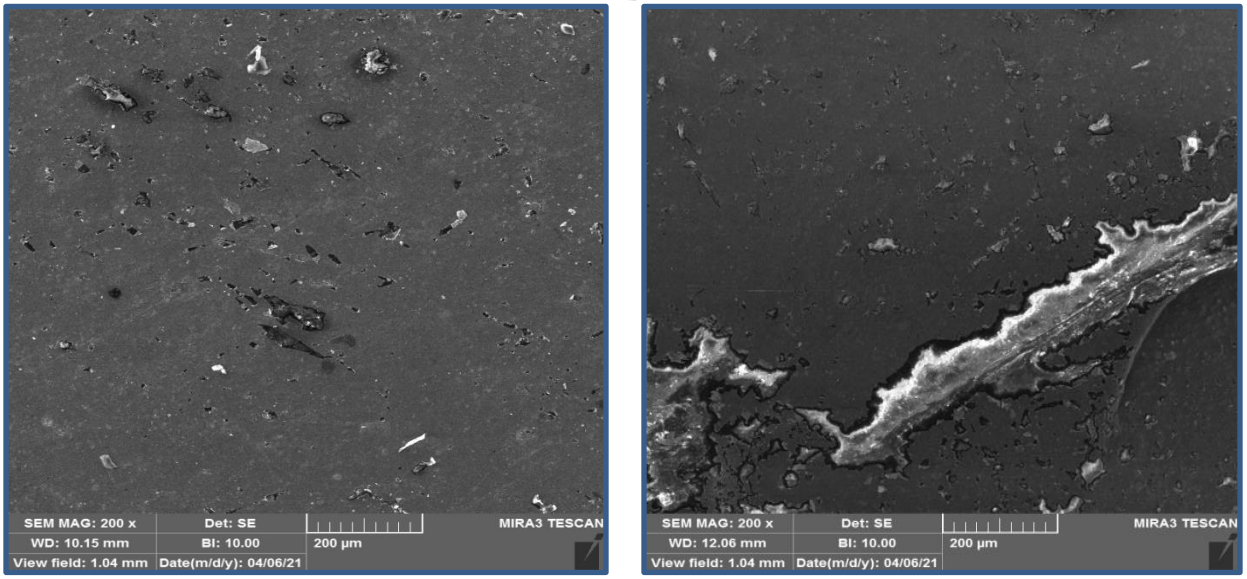

C D

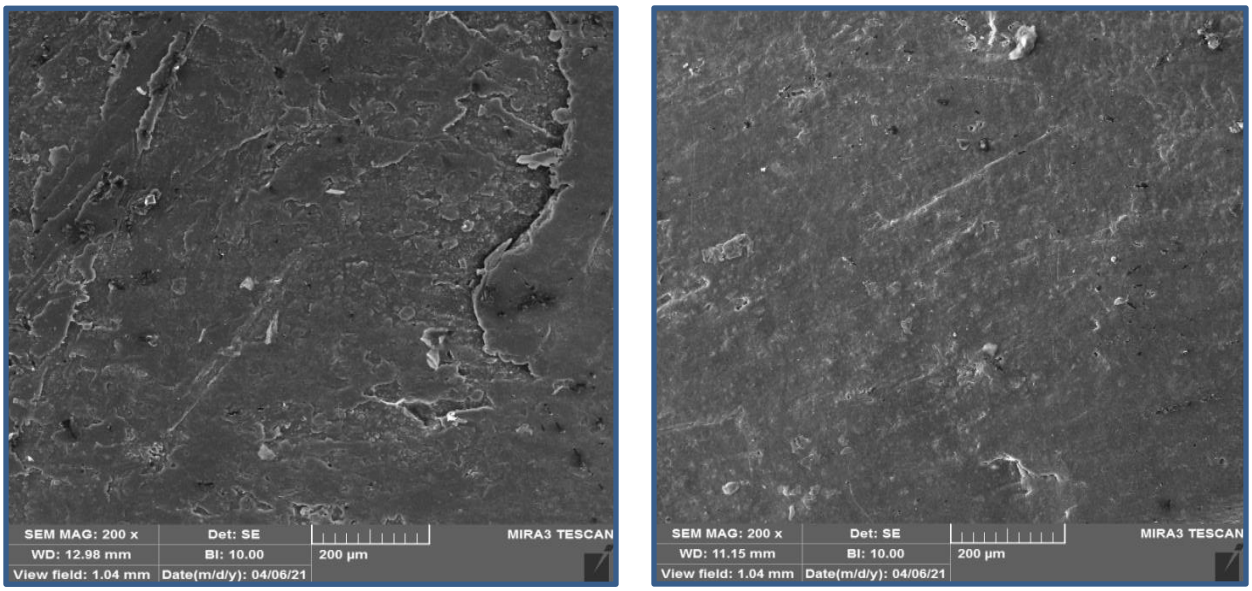

Figure 4.23: FESEM for (a) 90% LDPE/10%$CaCO_3$ (b) 80% LDPE/20 % $CaCO_3$ (c) 70% LDPE/30% $CaCO_3$ (d) 60% LDPE/40% $CaCO_3$

Figure (4.24) shows the sample (LDPE + 30wt% calcium carbonate) that was tested by the FESEM device to detect the presence of calcium carbonate. The (EDX) results indicated the presence of alumina in percentages (37w%).

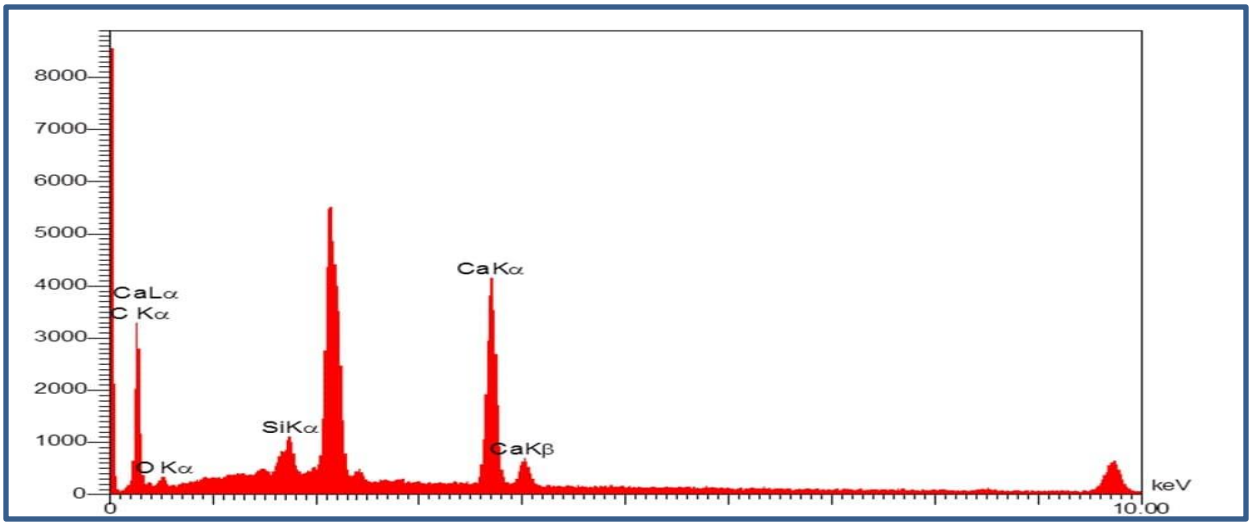

Figure 4.24: EDX for LDPE+30wt % $CaCO_3$.

Chapter Five

Conclusions and Recommendations

5.1 Conclusions

1. The addition of 10wt% alumina to the LDPE matrix provided the best performance of creep resistance, superior to the best performance provided by the LDPE matrix when introducing 20wt% calcium carbonate.
2. The sample that provided the best performance in resisting creep can withstand the highest temperature before failure, which is 50^0C
3. The results of (FTIR) indicated that a physical reaction occurred as a result of no the absence or disappearance of a new bond.
4. The highest tensile strength obtained was (11MPa) when inserting 10wt% calcium carbonate for (LDPE/$CaCO_3$) composites, while the highest for (LDPE/AL_2O_3) composites was (10MPa) also at 10wt% alumina.
5. The highest value Young's modulus obtained was (200GPa) when inserting 30wt% AL_2O_3 for (LDPE/ AL_2O_3composites, while the highest for (LDPE/$CaCO_3$) composites was (180GPa) at 10wt% $CaCO_3$whith Note the Height of stiffness rates of all modified LDPE compounds compared to virgin LDPE.
6. The highest impact resistance obtained was (23.825KJ / M^2) when inserting 30wt% $AL_2O_3$for (LDPE/AL_2O_3 composites, while the highest for (LDPE/$CaCO_3$) composites was (16.835KJ / M^2) at 30wt% $CaCO_3$
7. Density values increase when the filler content in the LDPE matrix increases
8. The decrease in MFR and shear rate and increase in viscosity occurs with increasing filler insertion into the LDPE matrix
9. The FESEM images showed us the level of the distribution of the filler particles and their proportions in the LDPE matrix.

5.2 Recommendations

1. Propose to study the rheological and thermal properties of virgin (LDPE) and (LDPE) reinforced by fillers.

2. Suggest the use of polypropylene (PP) or high-density polyethylene (HDPE) and the study of its mechanical and viscoelastic properties.

3. Suggest using other fillers or filler materials such as Silicon dioxide (SiO2) or Titanium dioxide (TiO_2) as reinforcing materials for (LDPE) and its studying their viscoelastic behavior.

4. Propose to study the properties of elasticity and plasticity properties in greater detail and the comprehensiveness of low-density polyethylene (LDPE) reinforced with fillers.

References

Reference

[1] F. C. Meral, T. J. Royston, and R. Magin, “Fractional calculus in viscoelasticity: An experimental study,” Commun. Nonlinear Sci. Numer. Simul., vol. 15, no. 4, pp. 939–945, 2010, doi: 10.1016/j.cnsns.2009.05.004.

[2] H. Münstedt, Rheological and Morphological Properties of Dispersed Polymeric Materials. 2016.

[3] F. M. Monticeli, H. L. Ornaghi, R. M. Neves, and M. Odila Hilário Cioffi, “Creep/recovery and stress-relaxation tests applied in a standardized carbon fiber/epoxy composite: Design of experiment approach,” J. Strain Anal. Eng. Des., vol. 55, no. 3–4, pp. 109–117, 2020, doi: 10.1177/0309324719892710.

[4] J. Aho, Rheological Characterization of Polymer Melts in Shear and Extension: Measurement Reliability and Data for Practical Processing. 2011.

[5] M. Tajvidi and L. C. Simon, “High-temperature creep behavior of wheat straw isotactic/impact-modified polypropylene composites,” J. Thermoplast. Compos. Mater., vol. 28, no. 10, pp. 1406–1422, 2015, doi: 10.1177/0892705713513283.

[6] R. Rothon, Sustainable and Recycled Particulate Fillers. 2016.

[7] J. S. Gutmann, Polymer Structure Characterization-From Nano to Macro Organization. By Richard A. Pethrick., vol. 9, no. 14. 2008.

[8] C. Hall, " Polymer Materials : An introduction for technologists

and Scientists ", 2nd ed., MacMillan education LTD, (1989).

[9] S. S. W. Grellman, Mechanical and Thermomechanical Properties of polymers. 2014

[10] S. S. Gupta, A. Meena, T. Parikh, and A. T. M. Serajuddin, “Investigation of thermal and viscoelastic properties of polymers relevant to hot melt extrusion - I: Polyvinylpyrrolidone and related polymers,” J. Excipients Food Chem., vol. 5, no. 1, pp. 32–45, 2014.

[11] M. Rudolf, D. Boutelier, M. Rosenau, G. Schreurs, and O. Oncken, “Rheological benchmark of silicone oils used for analog modeling of short- and long-term lithospheric deformation,” Tectonophysics, vol. 684, pp. 12–22, 2016, doi: 10.1016/j.tecto.2015.11.028.

[12] M. Johlitz, H. Steeb, S. Diebels, A. Chatzouridou, J. Batal, and W. Possart, “Experimental and theoretical investigation of nonlinear viscoelastic polyurethane systems,” J. Mater. Sci., vol. 42, no. 23, pp. 9894–9904, 2007, doi: 10.1007/s10853-006-1479-4.

[13] I. Agirre-Olabide, M. J. Elejabarrieta, and M. M. Bou-Ali, “Matrix dependence of the linear viscoelastic region in magnetorheological elastomers,” J. Intell. Mater. Syst. Struct., vol. 26, no. 14, pp. 1880–1886, 2015, doi: 10.1177/1045389X15580658.

[14] A. Wineman, Nonlinear viscoelastic solids - A review, vol. 14, no. 3. 2009.

[15] E. Ségard, S. Benmedakhene, A. Laksimi, and D. Laï, “Influence of the fibre-matrix interface on the behaviour of polypropylene reinforced by short glass fibres above glass transition temperature,” Compos. Sci. Technol., vol. 62, no. 15, pp. 2029–2036, 2002, doi: 10.1016/S0266-3538(02)00102-1.

[16] O. Starkova and A. Aniskevich, “Limits of linear viscoelastic behavior of polymers,” Mech. Time-Dependent Mater., vol. 11, no. 2, pp. 111–126, 2007, doi: 10.1007/s11043-007-9036-3.

[17] M. E. Rognes and R. Winther, “Mixed finite element methods for linear viscoelasticity using weak symmetry,” Math. Model. Methods Appl. Sci., vol. 20, no. 6, pp. 955–985, 2010, doi: 10.1142/S0218202510004490.

[18] N. Lahellec and P. Suquet, “Effective behavior of linear viscoelastic composites: A time-integration approach,” Int. J. Solids Struct., vol. 44, no. 2, pp. 507–529, 2007, doi: 10.1016/j.ijsolstr.2006.04.038.

[19] A. Ahmed and S. Erlingsson, “Viscoelastic Response Modelling of a Pavement under Moving Load,” Transp. Res. Procedia, vol. 14, pp. 748–757, 2016, doi: 10.1016/j.trpro.2016.05.343.

[20] M. Sasso, G. Palmieri, and D. Amodio, “Application of fractional derivative models in linear viscoelastic problems,” Mech. Time-Dependent Mater., vol. 15, no. 4, pp. 367–387, 2011, doi: 10.1007/s11043-011-9153-x.

[21] M. Aller, Handbook of materials Sensors, no. 0. 2000.

[22] Y. Jia and B. Fiedler, “Tensile creep behaviour of unidirectional flax fibre reinforced bio-based epoxy composites,” Compos. Commun., vol. 18, no. August 2019, pp. 5–12, 2020, doi: 10.1016/j.coco.2019.12.010.

[23] H. S. Lee and J. Kim, “Determination of Viscoelastic Poisson’s Ratio and Creep Compliance from the Indirect Tension Test,” J. Mater. Civ. Eng., vol. 21, no. 8, pp. 416–425, 2009, doi: 10.1061/(asce)0899-1561(2009)21:8(416).

[24] D. F. Castellanos and M. Zaiser, “Statistical dynamics of early creep stages in disordered materials,” Eur. Phys. J. B, vol. 92, no. 7, 2019, doi: 10.1140/epjb/e2019-100124-0.

[25] A. Plaseied and A. Fatemi, “Tensile creep and deformation modeling of vinyl ester polymer and its nanocomposite,” J. Reinf. Plast. Compos., vol. 28, no. 14, pp. 1775–1788, 2009, doi: 10.1177/0731684408090378.

[26] Q. Jiang, Y. Qi, Z. Wang, and C. Zhou, “An extended nishihara model for the description of three stages of sandstone creep,” Geophys. J. Int., vol. 193, no. 2, pp. 841–854, 2013, doi: 10.1093/gji/ggt028.

[27] M. Whittaker, W. Harrison, C. Deen, C. Rae, and S. Williams, “Creep deformation by dislocation movement in waspaloy,” Materials (Basel)., vol. 10, no. 1, 2017, doi: 10.3390/ma10010061.

[28] B. Schmidtke, M. Hofmann, A. Lichtinger, and E. A. Rössler, “Temperature dependence of the segmental relaxation time of polymers revisited,” Macromolecules, vol. 48, no. 9, pp. 3005–3013, 2015, doi: 10.1021/acs.macromol.5b00204.

[29] F. Meng, R. H. Pritchard, and E. M. Terentjev, “Stress Relaxation, Dynamics, and Plasticity of Transient Polymer Networks,” Macromolecules, vol. 49, no. 7, pp. 2843–2852, 2016, doi: 10.1021/acs.macromol.5b02667.

[30] T. Dalrymple, J. Choi, and K. Miller, "Elastomer rate-dependence: a testing and material modelling methodology," in … Meeting of the Rubber Division of …, 2007, no. October 2007, pp. 16–18, [Online]. Available: http://www.axelproducts.com/downloads/Elastomer_Rate_Dependence_Paper.pdf.

[31] F. Del Giudice, S. J. Haward, and A. Q. Shen, "Relaxation time of dilute polymer solutions: A microfluidic approach," J. Rheol. (N. Y. N. Y)., vol. 61, no. 2, pp. 327–337, 2017, doi: 10.1122/1.4975933.

[32] Y. Zhang, Z. Lian, M. Zhou, and T. Lin, "Viscoelastic behavior of a casing material and its utilization in premium connections in high-temperature gas wells," Adv. Mech. Eng., vol. 10, no. 12, pp. 1–8, 2018, doi: 10.1177/1687814018817452.

[33] T.-S. Chang and M. P. Singh, "Mechanical Model Parameters for Viscoelastic Dampers," J. Eng. Mech., vol. 135, no. 6, pp. 581–584, 2009, doi: 10.1061/(asce)0733-9399(2009)135:6(581).

[34] R. Lewandowski and B. Chorazyczewski, "Identification of the parameters of the Kelvin-Voigt and the Maxwell fractional models, used to modeling of viscoelastic dampers," Comput. Struct., vol. 88, no. 1–2, pp. 1–17, 2010, doi: 10.1016/j.compstruc.2009.09.001.

[35] Y. Y. Feng, X. J. Yang, and J. G. Liu, "On overall behavior of Maxwell mechanical model by the combined Caputo fractional derivative," Chinese J. Phys., vol. 66, no. January, pp. 269–276, 2020, doi: 10.1016/j.cjph.2020.05.006.

[36] F. Dubois, J. M. Husson, N. Sauvat, and N. Manfoumbi, "Modeling of the viscoelastic mechano-sorptive behavior in wood," Mech. Time-Dependent Mater., vol. 16, no. 4, pp. 439–460, 2012, doi: 10.1007/s11043-012-9171-3.

[37] R. J. Castelli, M. Asce, S. G. Engineer, P. Brinckerhoff, and N. M. St, "GeoFlorida 2010: Advances in Analysis, Modeling & Design (GSP 199) © 2010 ASCE 2012," GeoFlorida 2010 Adv. Anal. Model. Des., no. Gsp 199, pp. 2012–2021, 2012.

[38] Z. Yang, H. Peng, W. Wang, and T. Liu, "Crystallization behavior of poly(ε-caprolactone)/layered double hydroxide nanocomposites," J. Appl. Polym. Sci., vol. 116, no. 5, pp. 2658–2667, 2010, doi: 10.1002/app.

[39] S. Tang, M. Steven Greene, and W. K. Liu, "Two-scale mechanism-based theory of nonlinear viscoelasticity," J. Mech. Phys. Solids, vol. 60, no. 2, pp. 199–226, 2012, doi: 10.1016/j.jmps.2011.11.003.

[40] A. Zacharatos and E. Kontou, "Nonlinear viscoelastic modeling of soft polymers," J. Appl. Polym. Sci., vol. 132, no. 26, 2015, doi: 10.1002/app.42141.

[41] V. V Vasiliev, Advanced Mechanics of Composite Materials.pdf. 2007.

[42] Callister, Willi D., "An Introduction to Material Science and Engineering", 6th Edition, John Wiley & Sons, Inc., USA, 2003.

[43] G. Nowaczyk, S. Głowinkowski, and S. Jurga, "Rheological and NMR studies of polyethylene/calcium carbonate composites," Solid State Nucl. Magn. Reson., vol. 25, no. 1–3, pp. 194–199, 2004, doi: 10.1016/j.ssnmr.2003.07.003.

[44] S. S. R. Koloor, "Damage Mechanics of Composite Laminates Subjected to Cyclic Flexual Load." Universiti Teknologi Malaysia, 2009.

[45] E. E. Gdoutos, Composite Materials, vol. 263. 2020.

[46] M. A. Osman, A. Atallah, and U. W. Suter, "Influence of excessive filler coating on the tensile properties of LDPE-calcium carbonate composites," Polymer (Guildf)., vol. 45, no. 4, pp. 1177–1183, 2004, doi: 10.1016/j.polymer.2003.12.020.

[47] S. Y. Fu, X. Q. Feng, B. Lauke, and Y. W. Mai, "Effects of particle size, particle/matrix interface adhesion and particle loading on mechanical properties of particulate-polymer composites," Compos. Part B Eng., vol. 39, no. 6, pp. 933–961, 2008, doi: 10.1016/j.compositesb.2008.01.002.

[48] X. Yang, Semiconducting Polymer Composites: Principles, Morphologies, Properties and Applications. 2013.

[49] H. Up, C. Introduction, and C. Atomic, "Chapter 6 . Mechanical Properties of Metals," pp. 4–9.

[50] K. Chrissafis and D. Bikiaris, “Can nanoparticles really enhance thermal stability of polymers? Part I: An overview on thermal decomposition of addition polymers,” Thermochim. Acta, vol. 523, no. 1–2, pp. 1–24, 2011, doi: 10.1016/j.tca.2011.06.010.

[51] C. Vasile and M. Pascu, Practical Guide to Polyethylene. 2005.

[52] D. R. Askeland, materials scince and engineering. 2009

[53] G. Lazouzi et al., “Optimized preparation of alumina based fillers for tuning composite properties,” Ceram. Int., vol. 44, no. 7, pp. 7442–7449, 2018.

[54] S. Baskar, V. Vijayan, S. Saravanan, A. V. Balan, and A. Godwin Antony, “Effect of Al2O3 aluminium alloy and fly ash for making engine component,” Int. J. Mech. Eng. Technol., vol. 9, no. 12, pp. 91–96, 2018.

[55] T. Shirai, H. Watanabe, M. Fuji, and M. Takahashi, “Structural Properties and Surface Characteristics on Aluminum Oxide Powders,” Annu. Rep. Adv. Ceram. Res. Cent. Nagoya Inst. Technol., vol. 9, pp. 23–31, 2009.

[56] L. Kovarik et al., “Unraveling the Origin of Structural Disorder in High Temperature Transition Al2O3: Structure of θ-Al2O3,” Chem. Mater., vol. 27, no. 20, pp. 7042–7049, 2015, doi: 10.1021/acs.chemmater.5b02523.

[57] L. Samain et al., “Structural analysis of highly porous γ-Al2O3,” J. Solid State Chem., vol. 217, pp. 1–8, 2014, doi: 10.1016/j.jssc.2014.05.004.

[58] A. M. Abyzov, “Aluminum Oxide and Alumina Ceramics (review). Part 1. Properties of Al2O3 and Commercial Production of Dispersed Al2O3,” Refract. Ind. Ceram., vol. 60, no. 1, pp. 24–32, 2019, doi: 10.1007/s11148-019-00304-2.

[59] W. L. Suchanek, “Hydrothermal synthesis of alpha alumina (α-Al2O 3) powders: Study of the processing variables and growth mechanisms,” J. Am. Ceram. Soc., vol. 93, no. 2, pp. 399–412, 2010, doi: 10.1111/j.1551-2916.2009.03399.x.

[60] D. Gebauer, A. Völkel, and H. Cölfen, “Stable prenucleation calcium carbonate clusters,” Science (80-.)., vol. 322, no. 5909, pp. 1819–1822, 2008, doi: 10.1126/science.1164271.

[61] F. Manoli, J. Kanakis, P. Malkaj, and E. Dalas, “The effect of aminoacids on the crystal growth of calcium carbonate,” J. Cryst. Growth, vol. 236, no. 1–3, pp. 363–370, 2002, doi: 10.1016/S0022-0248(01)02164-9.

[62] E. Loste, R. J. Park, J. Warren, and F. C. Meldrum, “Precipitation of calcium carbonate in confinement,” Adv. Funct. Mater., vol. 14, no. 12, pp. 1211–1220, 2004, doi: 10.1002/adfm.200400268.

[63] O. A. Jimoh, K. S. Ariffin, H. Bin Hussin, and A. E. Temitope, “Synthesis of precipitated calcium carbonate: a review,” Carbonates and Evaporites, vol. 33, no. 2, pp. 331–346, 2018, doi: 10.1007/s13146-017-0341-x.

[64] G. A. Tribello, F. Bruneval, C. C. Liew, and M. Parrinello, “A molecular dynamics study of the early stages of calcium carbonate growth,” J. Phys. Chem. B, vol. 113, no. 34, pp. 11680–11687, 2009, doi: 10.1021/jp902606x.

[65] N. Durand, C. H. Monger, and M. G. Canti, Calcium Carbonate Features, no. August 2020. Elsevier B.V., 2018.

[66] J. Rohleder and E. Kroker, Calcium carbonate: from the Cretaceous period into the 21st century. Birkhäuser, 2012.

[67] A. Shenoy, Thermoplastic Melt Rheology and Processing. 1996.

[68] M. Subramanian, Basics of Polymers: Fabrication and Processing Technology. 2015.

[69] David I. Bower, Formerly at the University of Leeds, "An Introduction to Polymer Physics", Cambridge, New York, Melbourne, Madrid, Cape Town, Singapore, São Paulo , Published in the United States of America by Cambridge University Press, New York; 2002.

[70] mohd shamsul farid samsudin , " Rheologyical Behavior of Talc and Calcium Carbonate Filled Polypropylene Hybrid Composites" a Thesis, university sains Malaysia; 2008.

[71] Brian C. Smith, " Fundamentals of Fourier Transform Infrared Spectroscopy ", Second Edition, Taylor and Francis Group, CRC Press, (2011)

[72] Braun,H.Cherdron,M.Rehahn, H. Ritter, B.Voit, "Polymer Synthesis Theory and Practice",Springer-Verlag Berlin Heidelberg (2005).

[73] B. Stuart ,"Infrared Spectroscopy: Fundamentals and Applications " , John Wiley & Sons, Ltd ISBNs: 0-470-85427-8 (HB); 0-470-85428-6 (PB) , (2004).

[74] Mizi Fan, Dasong Dai, and Biao Huang,"Fourier Transform Infrared Spectroscopy for Natural Fibres" ISBN 978-953-51-0594- 7,(2012)

[75] S. Lanteri and M. Bronzoni, “Rheology Milestones 1687 Today Today,” pp. 1–54.

[76] Y. Hammache, A. Serier, and S. Chaoui, “The effect of thermoplastic starch on the properties of polypropylene/high density polyethylene blend reinforced by nano-clay,” Mater. Res. Express, vol. 7, no. 2, p. 25308, 2020

[77] J. Grum, Book Review: Handbook of Polymer Testing Short-Term Mechanical Tests, vol. 27, no. 3/4. 2006.

[78] A. R. Saeed and S. N. A. Rafiq, “Studying Mechanical Properties For Polyethylene Composites Reinforced By Fish Shell Particles,” Eng. Tech. J., vol. 29, no. 15, 2011.

[79] O. N. Nwoke, I. P. Okokpujie, and S. C. Ekenyem, “Investigation of creep responses of selected engineering materials,” J. Sci. Eng. Dev. Environmen Technol., vol. 7, no. 1, pp. 1–15, 2017.

[80] . H. F. Mark and J. I. Kroschwitz ,"Encyclopedia of Polymer Science and Engineering ", John Wiley &Sons, New York, (2004)

[81] William. D. Callister, "Materials science & Engineering an Introduction", Jown Wiley& Sons , Inc, 6th Ed, (2003).

[82] Weilie Zhou, and Zhong Lin Wang , "Scanning Microscopy for Nanotechnology: Techniques and Applications ", Springer Science & Business Media, (2007).

[83] Joseph Goldstein, Dale E. Newbury, David C. Joy, Charles E. Lyman, Patrick Echlin, Eric Lifshin, Linda Sawyer and J.R. Michael, " Scanning Electron

Microscopy and X-ray Microanalysis ", Third Edition, Springer Science & Business Media,(2012).

[84] R. H. Elleithy, I. Ali, M. AlhajAli, and S. M. Al-Zahrani, "High density polyethylene/micro calcium carbonate composites: A study of the morphological, thermal, and viscoelastic properties," J. Appl. Polym. Sci., vol. 117, no. 4, pp. 2413–2421, 2010, doi: 10.1002/app.32142.

[85] Y. Lu, H. Peng, K. Shen, and Z. Yan, "Study on creep behavior of PP/CaCO 3 molded by vibration injection molding at different vibration frequency and vibration pressure," Int. Polym. Process., vol. 26, no. 2, pp. 136–142, 2011, doi: 10.3139/217.2379.

[86] H. Salmah, B. Y. Lim, and P. L. Teh, "Rheological and thermal properties of palm kernel shell-filled low-density polyethylene composites with acrylic acid," J. Thermoplast. Compos. Mater., vol. 26, no. 9, pp. 1155–1167, 2013, doi: 10.1177/0892705711434193.

[87] M. M. Riara, A. S. Merenga, and C. M. Migwi, "Creep and recovery behavior of compression molded low density polyethylene/cellulose composites," J. Polym., vol. 2013, 2013.

[88] F. W. Qi, X. G. Luo, X. Y. Lin, and S. Z. Zhang, "Effect of CaCO3 particle size and size distribution on rheological and mechanical properties of polyethylene," in Advanced Materials Research, 2013, vol. 734, pp. 2252–2255.

[89] R. K. Hussain, H. F. Dagher, and R. R. Khudadad, "Reducing Creep Rate of polypropylene's by Soaking Solid solutions of CaCO 3," World Sci. News, vol. 49, no. 2, pp. 90–103, 2016, [Online]. Available: www.worldscientificnews.com.

[90] M. Tazi, M. S. Sukiman, F. Erchiqui, A. Imad, and T. Kanit, "Effect of wood fillers on the viscoelastic and thermophysical properties of HDPE-wood composite," Int. J. Polym. Sci., vol. 2016, 2016, doi: 10.1155/2016/9032525.

[91] M. Al-ibrahim, "The effect of adding carbon black and calcium carbonate on fluidity of polyethylene," vol. 1, pp. 501–514, 2019.

[92] X. Hao, X. Yi, L. Sun, D. Tu, Q. Wang, and R. Ou, “Mechanical properties, creep resistance, and dimensional stability of core/shell structured wood flour/polyethylene composites with highly filled core layer,” Constr. Build. Mater., vol. 226, pp. 879–887, 2019, doi: 10.1016/j.conbuildmat.2019.07.329.

[93] H. Sepet, B. Aydemir, and N. Tarakcioglu, “Evaluation of mechanical and thermal properties and creep behavior of micro- and nano-CaCO3 particle-filled HDPE nano- and microcomposites produced in large scale,” Polym. Bull., vol. 77, no. 7, pp. 3677–3695, 2020, doi: 10.1007/s00289-019-02922-9.

[94] K. Nwosu-Obieogu, F. O. Aguele, L. I. Chiemenam, K. N. Akatobi, K. Osoh, and C. S. Onyekwulu, “Creep and Stress Relaxation Behaviour of Rice Husk Reinforced Low Density Polyethylene Composites,” Eur. J. Sustain. Dev. Res., vol. 4, no. 4, p. em0144, 2020, doi: 10.29333/ejosdr/9284.

[95] Amir kabir petrochemical company, Tehran, Tehran Province, Iran, Q9FG+W9C.

[96] Thomas Baker (Chemicals) Pvt. Ltd. : 4/86 Bharat Mahal,, Marine Drive, Netaji Subhash Chandra Bose Rd, Churchgate, Mumbai, Maharashtra 400002 ، India.

[97] V. S. Chevali, D. R. Dean, and G. M. Janowski, “Flexural creep behavior of discontinuous thermoplastic composites: Non-linear viscoelastic modeling and time-temperature-stress superposition,” Compos. Part A Appl. Sci. Manuf., vol. 40, no. 6–7, pp. 870–877, 2009, doi: 10.1016/j.compositesa.2009.04.012.

[98] A. Pastrnak, A. Henriquez, and V. La Saponara, “Parametric study for tensile properties of molded high-density polyethylene for applications in additive manufacturing and sustainable designs,” J. Appl. Polym. Sci., vol. 137, no. 42, pp. 1–9, 2020, doi: 10.1002/app.49283.

[99] Astm-D6110-10, “Standard Test Method for Determining the Charpy Impact Resistance of Notched Specimens of Plastics,” Astm, no. April, p. 17, 2010, doi: 10.1520/D6110-10.1.

[100] J. Charles and G. R. Ramkumaar, “Qualitative analysis of high density polyethylene using FTIR spectroscopy,” Asian J. Chem., vol. 21, no. 6, pp. 4477–4484, 2009.

[101] S. Kormin, F. Kormin, M. D. H. Beg, and M. B. M. Piah, “Physical and mechanical properties of LDPE incorporated with different starch sources,” IOP Conf. Ser. Mater. Sci. Eng., vol. 226, no. 1, 2017, doi: 10.1088/1757-899X/226/1/012157.

[102] H. Salmah, B. Y. Lim, and P. L. Teh, “Melt rheological behavior and thermal properties of low-density polyethylene/palm kernel shell composites: Effect of polyethylene acrylic acid,” Int. J. Polym. Mater. Polym. Biomater., vol. 61, no. 14, pp. 1091–1101, 2012, doi: 10.1080/00914037.2011.617336.

[103] M. Al-ibrahim, “The effect of adding carbon black and calcium carbonate on fluidity of polyethylene,” vol. 1, pp. 501–514, 2019.

[104] A. Romisuhani, H. Salmah, and H. Akmal, “Tensile properties of low density polypropylene (LDPE)/palm kernel shell (PKS) biocomposites: The effect of acrylic acid (AA),” IOP Conf. Ser. Mater. Sci. Eng., vol. 11, p. 012001, 2010, doi: 10.1088/1757-899x/11/1/012001.

[105] A. K. Patel, P. Trivedi, and K. Balani, “Processing and Mechanical Characterization of Compression-Molded Ultrahigh Molecular Weight Polyethylene Biocomposite Reinforced with Aluminum Oxide,” J. Nanosci. Nanoeng. Appl., vol. 4, no. 3, pp. 1–11, 2014.

[106] F. H. Latief, A. Chafidz, H. Junaedi, A. Alfozan, and R. Khan, “Effect of alumina contents on the physicomechanical properties of alumina (Al2 o3) reinforced polyester composites,” Adv. Polym. Technol., vol. 2019, pp. 1–10, 2019, doi: 10.1155/2019/5173537.

[107] A. J. Mohammed, “Study the effect of adding powder Walnut shells on the Mechanical Properties and the flame resistance for Low Density Polyethylene (LDPE),” Int. J. Sci. Technol., vol. 3, no. 1, pp. 18–22, 2014.

[108] Lee Jie Shin, E. G. Barathi Dassan, M. S. Zainol Abidin, and A. Anjang, "Tensile and Compressive Properties of Glass Fiber-Reinforced Polymer Hybrid Composite with Eggshell Powder," Arab. J. Sci. Eng., vol. 45, no. 7, pp. 5783–5791, 2020, doi: 10.1007/s13369-020-04561-z.

[109] K. Chaochanchaikul, A. Kositchaiyong, and N. Sombatsompop, "Blending techniques affecting mechanical and morphological properties of fly ash/LDPE and CaCO3/LDPE composites," Polym. Polym. Compos., vol. 17, no. 5, pp. 281–290, 2009, doi: 10.1177/096739110901700502.

[110] S. Zhang, X. Y. Cao, Y. M. Ma, Y. C. Ke, J. K. Zhang, and F. S. Wang, "The effects of particle size and content on the thermal conductivity and mechanical properties of Al 2O 3/high density polyethylene (HDPE) composites," Express Polym. Lett., vol. 5, no. 7, pp. 581–590, 2011, doi:

[111] Y. cui, J. E. Campbell, M. burley, M. patel, K. hunt, and T. W. Clyne, "Effects of temperature and filler content on the creep behaviour of a polyurethane rubber," Mech. Mater., vol. 148, p. 103461, 2020, doi: 10.1016/j.mechmat.2020.103461.

[112] Sivarao, M. R. Salleh, A. Kamely, A. Tajul, and Taufik, "Mechanical properties modification of polyethylene (PE) for CaCO3 particulated composites," Adv. Mater. Res., vol. 264–265, pp. 880–887, 2011, doi: 10.4028/www.scientific.net/AMR.264-265.880.10.3144/expresspolymlett.2011.57.

جمهورية العراق
وزارة التعليم العالي والبحث العلمي
جامعة بابل
كلية هندسة المواد
قسم هندسة المواد البوليمرات والصناعات البتروكيمياوية

دراسة تاثير الحشوات على خواص اللزجة المرنة للبولي اثلين منخفض الكثافة (LDPE)

رسالة
مقدمة الى كلية هندسة المواد/ جامعة بابل وهي جزء من متطلبات نيل
درجة الماجستير في هندسة المواد/ البوليمر

من قبل

احمد سعيد هاشم عباس

بإشراف

أ.د. نجم عبد الامير سعيد

1442 هـ **2021م**

الخلاصة

تظهربعض البوليمرات سلوكًا مرنًا صلبًا وآخر سائل لزج ،خاصة البوليمرات ذات الوزن الجزيي المنخفض ،بعض البوليمرات تمتلك هذا السلوك في درجة حرارة الغرفة ،خاصة تلك التي تحتوي على درجة حرارة تحول منخفضة ،مما يؤثرسلبًاعلى خصائص وأداء الأجزاء أثناء الخدمة ،خاصة سلوك الزحف ،لذا فإن تحسين أداء هذه البوليمرات يتطلب إضافة مواد تقوية لتشكيل مواد مركبة جديدة قادرة على التغلب على هذا النوع من السلوك . تم استخدام مواد الحشو كمواد تقوية في هذا العمل .

في هذا العمل تم تحضيرنوعين من المواد المركبة ،البولي إيثيلين منخفض الكثافة المقوى بنسب وزنية (10,20,30,40)% من الالومينا ,البولي إيثيلين منخفض الكثافة المقوى بنسب وزنية (10,20,30,40) % من كاربونات الكالسيوم تم استخدام عمليتي الخلط الأولى هي الخلط الجاف الميكانيكي (المطحنة الكروية) والثانيةهي عملية الانصهارلخلط المواد بواسطة الطارد المزدوج ، لخلط البولي إثيلين المنخفض الكثافة مع الالومينا وكاربونات الكالسيوم للحصول على الموادالمركبة المعدلة الجديدة (البولي إيثيلين منخفض الكثافة/ الومينا) ,(البولي إيثيلين منخفض الكثافة / كاربونات الكالسيوم) على التوالي .

لغرض دراسة تأثير الحشوات على السلوك اللزج المرن والمورفولوجيا ، يتم إجراء العديد من الاختبارات بما في ذلك ،الأشعة تحت الحمراء ،وفحص مؤشر تدفق الذوبان ,والكثافة وقوة الشد ,والصدمة والزحف ,وفحص المجهرالإلكتروني الماسح .

كانت النتائج ،تحسنًا واضحًا في أداء الزحف لجميع مركبات البولي إثيلين المنخفض الكثافة عند إضافة مواد مالئة ،ولكن النسب المعقولة من الحشوات أعطت أفضل أداء ،حيث يتم توفير أفضل أداء لمقاومة الزحف بنسبة وزن (10 %) من الألومينا في في المادة الاساس (البولي إيثيلين منخفض الكثافة) متفوقًا لأفضل أداء يوفره البولي إيثيلين منخفض الكثافة عند إدخال وزن (20%) من كربونات الكالسيوم.أعلى درجة حرارة يمكن أن تتحملها العينة التي قدمت أفضل أداء لمقاومة الزحف هي 50 درجة مئوية, زادت قوة الشد بمقدار (22.22 %) عند إدخال وزن(10 %) من كربونات الكالسيوم وهي أعلى زيادة تم الحصول عليها ,بينما زادت مقاومة الشد بنسبة (11.111 %) عند ادخال وزن (10 %) من الألومينا. أما بالنسبة لأعلى نسبة زيادة تم الحصول عليها لمعامل يونغ فقد قدرت بحوالي (53.84 %) عند إدخال وزن(30 %) من الألومينا ،بينما زاد معامل يونغ بنسبة 38.46 %عند إدخال وزن (10 %) من كربونات الكالسيوم . زادت مقاومة الصدمات بنسبة (48.9 %) عند إدخال وزن (30 %) من الألومينا ، بينما زادت مقاومة الصدمات بنسبة (12.34 %) عند إدخال وزن (30 %) من كربونات الكالسيوم. زادت قيم الكثافة واللزوجة وانخفض معدل تدفق المنصهرمع زيادة محتوى الحشو في البولي

اثلين المنخفض الكثافة . أظهرت لنا صور الماسح الاكتروني مستوى تشتت جسيمات الحشو ونسبها في مادة الاساس (البولي إيثيلين منخفضة الكثافة).